RHEOLOGY OF LOW TO MEDIUM CONSISTENCY PULP FIBRE SUSPENSIONS

by

Babak Derakhshandeh

B.A.Sc., Shiraz University, 2004
M.A.Sc., Sharif University of Technology, 2006

A THESIS SUBMITTED IN PARTIAL FULLFILMENT OF
THE REQUIREMENTS FOR THE DEGREE OF

DOCTOR OF PHILOSOPHY

in

The Faculty of Graduate Studies
(Chemical and Biological Engineering)

THE UNIVERSITY OF BRITISH COLUMBIA
(Vancouver)

September 2011

Abstract

Papermaking is a major industry to manufacture products vital to education, communication, and packaging. Most operations in this industry deal with the flow of different mass concentrations of pulp suspensions. Therefore, the flow properties (rheology) of pulp suspensions are of great importance for the optimal functionality of most unit operations in the industry.

Yield stress is one of the most important rheological properties in designing process equipment, thus needs to be determined by a reliable technique. Two established and extensively used methods for determining yield stress were compared with a velocimetry technique. The yield stresses were determined for commercial pulp suspensions at fibre mass concentrations of 0.5 to 5 wt. %. The results were compared and models were proposed to predict the yield stress as a function of fibre mass concentration. The yield stress values obtained by the velocimetry technique were found to be the most reliable.

Conventional rheometry and local velocimetry techniques were further used to study the flow behaviour of pulp suspensions beyond the yield stress. Pulp suspensions were found to be shear-thinning up to a certain high shear rate. The Herschel–Bulkley constitutive equation was used to fit the local steady-state velocity profiles and to predict the steady-state flow curves obtained by conventional rheometry. Conventional rheometry was found to fail at low shear rates due to the presence of wall slip. Consistency between the various sets of data was found for all suspensions studied.

Finally, the same approach was used to study thixotropy and transient flow behaviour of concentrated pulp suspension of 6 wt.%. Pulp was found to exhibit a plateau in the flow curve where a slight increase in the shear stress generated a jump in the corresponding shear rate, implying the occurrence of shear banding. The velocity profiles were found to be discontinuous in the vicinity of the yielding radius where a Herschel-Bulkley model failed to predict the flow. Shear history and the time of rest prior to the measurement were found to play a significant role on the rheology and the local velocity profiles of pulp suspension.

Preface

The work of this thesis consists of four different manuscripts, which correspond to chapters one to four.

Chapter 1 has been published: Derakhshandeh, B., Kerekes, R.J., Hatzikiriakos, S.G., Bennington, C.P.J, 2011. Rheology of pulp fibre suspensions: A critical review. Chemical Engineering Science 66(15):3460-3470. I searched, criticised and reviewed the literature published on the topic. The written work was a collaborative effort between my supervisors Prof. Chad P.J. Bennington and Prof. Savvas G. Hatzikiriakos, me and Prof. Richard J. Kerekes.

Chapter 2 has been published: Derakhshandeh, B., Hatzikiriakos, S.G., Bennington, C.P.J., 2010. Apparent yield stress of pulp fibre suspensions. Journal of Rheology 54(5):1137-1154. I performed all the experimental measurements. The written work was a collaborative effort between my supervisors Prof. Chad P.J. Bennington, Prof. Savvas G. Hatzikiriakos and me.

Chapter 3 has been published: Derakhshandeh, B., Hatzikiriakos, S.G., Bennington, C.P.J., 2010. Rheology of pulp suspensions using ultrasonic Doppler velocimetry. Rheologica Acta 49 (11-12):1127-1140. I performed all the experimental measurements. The written work was a collaborative effort between my supervisors Prof. Chad P.J. Bennington, Prof. Savvas G. Hatzikiriakos and me.

Chapter 4 has been submitted for publication: Derakhshandeh, B., Vlassopoulos, D., Hatzikiriakos, S.G., 2011. Thixotropy, yielding and ultrasonic Doppler velocimetry in pulp fibre suspensions. I performed all the experimental measurements. The written work was a collaborative effort between my supervisor Prof. Savvas G. Hatzikiriakos and me. Prof. Dimitris Vlassopoulos revised the manuscript and provided insightful advices on the topic.

Check the first pages of these chapters to see footnotes with similar information.

Table of Contents

List of Tables

List of Figures

Nomenclature

A	fibre aspect ratio, (-)
a	constant, (Pa)
b	constant, (-)
c	sound velocity in the medium, (m/s)
C_m	fibre mass concentration, (%)
C_v	fibre volume concentration, (%)
C_s	sediment concentration, (%)
d	inner diameter of fibre, (mm)
D	outer diameter of fibre, (mm)
D_r	particle rotary diffusion, (s^{-1})
D_T	outer housing diameter, (m)
D_R	rotor diameter, (m)
E	fibre's modulus of elasticity, (Pa)
f_d	frequency shift of the reflected ultrasound pulses, (Hz)
f_0	ultrasound emission frequency, (Hz)
G'	storage modulus, (Pa)
G''	loss modulus, (Pa)
h	vane height, (mm)
K	HB consistency index
k_B	Boltztmann constant, ($m^2 Kg\ s^{-2}\ K^{-1}$)
L	fibre length, (mm)
m	constant
n	HB power-law index
N	crowding number, (-)
N_G	gel crowding number, (-)
r	local radius within the gap of the rheometer, (mm)
R	dimensionless radius
R_1	vane radius, (mm)

R_2	cup radius, (mm)
R_y	yielding radius, (mm)
t	time, (s)
t_f	time delay of the reflected ultrasound pulses, (s)
T	torque, (N.m)
T	absolute temperature, (K)
$u(r)$	local velocity across the gap of the rheometer, (mm/s)
$u(y)$	velocity in the direction of acoustic axis, (mm/s)
U	scaled velocity, (s^{-1})
V	pipe flow velocity, (m/s)
V_L	lumen volume per unit mass of fibre (m^3/kg fibre)
X_w	water mass located in the fibre wall, (kg water/kg fibre)
y	distance of fibres from the outer wall in Couette geometry, (mm)
ΔH	pipe friction loss, (Pa)

Greek letters

A	constant
B	constant
Γ	strain, (%)
$\dot{\gamma}$	shear rate, (s^{-1})
φ_g	volume fraction of gas phase in suspension, (-)
η	Instantaneous viscosity, (Pa.s)
η_s	medium viscosity, (Pa.s)
η_0	suspension viscosity prior to shearing, (Pa.s)
η_∞	suspension viscosity after shearing, (Pa.s)
μ_a	apparent viscosity, (Pa.s)
ρ_b	bulk density, (kg/m^3)
ρ_f	fibre density, (kg/m^3)
ρ_w	water density, (kg/m^3)

σ	shear stress, (Pa)
σ_i	pre-shear stress, (Pa)
σ_e	final shear stress in the step-wise experiments, (Pa)
σ_c	critical shear stress, (Pa)
σ_y	apparent yield stress, (Pa)
σ_T	steady-state shear stress at the vane, (Pa)
ε_f	power dissipation/unit volume, (w/m^3)
ω	fibre coarseness, (g/m)
θ	emission angle into the fluid
τ	structure build-up/breakdown time constant, s

Abbreviations

SBK	bleached softwood kraft pulp suspension
TMP	thermal mechanical pulp suspension
SGW	stone ground wood pulp suspension
HW	hardwood pulp suspension
UDV	ultrasound Doppler velocimetry

Acknowledgments

I offer my sincere gratitude and appreciation to my thesis supervisors Prof. Chad P.J. Bennington and Prof. Savvas G. Hatzikiriakos for giving me insightful scientific advice. They have supported me throughout my thesis with their patience and knowledge whist allowing me the room to work in my own way. One simply could not wish for better or friendlier supervisors.

My utmost gratitude to Prof. Chad P.J. Bennington who passed away unexpectedly on February 14, 2010 for introducing me into pulp and paper science and technology, for his smile, sincerity and encouragement. He will be in my thoughts and in my prayers for ever.

Working in the Dynamic Mixing and Rheology Group has been a privilege. I would love to thank all members, both past and present, for their hard work that has inspired so many ideas. I would like to thank my friends and ex-colleagues Dr. Christos Stamboulides and Dr. Anne-Marie Kietzig for their unconditional support.

I am grateful for the financial support of the University of British Columbia 4YF and DuPont fellowship in pulp and paper.

From the bottom of my heart, I thank my good friends Hooman Rezaei and Fahimeh Yazdanpanah, and my brother Maziar Derakhshandeh for helping me get through the difficult times, and for all the emotional support, camaraderie, entertainment, and caring they provided.

The most profound and loving thanks to my family, to my parents who have given me the greatest love and support anyone could ever expect. I am blessed to have them and I have missed them deeply during these years. They are my true inspiration.

Dedication

This thesis is dedicated to my parents, my sister and brother, for always encouraging and supporting me to achieve my goals.

1. Introduction[1]

Flow of fibre suspensions is a key factor in manufacturing a diverse range of products, for example, fibre-reinforced composites, food stuffs, carpeting, and textiles (Tucker and Advani, 1994; Papathanasiou and Guell, 1997; Piteira et al., 2006; Umer et al., 2007). Of these industries, none is larger than pulp and paper manufacture. It is a major industry in almost all countries, producing communication papers, packaging, boxes, tissue, hygiene products, and an assortment of disposable products. Fibre for this industry comes from pulping biomass, mostly trees in modern times. As such, the industry is based on a sustainable, renewable, carbon-neutral resource.

There is growing interest in new uses of biomass. The world's increasing population requires that more energy and products come from renewable resources that do not impinge upon the food supply. The forest biomass is a logical source. As in the case of pulp and paper, processing biomass for these new applications will require handling of fibres in suspension.

This work focuses on the rheological characterization of pulp fibre suspensions. Conventional stress-controlled and rate-controlled rheometers along with ultrasonic Doppler velocimetry are used to characterize commercial pulp fibre suspensions of various fibre mass concentrations. Particular objectives are to measure apparent yield stress, to study post-yield flow behaviour, and to investigate thixotropy and time dependent flow behaviour of pulp fibre suspensions. Constitutive models are proposed to describe the flow behaviour of pulp suspensions over a wide range of shear rates and fibre mass concentrations.

[1] A version of this chapter has been published. Derakhshandeh, B., Kerekes, R.J., Hatzikiriakos, S.G., Bennington, C.P.J., 2011. Rheology of pulp fibre suspensions-A critical review. Chemical Engineering Science 66(15): 3460-3470.

1.1. Literature Review

1.1.1. Background

1.1.1.1. Fibre Properties and Consistency Ranges

Wood pulp fibres are hollow tubes having typical average length 1-3 mm and diameter 15-30 μm. There is a wide variability around these averages, even within one species. Accordingly, fibre length is specified by various weighted averages, a typical one being length-weighted average for fibre length to give weight to the longer fibres in the distribution.

Wood fibres are composites made up of spirally-wound fibrils of cellulose. Some newer applications of wood pulp are being developed to exploit the unique properties of these fibrils. Examples are micro-fibrillated cellulose (MFC) and nano-crystalline cellulose (NCC). MFC are small fibrous particles of length 100 to 1000 nm and diameter 5-30 nm (Ankerfors and Lindström, 2010). NCC is smaller, in the range 20-200 nm in length (Dong et al., 1998; Pan et al., 2010). These fibrous particles are in the Brownian range and generally behave as colloidal suspensions in the dilute range and as gels when more concentrated. They are outside the range of interest in this study, although in producing them, for example in homogenizers, grinders, refiners and like, rheology of pulp suspensions plays a role.

Suspensions of pulp fibres are processed in various ranges by mass consistency, C_m (mass of fibres divided by the total mass of suspension). Kerekes et al. (1985) classified the ranges as follows: low consistency (C_m=0-5%) where the suspension is water-fibre slurry; medium consistency (C_m=5-20%) formed by mechanically pressing water from a medium consistency suspension and ultra-high consistency (C_m>40%) formed by evaporative drying.

At low consistency, the suspension is a two-phase slurry, changing at medium and higher consistencies into a three phase heterogeneous mixture of water, fibres and air. At the higher gas contents, it is useful to use volumetric concentration, C_v, in place of mass consistency. These are related as follows:

$$C_v = C_m \left(\frac{1}{\rho_f} + \frac{X_w}{\rho_w} + V_L \right) \rho_b \qquad (1\text{-}1)$$

where C_m is the fibre mass fraction, ρ_f is the fibre density (kg/m^3), ρ_w is the water density (kg/m^3), ρ_b is the bulk density (kg/m^3), X_w is the water adsorbed within the fibre wall (kg water/kg fibre) and V_L is the volume per unit mass of the hollow channel in the middle of the fibre referred to as lumen (m^3/kg fibre).

All of the above consistency ranges are found in the processes for pulp and paper manufacture. They are likely to be important in new processes for fibrous biomass.

1.1.1.2. Fibre Contacts and Forces

The large aspect ratio of pulp fibres (40 to 100) induces significant contact among fibres at all consistencies. This has a strong effect on suspension rheology. In the low consistency range, with increasing consistency the nature of contacts changes from occasional collisions, to forced contacts, to continuous contact. These contact regimes have been described by a crowding number, *N*, defined as the number of fibres in a volume swept out by the length of a single fibre (Kerekes et al., 1985). This parameter can be expressed in terms of a volumetric concentration C_v, fibre length *L,* and diameter *d*. Pulp fibres have a distribution of fibre lengths, variable diameters, and like all lignocelluloses materials, tend to swell in water. Accordingly mass is more suitable than volume for calculating numbers of fibres and thereby *N*. Kerekes and Schell (1992) provide a mass-based expression for this calculation shown below:

$$N = \frac{2}{3} C_v \left(\frac{L}{d} \right)^2 \approx 5 C_m \frac{L^2}{\omega} \qquad (1\text{-}2)$$

In this equation, *L* is the length-weighted average length of the pulp fibres (m); C_m is the mass consistency (%), and ω is the fibre coarseness (weight per unit length of fibre, kg/m). The latter is a commonly measured property of pulp fibres. Accordingly, the constant has units kg/m^3**.**

In early work, Mason (1950) identified $N = 1$ as a "critical concentration" at which, collisions first occur among fibres in shear flow. In later work, Soszynski and Kerekes (1988a) and Kerekes and Schell (1992) showed that at $N \approx 60$ fibre suspensions have about three contacts per fibre. This is a critical value because fibres are restrained by three-point contact. Upon cessation of shear, fibres become locked in the network in a bent configuration. This elastic bending creates normal forces at contacts, and the resulting frictional force imparts mechanical strength to the network.

In later work, Martinez et al. (2001) identified another critical value of N, $N \approx 16$, calling this a "gel crowding number". Below this value, the suspension behaves as essentially dilute. In recent work, the limits N=16 and N=60 were shown to correspond respectively to the "connectivity threshold" and "rigidity threshold" of fibre networks as predicted by effective-medium and percolation theories (Celzard et al., 2009).

1.1.1.3. Forces on Fibres and Flocculation

In addition to friction forces, other forces may contribute to strength at contacts, such as forces from chemical flocculants, hooking of curved fibres, and surface tension when air content is substantial (Kerekes et al., 1985). These forces impart mechanical strength to fibre networks.

In shear flow, fibres aggregate into local mass concentrations called flocs, which are typically a few fibre lengths in size. When N<60, the flocs are loose aggregates, but when N>60 the flocs adopt mechanical strength. Their size and strength are affected by the flow conditions, for example, shear history such as nature of the decaying turbulence in the wakes of pumps and mixers where most flocs form (Kerekes, 1983b). Having a larger concentration than the suspension average, flocs also have a larger strength than the suspension average. Consequently, fibre suspensions are heterogeneous in both mass and strength, an important factor in pulp suspension rheology.

The mechanism of floc formation has been studied in various past works. Kerekes (1983b) examined the role of decaying turbulence in floc formation, and later Soszynski and Kerekes (1988b) studied the role of flow acceleration and turning on local fibre

crowding to produce coherent flocs. Valuable insights have also been gained from particle level simulation techniques modeling fibres as chains of rigid rods connected with hinges (Ross and Klingenberg, 1998; Schmid and Klingenberg, 2000a,b,c).

In summary, fibre suspensions display a large range of behaviour, from dilute slurries, to heterogeneous two-phase suspensions, to discontinuous three-phase mixtures of wet fibres in a gas. In commercial papermaking, pulp suspensions are formed into paper by filtration in the range $16 < N < 60$ to minimize both water usage and flocculation. However, most of the unit operations for processing pulp before papermaking take place at one or other of the higher consistency ranges.

1.1.1.4. Rheology of Fibre Suspensions

The complexities described above make the rheology of pulp suspensions complex. The suspension often cannot be treated as a continuum because fibres and flocs are large relative to the dimensions of the flow field. Both shear history and time in a given shear flow (thixotropy) may cause floc size and strength to differ among suspensions even when suspension averages are the same. Fibre orientation and migration away from solid boundaries create a depletion layer near walls which complicates rheological measurements (Nguyen and Boger, 1992; Barnes, 1997; Swerin, 1998; Wikström and Rasmuson, 1998). Given these factors and those described earlier, not surprisingly defining and measuring rheological properties of fibre suspensions is complex. The complexities involved in the rheological measurement of pulp fibre suspensions will be discussed in more detail throughout the next chapters of this thesis.

1.1.2. Yield stress

Yield stress is arguably the most important rheological property of fibre suspensions. Unless it is exceeded, flow does not take place. As a rheological property, yield stress has various definitions and means of measurement. These will be discussed in detail in chapter 2 of this thesis although a brief overview of the yield stress measurement techniques, definitions, and findings of past work is summarized here.

In the simple case of a Bingham fluid, yield stress is the shear stress required to initiate continuous motion in the form of Newtonian flow. However, non-Newtonian fluids often exhibit no clear demarcation as found in a Bingham fluid. Indeed there is some controversy over whether yield stress is a true material property (Scott, 1933; Barnes and Walters, 1985). Accordingly, it is common to define an "apparent yield stress" by the method of measurement. There are several approaches for doing so that are relevant to fibre suspensions:

"Maximum viscosity": This yield stress is the value of shear stress at which the instantaneous viscosity exhibits a significant decrease as shear stress is increased, as shown in Figure 1-1 (Cheng, 1986; Zhu et al., 2001; Brummer, 2005; Coussot, 2005; Nguyen et al., 2006).

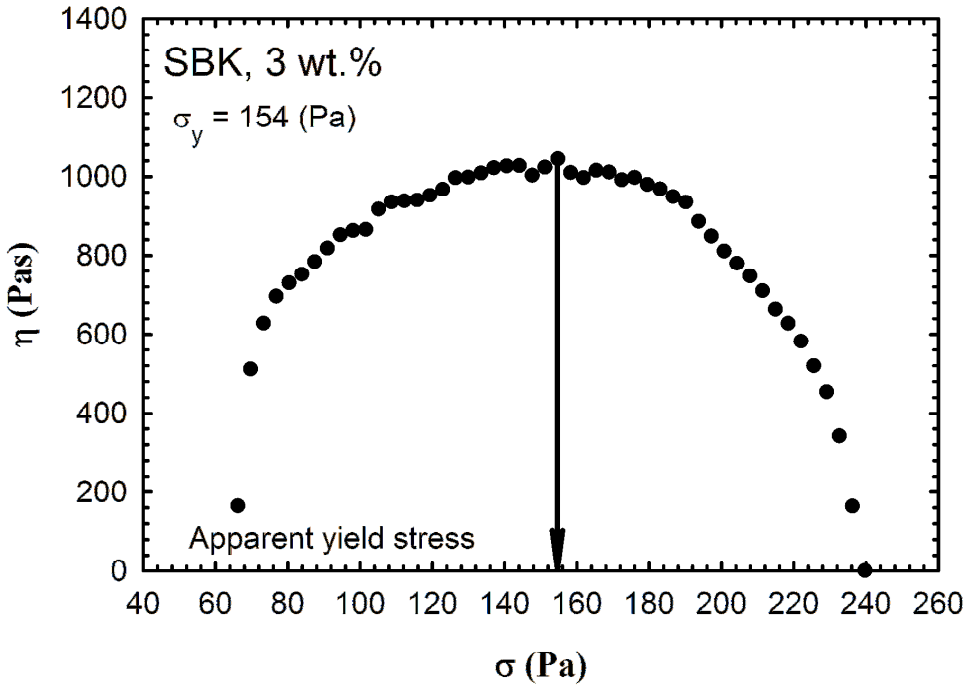

Figure 1-1: Instantaneous viscosity versus shear stress by applying a linear shear stress ramp. Apparent yield stress is defined as the shear stress at which, the instantaneous viscosity starts dropping.

"Apparent stress to initiate flow": This apparent yield stress is the intercept obtained by extrapolating shear stress to zero shear rate, usually from the linear portion of the shear stress-shear rate curve (Figure 1-2).

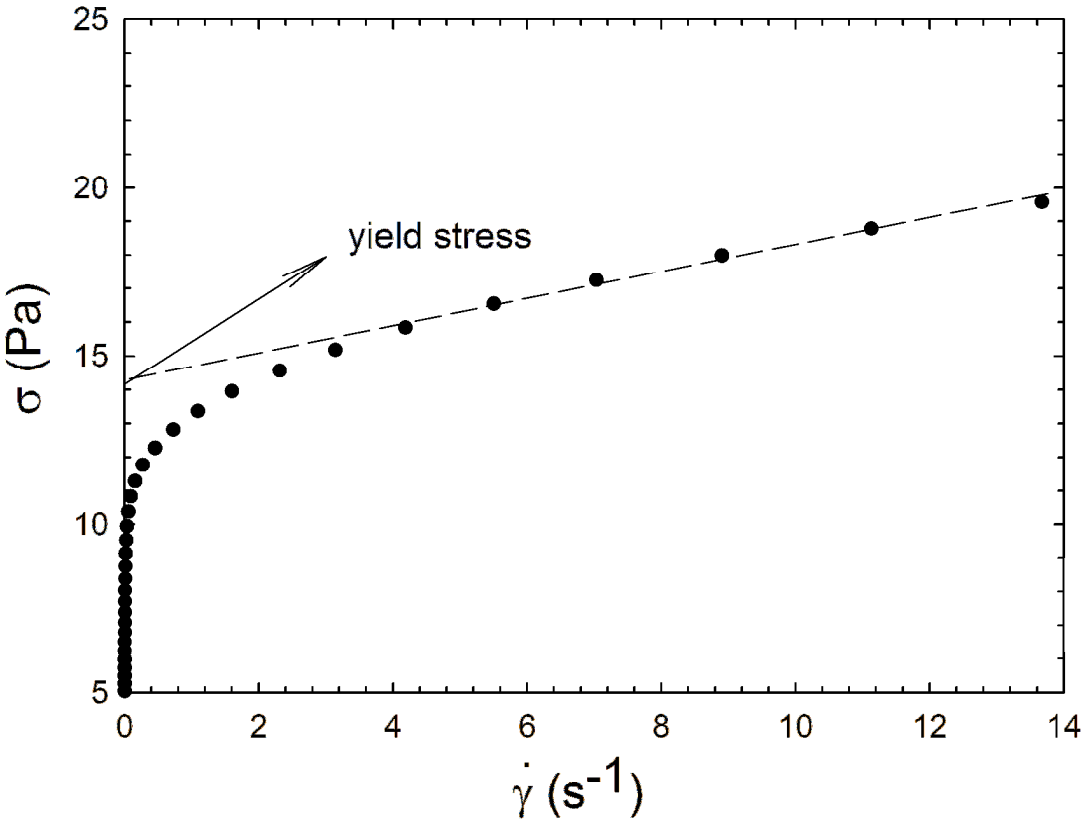

Figure 1-2: Apparent stress to initiate flow

"Ultimate Shear Strength": This yield stress is the maximum stress reached as strain is increased to initiate flow, after which the stress decreases. The maximum is called the ultimate shear strength (Figure 1-3), and used as a measure of the apparent yield stress (Thalen and Wahren, 1964; Nguyen and Boger, 1985; Cheng, 1986; Liddell and Boger, 1996). The rationale here is that this stress must be exceeded for flow to take place.

1.1.2.1. Yield Stress of Fibre Suspensions

There have been two general approaches to measuring yield stress of pulp fibre suspensions (Kerekes et al., 1985). The first, a "quasi-static" shear strength, employs conventional stress-controlled or rate-controlled rheometers or devices that rupture the fibre network at rest. The second, a "dynamic network strength", is obtained in flowing suspensions by estimating the shear stress at the surface of plugs of fibre networks at the onset of plug surface disintegration. This gives a "disruptive shear stress" (Daily and

Bugliarello, 1961; Meyer and Wahren, 1964; Mih and Parker, 1967; Duffy and Titchener, 1975; Bennington et al., 1990).

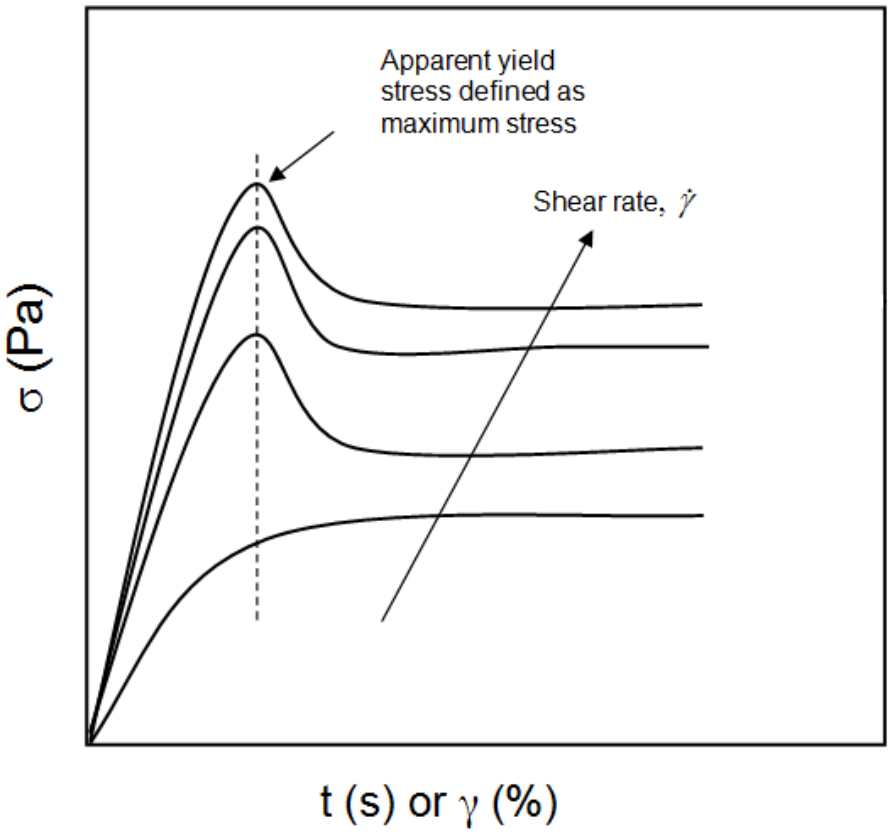

Figure 1-3: Ultimate shear strength

1.1.2.2. Modified Rheometers

Narrow-gap, smooth-walled rheometers must be modified to measure pulp suspensions for reasons described earlier. To accommodate the size of fibres and flocs, the gap size is increased. To overcome the depletion layer, rheometer walls may be roughened with asperities that are large relative to the thickness of the depletion layer. Swerin et al. (1992) and Damani et al. (1993) measured the apparent yield stress of pulp suspensions in a parallel-plate rheometer having roughened walls of 105-125 μm and a gap size of 10 mm.

Oscillatory shear is another approach to measure the apparent yield stress. The suspension is subjected to an oscillatory small-amplitude strain to measure material properties such as elastic and viscous modulus (Dealy and Wissbrun, 1990). Swerin et al. (1992) and Damani et al. (1993) used oscillatory rheometry to measure the apparent yield stress of softwood pulp suspensions from the product of the storage modulus G' and the critical strain for the onset of decrease of G' in oscillatory shear modes (Figure 1-4). In this measurement small strains are applied which may cause strain and rupture only between flocs, not within them. Swerin et al. (1992) found the critical strain to be almost independent of the mass concentration, which suggests that the strain was confined to zones between flocs.

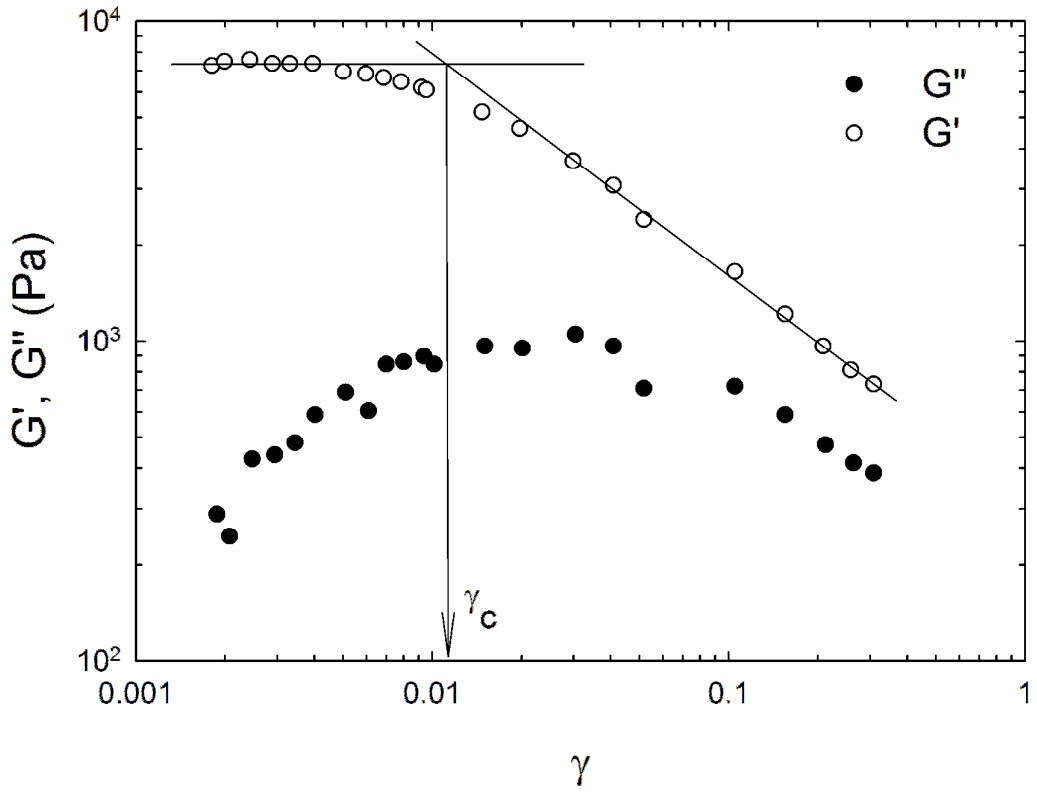

Figure 1-4: Storage modulus (○) and loss modulus (●) as a function of strain. The critical shear strain (γ_c) defines the limit of linear viscoelasticity and is used to obtain the apparent yield stress of pulp suspensions (Swerin et al., 1992).

1.1.2.3. Vaned-Geometry Devices

Another approach to overcome issues of gap size and wall slip to measure the apparent yield stress is by use of vaned rotors in housings having baffles, as shown in Figure 1-5 (Head, 1952; Duffy and Titchener, 1975; Gullichsen and Harkonen, 1981; Bennington et al., 1990). This approach moves the shear layer away from the wall surface to a circle swept out by the tips of the rotor vanes, that is, into the body of the suspension. The shear plane lies in the circle swept out by the rotor tips.

Head (1952), Thalen and Wahren (1964 a,b), Duffy and Titchener (1975), Gullichsen and Harkonen (1981), Bennington et al. (1990), Ein-Mozaffari et al. (2005) and Dalpke and Kerekes (2005) employed vaned-geometry devices to measure the apparent yield stress of pulp suspensions. They applied increasing strain on the rotor and reported the apparent yield stress as the maximum stress sustained by the suspension at the onset of continuous motion. This corresponds to the "ultimate shear strength" discussed earlier. Most of the studies were for low and medium consistency pulp suspensions, but Bennington et al. (1995) extended measurement of apparent yield stress to high consistency which contained significant amounts of air.

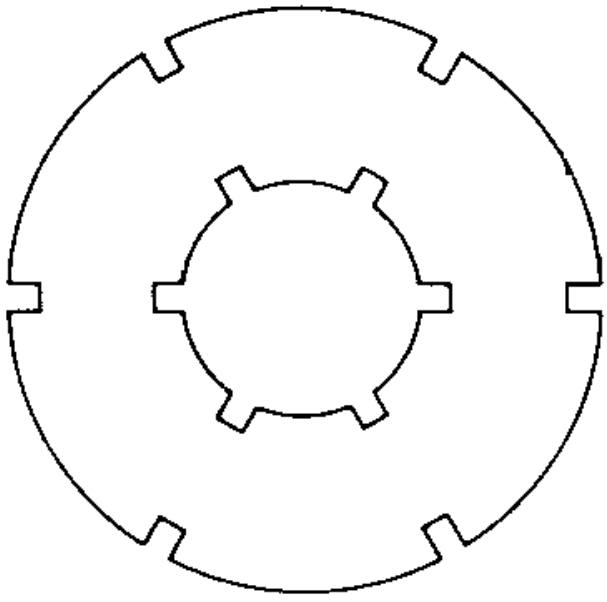

Figure 1-5: Vane in baffled housing used to study pulp fibre suspensions (Head, 1952).

1.1.2.4. Findings of Various Approaches to Measure Yield Stress

All workers found the apparent yield stress to depend on a power of the consistency. At low consistency, the power dependence is for the difference between the consistency being tested and a threshold consistency at which networks form. The premise here is that consistencies below the threshold do not contribute to mechanical strength. Thalen and Wahren (1964a) defined the threshold by a sediment concentration, C_s, as shown in Eq. (1-3) below. Later, Martinez et al. (2001) defined it by the gel crowding number N_G as shown in Eq. (1-4).

$$\sigma_y = a\left(C_m - C_s\right)^b \tag{1-3}$$

or

$$\sigma_y = a\left(N - N_G\right)^b \qquad \text{where} \qquad N_G = 16 \tag{1-4}$$

These equations apply for low consistency pulp suspensions, typically in the range in which paper is formed, typically C_m=0.5 to 1%. However, most processing of fibre suspensions takes place at larger consistencies, typically are 3% or more. In this range, the apparent yield stress equations can be simplified to:

$$\sigma_y = aC_m^{\ b} \tag{1-5}$$

where C_m is consistency in % and a has units of Pa.

Values for a and b measured in earlier studies were summarized by Kerekes et al. (1985). The studies examined apparent yield strength in various ways, including shear strength of pulp plug surfaces in flowing suspensions, and defined these strengths in differing ways. In addition, many other factors differed among the studies, such as wood species and pulping method. Not surprisingly, results varied considerably. Values of a were in the range $1.8 < a < 24.5$ (Pa) and b in the range $1.69 < b < 3.02$. Many key variables contributing to these differences were not measured or reported. For example, Dalpke and Kerekes (2005) found fibre length to be very important, with longer fibres causing larger apparent yield stress.

At consistencies C_m>8%, fibre suspensions generally contain substantial air. Bennington et al. (1995) measured the apparent yield stress in ranges of consistency having up to 90% air content by volume, obtaining the following expression for yield stress:

$$\sigma_y = 7.7\times10^5 C_m^{\,3.2}\left(1-\varphi_g\right)^{3.4} A^{0.6} \tag{1-6}$$

$$0.004 \le C_m \le 0.5 \quad \text{and} \quad 0 \le \varphi_g \le 0.9$$

where φ_g is the fractional gas content and A is the fibre axis ratio with the pre-factor numerical constant in Pa. This equation is valid for both mechanical and chemical pulps. At high gas contents, it was found that the apparent yield stress could be well described by volumetric fibre concentration C_v (Bennington et al, 1990):

$$\sigma_y = aC_v^b \tag{1-7}$$

All the measurements of apparent yield stress have considerable scatter, often as much as 100%. To determine an average value, Bennington et al. (1990) defined a relative apparent yield stress to be that measured in a single test divided by the average apparent yield stress for all tests performed under the same experimental conditions. Using the relative apparent yield stress, experimental data were compared on a normalized basis and approximated by a Gaussian distribution. The coefficient of variation for the apparent yield stress of pulp suspensions was found to be 20% and for synthetic fibres to be 45%.

Scatter in the data is due to many factors, including how apparent yield stress is defined and the method of measurement. For example, apparent yield stresses obtained by quasi-static methods were all larger than those measured using dynamic methods. Other difference are illustrated in the methods and definitions employed in studies of Gullichsen and Harkonen (1981), Bennington et al. (1990), Swerin et al. (1992), Wikström et al. (1998), and Dalpke and Kerekes (2005). An example is given in Table 1-1 for apparent yield stress of a bleached softwood kraft pulp. The values range from 19.3 to 350 Pa for a consistency of 3%, and from 60 to 1220 Pa for a consistency of 6%.

Table 1-1: Apparent yield stress of SBK suspension obtained using different methods

Reference	Measurement method	σ_y (Pa) C_m=3%	σ_y (Pa) C_m=6%
Bennington et al. (1990)	Baffled concentric-cylinder, Ultimate shear strength	176	1220
Swerin et al. (1993)	Couette cell, Oscillatory experiments	19.3	117
Damani et al. (1993)	Parallel plate geometry, Oscillatory experiments	------	60
Wikström et al. (1998)	Baffled concentric-cylinder, Ultimate shear strength	131	1100
Ein-Mozaffari et al. (2005)	Concentric-cylinder, Ultimate shear strength	350	------
Dalpke and Kerekes (2005)	Vane in large cup geometry, Ultimate shear strength	130	------

1.1.2.5. Modeling Yield Stress

Several workers developed mathematical models of fibre networks to predict yield stress. Bennington et al. (1990) derived an equation based on network theory that included fibre aspect ratio and Young's modulus as follows:

$$\sigma_y = cEA^2 C_v^{\ 3} \tag{1-8}$$

where A is the fibre aspect ratio, E is the fibre's Young's modulus, c is a constant and C_v is the volume concentration of the pulp suspension. All fibres were assumed to be rod-like with a common area moment of inertia. In later work, Wikström et al. (1998) considered differing area moments of inertia for pulp fibres and modified Eq. (1-8) by using the fibre stiffness (the product of elastic modulus and area moment of inertia). This modification led to the following equation proposed for the apparent yield stress values:

$$\sigma_y = cEA^2 \left[1 - \frac{d^4}{D^4}\right] C_v^{\ 3} \tag{1-9}$$

where d and D are the inner and outer diameters of the fibres.

1.1.3. Shear viscosity

1.1.3.1. Suspensions of Synthetic Fibres

Relatively few studies have been devoted to measuring the viscosity of pulp suspensions, although there have been a substantial number for the simpler case of synthetic (plastic, glass) fibres of uniform size and shape. Although this study is focused on pulp fibres, there are sufficient similarities to synthetic fibres to warrant a brief discussion here.

References to many of the major studies of synthetic fibres can be found in review papers and literature surveys in papers on the subject, for example Ganani and Powell (1985), Bennington and Kerekes (1996), Petrie (1999), Kerekes (2006), and Eberle et al. (2008). Some studies are particularly relevant to pulp fibre suspensions. Nawab and Mason (1958) measured the viscosity of dilute suspensions of thread-like rayon fibres in castor oil. They employed a bob and cup viscometer equipped with a microscope to check for wall slippage. Fibre aspect ratio had a strong effect on suspension viscosity and its shear dependence. In other work, Blakeney (1966) examined the effect of fibre concentration on the relative viscosity of suspensions of straight, rigid nylon fibres with aspect ratio of about 20. He found that at C_v>0.0042, viscosity increased dramatically with concentration. Interestingly, this condition is $N \approx 1$.

Ziegel (1970) measured the viscosity of suspensions of glass rods, glass plates and asbestos fibres in high viscosity polymer fluids and compared them with those of spherical particles. Horie and Pinder (1979) measured the viscosity of suspension of nylon fibres over a wide range of consistency and shear rates; they found thixotropy and that thickness of the shearing layer in the viscometer to depend on time of shearing.

Kitano and Kataoka (1981) employed a cone-plate rheometer to study the steady shear flow properties of suspensions of vinylon fibres in silicone oil up to C_m=7%. Ganani and Powell (1986) studied the rheological behaviour of monodisperse glass fibres both in Newtonian and non-Newtonian suspending media at fibre volume fractions of 0.02, 0.05 and 0.08. Milliken et al. (1989) employed falling-ball rheometry to measure viscosity of monodisperse randomly oriented rods in a Newtonian fluid. Suspensions

exhibited Newtonian behaviour at $C_v < 0.125$ and a sharp transition at $C_v > 0.125$ at which viscosity depended on the third power of concentration. This corresponds to N=33.

Petrich et al. (2000) studied the relationship between the fibre orientation distribution, fibre aspect ratio, and the rheology of fibre suspensions. They measured both specific viscosity and normal stress differences. Chaouche and Koch (2001) examined the effect of shear stress and fibre concentration on the shear-thinning behaviour of rigid fibre suspensions. They showed that fibre bending and a non-Newtonian suspending liquid played a major role in shear-thinning behaviour of suspension at high shear rates. Switzer and Klingenberg (2003) modelled the viscosity of fibre suspensions. They showed viscosity to be strongly influenced by fibre equilibrium shape, inter-fibre friction, and fibre stiffness.

1.1.3.2. Shear Viscosity of Pulp Suspensions

Steenberg and Johansson (1958) studied flow behaviour of suspensions of unbleached sulphite pulp in a custom-made parallel-plate viscometer. They measured shear stress-shear rate relationships over a wide range of flow velocity and consistencies up to 2.5%. They observed two transition points: a maximum at low shear rates and a minimum at high shear rates. These correspond to similar observations in pipe flow (discussed later). The transition points shifted towards higher shear rates as the gap clearance decreased. They measured viscosities at shear rates above the second transition point where pulp was considered to be a fully sheared medium. At these high shear rates, they found Newtonian behaviour up to about $N \approx 100$, with viscosity slightly larger than water. This work showed that various flow regimes may exist in rheometers.

In another early study, Guthrie (1959) measured the apparent viscosities of pulp suspensions at C_m<2% to calculate Reynolds numbers in a pipe. He found viscosity increased dramatically with consistency above a critical value of C_m=1.4%. Below this, pulp suspension viscosity showed no significant dependence on the fibre length over the length range of 0.2-0.67 mm. The likely explanation for this observation is that consistency 1.4% at fibre length 0.67 mm give about $N = 20$, which is near the gel crowding number. Below this the suspension behaves as dilute and length would not be

expected to be important. An abrupt change in suspension behaviour at this point is to be expected.

Chase et al. (1989) surveyed the variation of torque versus rotational rate of hardwood and softwood pulp suspensions to study the effects of fibre concentration and freeness on the viscosity parameter. For both suspensions, viscosities increased linearly with consistency. The viscosity of hardwoods decreased linearly with freeness, while the viscosity of softwoods increased initially and then decreased with a decrease in freeness. They also concluded that pulp behaves as a Bingham plastic fluid on the basis that exhibits an apparent yield stress.

Chen et al. (2003) studied the flow behaviour of pulp suspensions in a modified parallel-plate rheometer. The lower plate was replaced with a Petri dish to prevent the suspension overflow, but no modification was made to minimize wall slippage. Softwood and hardwood bleached kraft pulps were mixed in different ratios, but the total mass concentration was kept at 0.05%, giving a very dilute suspension i.e. $N \approx 5$. They measured shear stress as a function of shear rate and performed stress relaxation experiments. Using a CCD camera, they identified three flow regimes as illustrated in Figure 1-6. In the first regime, Newtonian flow was observed at low shear rates. In the second regime, they observed unstable flow, with jumps in the shear stress dependent on shear rate. The stress jumps were attributed to the flocculation of pulp fibre suspensions. The third region was found to be a dynamic equilibrium zone which showed Newtonian behaviour at high shear rates.

These studies clearly show that differing flow regimes may exist in rheometers caused by differences in fibre orientation, a depletion layer, and the onset of shear over the entire gap as opposed to a depletion layer near the wall. No consistent picture has been established of when these regimes exist.

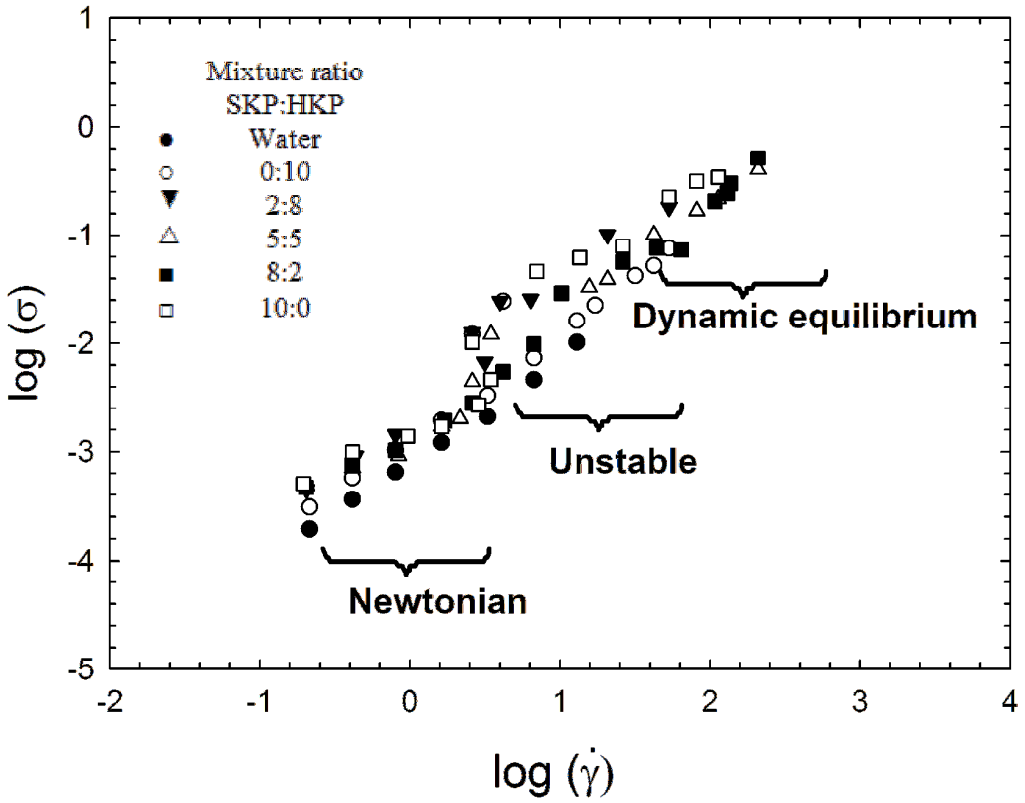

Figure 1-6: Shear stress versus shear rate for 0.05% mixed pulp fibre suspensions. Three different regimes were observed for pulp suspensions (Chen et al., 2003).

To avoid wall effects and ensure flow throughout the vessel, Bennington and Kerekes (1996) measured viscosity by an indirect approach. They created turbulence in a large-gap device and obtained viscosity from the relationship between power dissipation and microscale turbulence. They noted, but did not measure, the dependence of viscosity on shear rate. They found viscosities to depend upon the third power of consistency for fibre mass consistencies over 1% as shown below:

$$\eta = 1.5\times10^{-3} C_m^{\,3.1} \tag{1-10}$$

where C_m is mass consistency and η is in Pas. Interestingly, the consistency dependence of the pulp viscosity is similar to that of suspensions of rod-like particles in Newtonian fluids (Miliken et al., 1989; Powell et al., 2001).

Another approach to characterizing the viscosity of a pulp suspension is by considering flocs rather than fibres as the suspended solid, specifically flocs to be solid

spheres. This is possible in some cases of low velocity flows. Van de Ven (2006) used this approach to correlate spouting velocity to fibres mass in spouted beds.

Other recent work has addressed the question of viscosity of pulp suspensions in narrow channels much smaller than a fibre length. In this case, continuum conditions clearly do not exist and therefore the suspension cannot be considered a fluid. Consequently, a meaningful viscosity cannot be measured. For practical applications in process equipment, Roux et al. (2001) introduced the concept of a "shear factor", a parameter to be multiplied by velocity divided by a gap size.

1.1.3.3. Extensional Viscosity of Fibre Suspensions

Extensional (elongational) viscosity is the resistance of a fluid element to stretching in flow. There are few studies of extensional viscosity of pulp fibre suspensions although there have been some for synthetic fibres. Mewis and Metzner (1974) measured apparent extensional viscosity of glass fibre suspensions in the range $N>60$. They found the extensional viscosity to be one to two orders of magnitude greater than that of the suspending fluid. Ooi and Sridhar (2004) employed filament stretching technique to study extensional flow of fibre suspensions in Newtonian and non-Newtonian fluids.

Studies on extensional flow of pulp fibre suspensions have largely been confined to measuring stretching and rupture of individual flocs. This work was stimulated by early findings of Kao and Mason (1975) which showed that flocs ruptured primarily in tension rather than shear, suggesting that extensional flows were likely to be more effective than shear flow in dispersing flocs in papermaking.

Kerekes (1983a) employed a high speed camera to study the behaviour of 0.5% long-fibred pulp suspensions in entry flow into constrictions. These strong flocs were found to stretch by a ratio up to 5:1 before rupture. The necessary degree of contraction in the sharp-edge constriction to create this elongational strain was such that flocs came into contact with constriction edges, which introduced shear on the floc. In other work, Li et al. (1995a) examined pulp suspensions in extensional flows by nuclear magnetic resonance imaging technique. They measured the axial velocity profiles for hardwood

kraft pulps of 0.5% flowing through a 1.7:1 tubular contraction. James et al. (2003) employed a novel extensional flow apparatus to apply constant extensional strain rates in fibre flocs. They examined softwood kraft pulp at C_m=0.01% ($N \cong 1$) and found a critical extensional strain rate of ~ 3 s^{-1} required to rupture these weak flocs. More recently, Yan et al. (2006) designed a flow device to simulate the extensional flow in paper-machine headboxes. They observed that about 20% of the flocs in a 2:1 contraction ruptured in this extensional flow.

1.1.4. Viscoelasticity

Pulp fibre suspensions exhibit elastic as well as viscous behaviour and therefore are considered viscoelastic. As in the case of measuring viscosity, measuring viscoelasticity in fibre suspensions is not simple. Here too some relevant work was carried out on suspensions of synthetic fibres.

One approach to measurement has been by normal stress differences. Nawab and Mason (1958) were the first to observe viscoelasticity in concentrated fibre suspensions at N>56 in the form of the Weissenberg or rod-climbing effect. Kitano and Kataoka (1981) employed a cone-plate rheometer to study the steady shear flow properties of suspensions composed of vinylon in silicone oil up to C_m=7%. First normal-stress differences increased with fibre concentration, aspect ratio, and shear rate. Petrich et al. (2000) measured the first normal stress difference of a glass fibre suspension using a parallel-plate rheometer. They found that, for fibre suspensions, the first normal stress difference is directly proportional to the shear rate. It is of interest to note that a similar dependence was found between first normal stress difference and shear rate in dilute suspensions of rigid, axisymmetric Brownian particles in a Newtonian fluid (Brenner, 1974).

Another approach to measuring viscoelasticity is by oscillatory shear. Here the Boltzmann superposition principle is employed whereby a relaxation spectrum determined by a single experiment for small amplitude oscillatory shear, and this is used to determine the response in any other case (Dealy and Wissbrun, 1990). This approach is only valid when the deformation is either small or very slow.

Using oscillatory strain in a parallel-plate rheometer, Swerin et al. (1992) measured viscoelastic properties of pulp suspensions in the consistency range of 3 to 8% in terms of storage and loss moduli. Storage and loss moduli were found to increase with fibre mass concentration and to be independent of the applied frequency. A power-law equation was proposed to predict the storage modulus as a function of fibre mass concentration.

Damani et al. (1993) employed the same approach and found the elastic modulus to be independent of the applied frequency. This is consistent with the results of Swerin et al. (1992). The level of strain was found to have a significant effect on the elastic modulus, especially at low fibre concentrations.

Later, Swerin (1998) examined the viscoelasticity of two fibre suspensions with different fibre sizes (0.9 and 2.8 mm) up to C_m=1% in the presence of flocculants. All measurements were performed in the oscillatory mode using a roughened cup-and-bob geometry to minimize wall slippage. By measuring the variation of elastic and viscous modulus versus straining frequency, with and without flocculants, it was shown that the effect of flocculants on the modulus was very large because they caused significant flocculation. The storage modulus was found to increase with increasing frequency, while the viscous modulus was almost independent of the frequency.

Stickel et al. (2009) measured the viscoelasticity of bio-mass slurries having average fibre lengths of 0.1 mm and aspect ratio of 1 to 20 using both parallel-plate and vaned geometries. They found that elastic and viscous moduli depended slightly on frequency. The elastic modulus was larger than the viscous modulus by about an order of magnitude.

A limitation of these oscillatory methods is the use of small strains. This is likely to produce strain and rupture between flocs rather than within them. In many processes, flocs must be dispersed as well, and therefore this rheological measurement may have limited value.

1.1.5. Fluidization of pulp suspensions

Fluidization describes a state of pulp suspensions in which elements of the suspension move relative to one another such that the suspension adopts properties of a fluid. An important property is pressure energy and the ability to recover this from kinetic energy (obey the Bernoulli equation). For example, this feature permits use of centrifugal pumps, even for medium consistency suspensions, in place of displacement pumps to transport the suspension.

To attain fluidization, apparent yield stress must be exceeded throughout the suspension. The stresses necessary for this pulp suspension can generally only be attained in the turbulent state. For this reason, the terms fluidization and turbulence in pulp suspensions are often used interchangeably.

Gullichsen and Harkonen (1981) pioneered the use of fluidization for pumping. They determined the conditions necessary for fluidization in a rotary device. Based on their findings, they developed a centrifugal pump capable of handling pulp suspension up to 15% consistency. In later work a number of workers studied fluidization in more detail (Bennington et al., 1991; Hietaniemi and Gullichsen, 1996; Bennington and Kerekes, 1996). It was found that fluidization could occur at two levels, floc level and fibre level, because of their large difference in the apparent yield stress (Kerekes, 1983b; Bennington et al., 1991; Hietaniemi and Gullichsen, 1996). Floc level fluidization was sufficient for pumping, but fibre-level fluidization was necessary in some processes, for example micro-scale mixing of fast-reacting chemicals with pulp. Both scales are commonly found in mixing vessels as well as in other process equipment, often along with zones having no relative velocity at all (dead spots).

Fluidization has been difficult to quantify because methods to measure velocity in concentrated fibre suspensions are lacking. Accordingly, indirect methods have been employed. One method is by the torque necessary to produce turbulent motion in a vessel of prescribed dimensions (Gullichsen and Harkonen, 1981). Another is method by the power dissipation per unit volume, ε_F, necessary for the onset of fluidization (Wahren, 1980). An issue in this characterization is the presence of large gradients of power

dissipation in vessels, making power dissipation equipment-specific. Bennington et al. (1991) addressed this by determining power dissipation as a function of equipment size, as shown by Eq. (1-11) below:

$$\varepsilon_f = 4.5\times10^4 C_m^{2.5}\left(\frac{D_T}{D_R}\right)^{-2.3} \tag{1-11}$$

where $1\% < C_m < 12\%$, D_T is the outer housing diameter, D_R is the rotor diameter with ε_f the power dissipation/unit volume (w/m^3).

Bennington (1991) observed fibre-level fluidization at the rotor vane tips and largely floc-level fluidization in zones away from the rotor. The power dissipation at the impeller tip was obtained by extrapolating Eq. (1-11) to zero gap size ($D = D_T$). This showed that power dissipation for fibre-level fluidization is about an order of magnitude greater than that for floc-level fluidization in the vessel.

Other recent studies have extended knowledge of pulp suspension fluidization (Hietaniemi and Gullichsen, 1996; Chen and Chen, 1997; Wikstrom et al., 2002). The latter workers measured the onset of fluidization using a vaned narrow-gap viscometer, defining the onset of fluidization as the condition at which the Power Number becomes constant with Reynolds number (based on rotational speed) as is common for turbulent flow in mixing vessels. They developed a correlation which gave values similar to those of Gullichsen and Harkonen (1981), but smaller than those of Bennington et al. (1996). This suggests that floc-level rather than fibre-level fluidization was measured.

Although fluidization generally occurs in a turbulent regime, fluid-like behaviour at a floc level can be attained under some non-turbulent conditions. One example is the flow induced in a rotary device at slow rotational speeds just above the apparent yield stress (Bennington et al., 1991). Another example was found in spouted beds (van de Ven, 2006).

1.1.6. Applications in pipe flow

In concluding this review chapter, it is useful to illustrate how the rheology described above affects one of the most important flows—pipe flow. A key early study by Robertson and Mason (1957), followed by numerous other studies cited in the review papers in the Introduction, identified three regimes of flow behaviour which take place with increasing velocity. These regimes give an "S" shaped friction loss curve as shown in Figure 1-7 where pipe friction loss, ΔH (Pa), has been plotted against pipe flow velocity, V (m/s).

At low velocity, a "plug flow" exists in which the suspension scrapes along the wall, with some rolling of fibres at the wall (Region 1). As velocity increases, a clear water annulus develops between the pulp plug and pipe wall (starting at peak of Region 1). Shear is concentrated in this annulus. With increasing velocity, the size of this annulus increases in greater proportion than the velocity increase, thereby causing a decrease in wall shear and consequently a decrease in friction loss with increasing velocity (Region 2 between peak and minimum). As velocity increases further, the annulus turns turbulent, pulling and mixing fibres in the annulus (Region 2, minimum). This starts the "mixed flow regime". As velocity increases, the size of the turbulent annulus increases and the plug core decreases. At a point in this mixed regime, the friction loss of the suspension becomes less than that of the water flowing alone at the same rate, i.e., the flow exhibits "drag reduction". As velocity increases further in Region 3, eventually a fully "turbulent regime" is attained over the whole diameter.

The above regimes occur in the low consistency range. Clearly, the range of flow behaviour is very broad, extending from mechanical friction at the wall to turbulent drag reduction. In the case of drag reduction, pulp fibre suspensions are one of the earliest and most consistent solid-liquid suspensions in which this phenomenon has been observed. The phenomenon is also found in suspensions of synthetic fibres (Kerekes and Douglas, 1972).

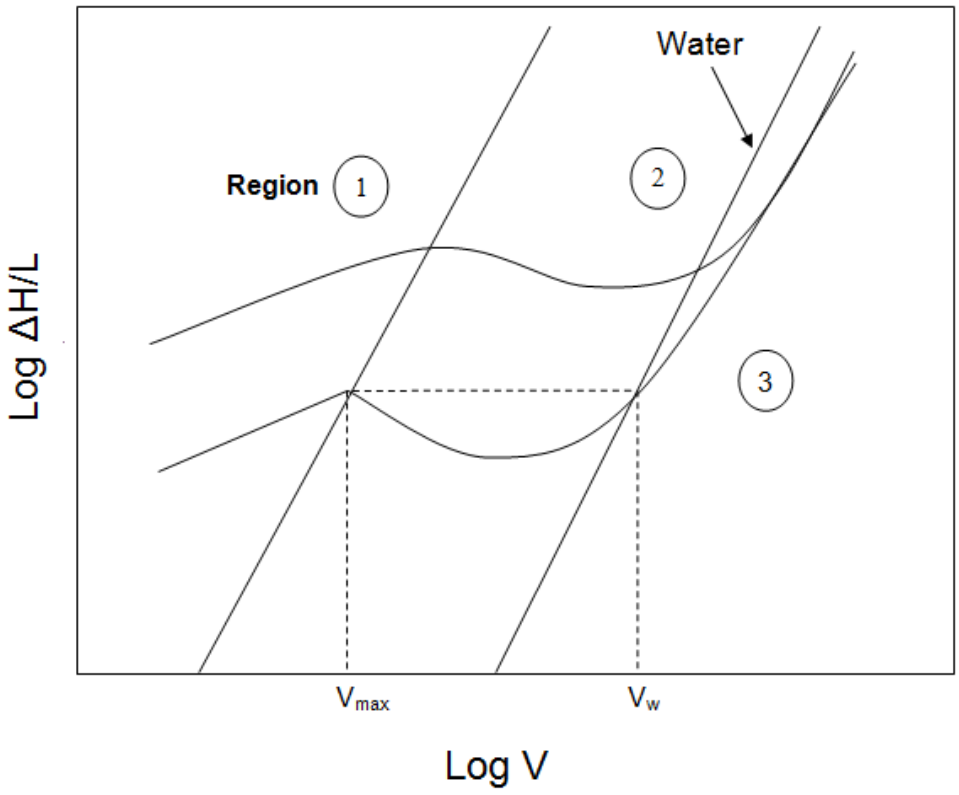

Figure 1-7: Friction loss curve for chemical pulp.

At medium consistency, suspensions are virtually always in plug flow. Furthermore, in this range, the suspension is compressible because of its high air content, and therefore pressure, as well as pressure difference, is important for flow. A larger pressure causes the suspension to compress and thereby exert greater mechanical force on the wall, which leads to greater friction loss (Longdill et al., 1988).

Attempts have been made over the years to model friction loss of pulp suspensions in pipe flow, for example Daily and Bugliarello (1961), Luthi (1987) and Pettersson (2004), but these have found limited use. Reasons for this are many, as discussed in this paper and by Duffy (2003). Accordingly, predictions of friction loss in pipe flow in the pulp and paper industry are commonly made by empirical procedures (Duffy, 1978) that have been adopted as industry standard methods (Tappi Press TIS 0410-12).

1.1.7. Summary and conclusions

This chapter has described the various methods and approaches used over the years to measure key rheological properties of pulp suspensions. Previous studies on pulp suspension rheology are generally limited to the apparent yield stress measurements, viscoelasticity and pipe flow experiments.

Apparent yield stress has been measured and reported for pulp fibre suspensions using different experimental procedures and definitions. The reported values vary over a wide range due to dissimilar definitions, different experimental approaches, and perhaps dissimilar structural state of the suspensions used in various studies. Therefore, it is important to study the yielding behaviour of these suspensions in a more detailed manner to eliminate factors which may lead to dissimilar apparent yield stress values.

This literature review shows that there is little known about the flow behaviour of pulp suspensions beyond the apparent yield stress at industrially relevant concentrations. This is due to the difficulties associated with the experimental testing of these suspensions. On the other hand, the lack of sufficient rheological experimental data has led to the lack of reliable constitutive rheological models which are required to design processing machines in the pulp industry.

Pulp suspensions are composed of fibre microstructures which evolve and/or rupture with time and under influence of shear. This in turn makes pulp suspension a thixotropic material with a time dependant rheological behaviour. Thixotropy and time dependant rheology of pulp fibre suspensions should be examined in detail as there is no study concerning these topics in the open literature.

1.2. Thesis Objectives

The overall objective of this research work was to first determine an appropriate and reliable experimental approach to measure the rheological properties of pulp fibre suspensions. Next, to implement such technique to improve our understanding on the flow properties (rheology) of dilute and medium consistency pulp suspensions (0.5-6 wt.%) to open opportunities for applying these concepts in the pulp preparation stages in the paper industry in the future. The particular objectives of this thesis can be summarized as follows:

1. To determine a reliable experimental approach to study the rheology of pulp fibre suspensions that yields consistent results (addressed in Chapters 2-4).

2. To propose a reliable technique to measure the apparent yield stress of commercial pulp fibre suspensions that can particularly be incorporated in the designing of mixing processes (addressed in Chapter 2).

3. To study the post yield flow behavior of various types of pulp fibre suspensions and propose a rheological model to predict the flow behavior at steady-state (addressed in Chapter 3).

4. To investigate effects such as thixotropy and shear banding in pulp fibre suspensions, effects which have not been studied for pulp suspensions in the past (addressed in Chapter 4).

1.3. Thesis Organization

The present chapter of the thesis discusses the basic motivation of the present work. It includes a historical overview of pulp fibre suspension rheology, a brief introduction to the terms and definitions related to pulp and paper science, and a brief introduction into inter fibre forces and consistency ranges. In addition, this chapter includes a review on the different experimental methods previously used for

measurement of pulp fibre suspension rheology and therewith identified parameters influencing the rheology of such materials. This chapter is based on a review paper that has been published (Derakhshandeh, B., Kerekes, R.J., Hatzikiriakos, S.G., Bennington, C.P.J., 2011. Rheology of pulp fibre suspensions-A critical review. Chemical Engineering Science 66(15): 3460-3470.

Chapter 2 describes a new approach to measure apparent yield stress of pulp fibre suspensions using a velocity profile determination technique coupled with a rheometer. Unlike previous approaches, which assumed the nature of velocity profiles in the rheometers, this approach measures the velocity profiles directly and links them to the shear stress evolution in the suspension, thereby measuring the apparent yield stress. The experimental techniques used in this research work and the pulp suspension preparation procedures are described in this chapter in detail. This chapter is based on a journal paper that has already been published (Derakhshandeh, B., Hatzikiriakos, S.G., Bennington, C.P.J., 2010. The apparent yield stress of pulp fibre suspensions. Journal of Rheology 54(5): 1137-1154).

Chapter 3 studies the behaviour of pulp fibre suspensions beyond the apparent yield stress. Conventional rheometry and a velocity profile determination technique have been used and the obtained results are compared. Models have been proposed to describe the flow behaviour using the local velocity profiles within the rheometer. Effects of lignin content and pH on the rheology of pulp fibre suspensions have also been discussed. This chapter is based on a journal paper that has already been published (Derakhshandeh, B., Hatzikiriakos, S.G., Bennington, C.P.J., 2010. Rheology of pulp fibre suspensions using ultrasonic Doppler velocimetry. Rheologica Acta 49(11-12): 1127-1140).

Chapter 4 studies thixotropy and transient behaviour of pulp fibre suspensions. A velocity profile determination technique is used to measure velocity profiles within the suspension at steady-state and transient flow conditions. The effects of rest time and shear history are studied and mechanisms of structure build-up and breakdown are discussed. Moreover, the possibility of shear-banding instability in concentrated pulp suspensions is examined and models have been proposed to describe the flow of concentrated pulp fibre suspensions. This chapter is based on a manuscript that has been

submitted for publication (Derakhshandeh, B., Vlassopoulos, D., Hatzikiriakos, S.G., 2011. Thixotropy, yielding and ultrasonic Doppler velocimetry in pulp fibre suspensions. Rheologica Acta).

Finally, the conclusions, contributions to knowledge and recommendations for future research are summarized in chapter 5. A general summary of the most significant findings from this work is also presented.

2. The Apparent Yield Stress of Pulp Fibre Suspensions[2]

2.1. Introduction

Pulp fibre suspensions consist of fibre networks having considerable strength. Before they begin to flow, a minimum shear stress must be applied to disrupt the fibre networks referred to as the yield stress. We will refer to this quantity as apparent yield stress since different methods may result in different values. Despite the controversial concept of the yield stress as a true material property (Scott, 1933; Barnes and Walters, 1985) the apparent yield stress is considered as one of the most important rheological properties of pulp fibre suspensions in designing process equipment for the pulp and paper industry.

As discussed in chapter 1, several methods and definitions have been proposed/developed to predict and measure the apparent yield stress both directly and indirectly (Pryce-Jones, 1952; Head and Durst, 1957; Thalen and Wahren, 1964; Van den Tempel, 1971; Papenhuijzen, 1972; Duffy and Titchener, 1975; Nguyen and Boger, 1992; Liddell, 1996). These methods make use of various pieces of equipment such as a concentric cylinder shear tester (Gullichsen and Harkonen, 1981), a rotary shear tester (Bennington et al., 1990) and a reservoir-type parallel plate geometry (Damanai et al., 1993; Swerin et al., 1993; Wikström et al., 1998). In addition to experimental studies, models of the form $\sigma_y = aC_m^{\ b}$ have been proposed to represent the apparent yield stress as a function of mass concentration (Meyer et al., 1964; Kerekes et al., 1985; Bennington et al., 1990; Bennington et al., 1995).

Pulp rheological characterization is no easy task due to the unique and complex behaviour of wood fibre suspensions described in chapter 1. Pulp suspensions consist of roughly cylindrical fibres of average length ranging from 1 mm to 3 mm having aspect ratios of 40 to 100. Fibres entangle mechanically to form regions of higher fibre mass

[2] A version of this chapter has been published. Derakhshandeh, B., Hatzikiriakos, S.G., Bennington, C.P.J., 2010. The apparent yield stress of pulp fibre suspensions. Journal of Rheology 54(5): 1137-1154.

concentrations of average size of 2 cm to 3 cm referred to as fibre flocs (Mason, 1950; Stockie, 1997).

Increasing the fibre concentration, the number of fibre-fibre contacts increases which results into formation of network structures throughout the suspension (Kerekes and Schell, 1992). Presence of individual fibres, fibre flocs and networks makes pulp fibre suspensions heterogeneous and multiphase systems. This is against the basic homogeneity assumption which is made to predict simple fluid flow characteristics. The presence of millimetre-sized fibres and centimetre-sized fibre flocs in a heterogeneous suspension makes it complicated to obtain reproducible rheological data. Pulp suspensions contain a dispersed phase with dimensions comparable to the characteristic dimensions of the geometry of the measuring apparatus in rheological devices and therefore fibre rotation is limited.

Another common behaviour of pulp fibre suspensions is their orientation around the measuring elements and migration of fibres away from solid boundaries which leads to formation of a depletion layer that complicates further rheological measurements (Nguyen and Boger, 1992; Barnes, 1995; Swerin, 1998; Wikström, 1998; Archer, 2005).

Due to these complications and those discussed in chapter 1, the selection of an appropriate measuring device to provide large measurement gaps (compared with the dimensions of the fibre domains to eliminate fibre jamming) as well as decrease the possibility of apparent slip at solid boundaries is required to obtain reliable data.

Various methods have been proposed in the literature to interpret the rheological data which are affected by wall slip, particularly for foams, emulsions and polymers (Mooney, 1931; Jastrzebski, 1967; Yoshimura and Prud'homme, 1988; Hatzikiriakos and Dealy, 1991). These corrections cannot be applied to raw rheological data obtained from pulp suspensions. For instance, Yoshimura and Prud'homme (1988) considered the wall slip to be a function of wall shear stress and proposed a method to correct the rheological data by examining the dependency of the rheological data on the gap size in a parallel-plate geometry. Decreasing the gap size in the case of pulp suspensions squeezes water out, and, as a result, the fibre mass concentration increases. This leads to imprecise rheological data.

Another approach to minimize the effect of slip is to make use of complex geometries such as the vane geometry (Nguyen and Boger, (1983, 1985); Barnes et al., 1990; Barnes et al., 2001; Cullen et al., 2003). Vane geometry is basically a small shaft with a small number of thin blades (usually 2-8) arranged at equal angles. Application of the vane geometry requires that a number of assumptions be made. First, it is assumed that the fluid in between the blades rotates along with them so that it generates a cylindrical surface with a radius close to that of the vane. It has been shown that this assumption is valid for highly shear-thinning fluids with power-law indices less than 0.5. In this case little or no shearing occurs in between the blades of the vane. Therefore, the fluid is sheared at the virtual cylinder prescribed by the tips of the vane blades (Barnes and Carnali, 1990). Second, the shear stress distribution is assumed to be uniform at the outer virtual cylindrical surface described by the outer edge of the vane and finally, the fluid which is trapped between the blades of the vane is assumed to act as a rigid body without any secondary flow.

These assumptions are valid in vanes with four or more blades (Nguyen and Boger, 1983). Despite these assumptions, the vane geometry has many advantages over the other geometries. Particularly, when used to study complex systems such as pulp suspensions. In a vane geometry, the fluid is sheared within itself. Therefore, the wall slippage is minimized (Barnes and Nguyen, 2001). In addition to the decrease of the wall slip, insertion of the vane generates the least amount of disturbances to the structure of the sample although it can be significant, particularly in the case of thixotropic fluids (Nguyen and Boger, 1983).

Most commercial rheometers utilize narrow gaps which impose practical restrictions to sample rheological behaviour. These include fibre jamming, tumbling, orientation and the formation of depletion layers. Vane geometry with large cups provides wide gaps which enable the investigation of fluids containing large particles or fibres that can exhibit considerable apparent wall slip (Bennington et al., 1990; Zhang et al., 1998; Baravian et al., 2002; Martin et al., 2005; Ramírez-Gilly et al., 2007).

A significant amount of discrepancy can be found among the reported apparent yield stress values (Gullichsen and Harkonen, 1981; Bennington et al., 1990; Swerin et

al., 1993; Damani et al., 1993; Wikström et al., 1998; Ein-Mozaffari et al., 2005). An example is given in Table 1-1, where the reported values for the apparent yield stress of a 3 wt.% bleached softwood kraft pulp range from 19.3 to 350 Pa, while those of a 6 wt.% range from 60 to 1220 Pa. These discrepancies are due to differences in pulp type, the way the apparent yield stress is defined and the technique used to measure it.

As discussed in chapter 1, the apparent yield stress can be measured by means of either stress-controlled or rate-controlled rheometers by performing creep or steady shear tests respectively. Using a rate-controlled rheometer and applying a constant strain rate, the shear stress can be measured as a function of strain or time. The apparent yield stress can then be calculated as the maximum shear stress measured, the steady-state shear stress or the shear stress at which departure from linearity begins (very difficult to establish uniquely). Each of these definitions gives a different value for the apparent yield stress (Thalen and Wahren, 1964; Nguyen and Boger, 1985; Liddell and Boger, 1996).

Another approach is to apply a slow shear rate ramp to obtain the variation of torque as a function of rotational speed. The apparent yield stress is calculated using the maximum torque measured during the experiment (Bennington et al., 1990). Using a stress-controlled rheometer and increasing the shear stress in a linear manner, the variation of the instantaneous viscosity (instantaneous shear stress divided by the instantaneous shear rate) versus shear stress can be obtained. The apparent yield stress is the value at which the instantaneous viscosity drops significantly or is a maximum (Cheng, 1986; Zhu et al., 2001; Brummer, 2005; Coussot, 2005; Nguyen et al., 2006).

The main objective of this chapter is to identify a reliable technique for measuring the apparent yield stress of pulp fibre suspensions that yields consistent results. To establish this technique, the apparent yield stress of several commercial pulp fibre suspensions over a wide range of mass concentrations is measured by using conventional apparent yield stress measurement methods utilizing both a stress-controlled and rate-controlled rheometer. The apparent yield stress values obtained using these techniques are compared with those obtained from a velocity profile determination technique using ultrasonic Doppler velocimetry (described in the next section). The reliable data from this

comparison are used to obtain models for the apparent yield stress of pulp fibre suspensions.

2.2. Velocity Profile Determination Using Ultrasonic Doppler Velocimetry

While conventional rheometry is the most widely used technique for rheological characterization, fluid visualization methods have also been found useful in rheology (Takeda, 1986; McClements et al., 1990; Bachelet et al., 2004; Be´cu et al., 2006; Koseli et al., 2006).

These techniques primarily make use of light to measure instantaneous velocities in a flowing fluid. Among others, Particle Image Velocimetry (PIV) and Laser Doppler Velocimetry (LDV) are the most common ones in fluid flow measurements. In these techniques, fluid is often seeded with tracer particles which are assumed to follow the fluid flow dynamics. Tracking the motion of the seeded particles, the fluid velocity can be obtained instantaneously. These two techniques often require a complicated set-up and as they utilize laser light to follow the flow field they are exclusive to the transparent systems. Therefore, in the case of opaque systems such as pulp fibre suspensions other techniques such as ultrasonic Doppler velocimetry (UDV) should be implemented.

Ultrasonic Doppler velocimetry (UDV) is a simple, non-intrusive acoustic measurement technique based on the Doppler effect (more detail can be found in Appendix A). In this technique, a short ultrasonic burst with an angle θ_0 relative to the normal to the wall is sent to the fluid periodically and the echoes issuing from the suspended particles are collected (Figure 2-1). However, as the ultrasound travels through the wall, the initial angle θ_0 changes to θ the value of which is given by the law of refraction (Manneville et al., 2004). Using the time delay, t_f, and the frequency shift of the reflected pulses, f_d, the location and the velocity of the particles in the direction of the acoustic axis are obtained using Eqs. (2-1) and (2-2) (Hein and O'Brien, 1993).

$$y = \frac{ct_f}{2} \tag{2-1}$$

$$u(y) = \frac{cf_d}{2f_0 \cos\theta} \tag{2-2}$$

where c is the sound velocity in the medium, f_0 is the ultrasound emission frequency and θ is the emission angle into the fluid.

The radial position and the orthoradial velocity of the reflecting particles in Couette geometry can then be found by using Eqs. (2-3) and (2-4) based on the geometry shown in Figure 2-1 (Manneville et al., 2004).

$$u(r) = \frac{r}{R_2 \sin\theta} u(y) \tag{2-3}$$

$$r = \sqrt{R_2^{\,2} + y^2 - 2R_2 y \cos\theta} \tag{2-4}$$

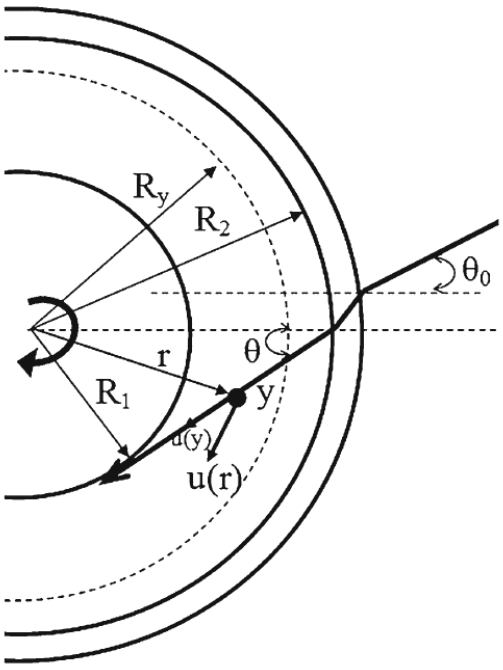

Figure 2-1: Ultrasonic Doppler velocimetry in Couette geometry. r is the radial distance from the rotor, y is the distance from the outer wall along the acoustic axis and R_y is the yielding radius.

As UDV measures accurately the velocity profiles of a flowing fluid, it can be coupled with conventional rheometers to study the rheological behaviour of complex

fluids in a more precise manner. Particularly, when coupled with a Couette geometry, the torque T imposed on the moving cylinder by the rheometer yields the stress distribution $\sigma(r)$ across the gap, while the velocity profile obtained by UDV permits determination of the local shear rate $\dot{\gamma}(r)$ according to Eqs. (2-5) and (2-6) (Bird et al., 2001).

$$\sigma(r) = \frac{\mathrm{T}}{2\pi h r^2} \tag{2-5}$$

$$\dot{\gamma}(r) = -r\frac{\partial}{\partial r}\left(\frac{u_{(r)}}{r}\right) \tag{2-6}$$

where h is the cylinder height., R_1 is the cylinder radius, R_2 is the cup radius with $R_1 \le r \le R_2$ (Figure 2-1).

By using large gaps to study the rheological properties of viscoplastic fluids that exhibit an apparent yield stress, such as paper pulps, polymers and ceramic pastes, the vane creates a sheared (yielded) zone within which the material is in flow. However, as the shear stress falls below the apparent yield stress, the flow stops generating an un-yielded zone, i.e. the velocity is practically equal to zero between R_y and R_2 (Figure 2-2).

By knowing the radius of shearing R_y obtained using UDV measurements and the steady-state shear stress at the vane surface σ_T obtained using the torque reading from the rheometer, the apparent yield stress σ_y can be calculated from Eq. (2-7) (Fisher et al., 2007).

$$\sigma_y = \sigma_T\left(\frac{R_1}{R_y}\right)^2 \tag{2-7}$$

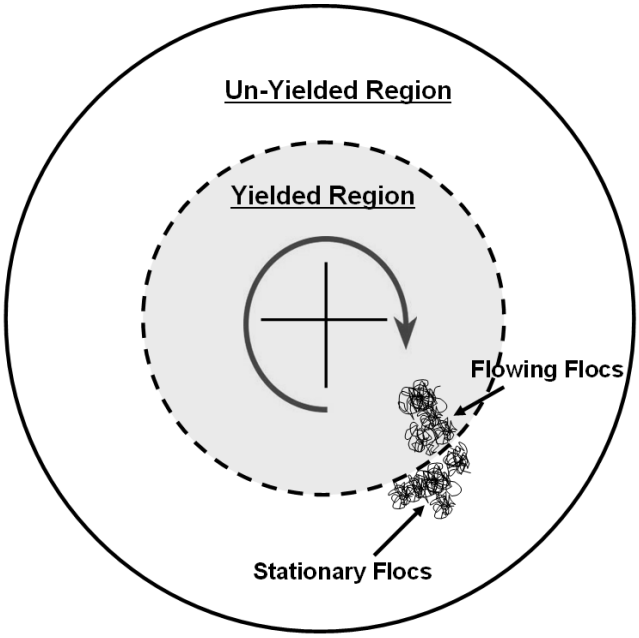

Figure 2-2: Schematic of vane in large cup geometry with yielded and un-yielded regions.

2.3. Materials and Experimental Testing

Pulp fibre suspensions were prepared from bleached softwood kraft (SBK) and bleached hardwood kraft (HW) (Domtar Inc., Windsor, QC), thermal-mechanical-pulp (TMP) (Howe Sound Pulp and Paper Limited Partnership, Port Melon, BC) and stone-ground wood (SGW) (Paprican, Pointe-Claire, QC) by breaking up the dried pulp sheets and rehydrating the fibres with tap water using a disintegrator (TMI, Montreal, QC) for 30 minutes at 120 rpm. Suspensions of 0.5, 1.0, 2.0, 2.5, 3.0, 4.0 and 5.0 wt.% were prepared. The pulp fibre properties are summarized in Table 2-1. The mean fibre length is an important parameter as shown below. In this study, it varies from 0.67 to 2.96 mm (Table 2-1). Fibre Curl Index is the ratio of actual fibre length to the distance between the 2 fibre ends minus 1. It indicates the continuous curvature of the fibres greater than 0.5 mm in length and within the selected range limits. Fibre Kink Index is the sum of the number of kinks (an abrupt change in fibre curvature) within a range of kink angles divided by the total fibre length of all the fibres.

Table 2-1: Properties of pulp fibres used in the present study

Fibre System	*Fibre Properties*			
	Mean length L_w (mm)	Percent fines (L=0.07-0.2 mm)	Mean curl index	Mean kink index
SBK	2.96	1.9	0.27	2.11
HW	1.28	8.17	0.105	1.98
TMP	1.36	11.9	0.05	0.50
SGW	0.67	23.1	0.09	1.43

A four-bladed vane, 38.5 mm in height and 25 mm in diameter, was placed in a transparent cylindrical cup having an internal diameter of 100 mm and a height of 64 mm resulting in a gap size of 37.5 mm. To obtain consistent rheological data for pulp suspensions and to eliminate shear history after loading the sample into the measuring device, all samples should have the same structural state prior to experimental testing. To achieve this, the suspension should be pre-sheared with a preset shear stress or shear rate over a fixed time span in order to rupture most of the fibre structures. The suspension should then be kept at rest for another specific period of time to recover its structure to a certain level for all subsequent experiments. The effectiveness of the pre-shearing conditions can be examined by checking the dependency of the viscosity on the shear rate after applying the pre-shearing conditions. The optimum pre-shearing conditions are those for which different samples of the same suspension exhibit the same viscosity versus shear rate relationship.

Given this, a series of tests was conducted to determine the optimum pre-shearing conditions for each sample. Tests were performed at each suspension mass concentration with different levels of shear stress applied for different lengths of time. Samples were then redistributed evenly in the gap and left to rest for 15 minutes followed by checking the dependency of the viscosity on the shear rate. The optimum pre-shearing conditions were identified as those for which different samples exhibited the same viscosity-shear rate relationship. These conditions were then used in all subsequent tests (Table 2-2).

The apparent yield stress values of the pulp suspensions were measured using three methods. In the first, a stress-controlled Bohlin C-VOR rheometer (Malvern, Worcestershire, UK) was used to linearly increase the shear stress in steps and the

variation of the instantaneous viscosity (instantaneous shear stress divided by the instantaneous shear rate) versus shear stress was obtained. The apparent yield stress was measured as the stress value for which the instantaneous viscosity exhibited a maximum (Cheng, 1986; Zhu et al., 2001; Brummer, 2005; Coussot, 2005; Nguyen et al., 2006).

Table 2-2: Optimum pre-shearing conditions applied on pulp suspensions

C_m	*SBK*		*HW*		*TMP*		*SGW*	
	σ(Pa)	t(s)	σ(Pa)	t(s)	σ(Pa)	t(s)	σ(Pa)	t(s)
0.01	50	10	15	5	10	10	5	5
0.02	120	15	40	10	45	10	50	10
0.025	230	20	80	20	72	10	80	15
0.03	300	20	125	30	95	30	75	15
0.04	460	30	200	30	240	40	170	35
0.05	580	40	365	35	350	40	260	40

The second method used a rate-controlled Haake RV12 Rotovisco viscometer (Thermo Fisher Scientific Inc., Waltham, MA) at a rotational speed of 8 rpm. For this experiment the torque–time response was measured with the peak torque used to calculate the apparent yield stress. This technique has commonly been used to measure the apparent yield stress of various substances (Cadling and Odenstad, 1950; Donald et al., 1977; Bowles, 1977; Nguyen et al., 1981; Nguyen and Boger, 1983; Ein-Mozaffari et al., 2005).

The third method used the Haake RV12 viscometer at two rotational speeds of 8 and 16 rpm and a pulsed ultrasonic Doppler velocimeter (Model DOP2000, Signal Processing, Switzerland) to measure the velocity profiles across the gap. The ultrasonic transducer has an active diameter of 20 mm and a pulse repetition frequency of 100 Hz to 15.6 KHz which can be changed depending on the magnitude of the expected velocity. A cup, identical to those used in the other methods, was made with an indentation of 14° at the surface to attach the UDV probe. The space between the transducer and the Plexiglas wall was filled with an ultrasonic gel to establish an efficient acoustic coupling between the probe and the vessel. The Plexiglas interface between the transducer and suspension was machined as thin as possible so that the refraction of the beam due to the interface can be neglected i.e. $\theta_0 \sim \theta$ in Figure 2-1.

2.4. Results and Discussion

2.4.1. Apparent yield stress measurement by linear stress ramps

Figure 2-3 depicts a typical apparent yield stress measurement for a 1 wt.% bleached softwood kraft pulp suspension at 23°C. Measurements were performed at least five times to check the reproducibility and minimize experimental error.

Figure 2-4 shows the typical behaviour of the transient strain $\gamma(t)$ when shear stresses lower and greater than the apparent yield stress are applied to the pulp suspension. For stresses lower than the apparent yield stress an initial jump in strain (elastic response) was observed followed by a gradual increase in the strain until reaching a constant value (solid-like behaviour). For stresses above the apparent yield stress value, the strain increases monotonically, reaching a constant slope (fluid-like behaviour).

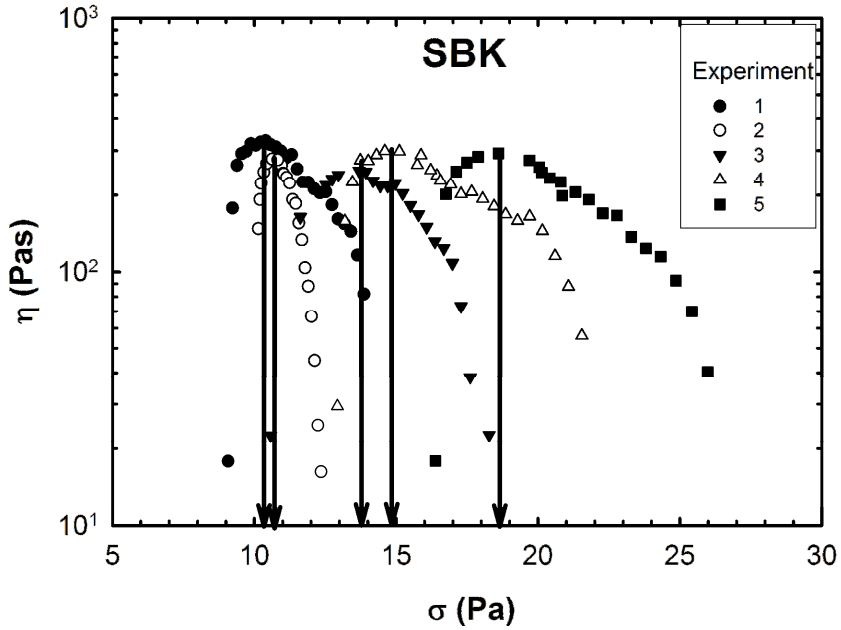

Figure 2-3: Repeats of apparent yield stress measurements for a bleached softwood kraft pulp suspension (SBK) of mass concentration of 1 % at 23 °C applying a linear shear stress ramp.

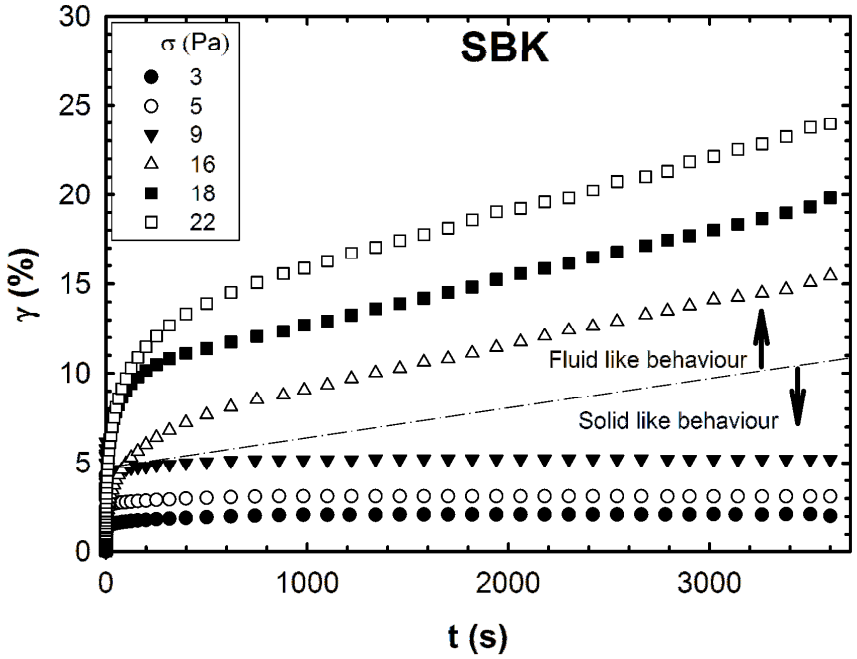

Figure 2-4: Creep response of a bleached softwood kraft pulp suspension (SBK) of mass concentration of 1 % at 23 °C for shear stress values lower and higher than the apparent yield stress. Note that pulp suspension exhibits a solid behaviour below the apparent yield stress while a fluid behaviour can be observed above the apparent yield stress.

The apparent yield stress values obtained by applying linear shear stress ramps are listed in Table 2-3 and plotted in Figure 2-5 as a function of mass concentration.

Table 2-3: Apparent yield stress values obtained by using the linear shear stress ramp method

C_m	*Apparent Yield Stress (Pa)*			
	SBK	HW	TMP	SGW
0.005	2±0.60	0.33±0.1	0.18±0.05	0.11±0.03
0.01	13±4	4±1.5	1±1	0.73±0.1
0.02	57 ±6	14±2	16±3	9±1
0.025	114±16	26±4	27±1	17±1
0.03	154±13	48±8	50±11	28±4
0.04	242±45	80±10	125±12	69±2
0.05	384±49	166±7	245±32	150±9

The dependency of the apparent yield stress values on fibre mass concentration has been correlated using a power-law model ($\sigma_y = aC_m^{\ b}$). The resulting fitted constants are listed as an insert in Figure 2-5. These are within the range of previously reported results (Kerekes et al., 1985).

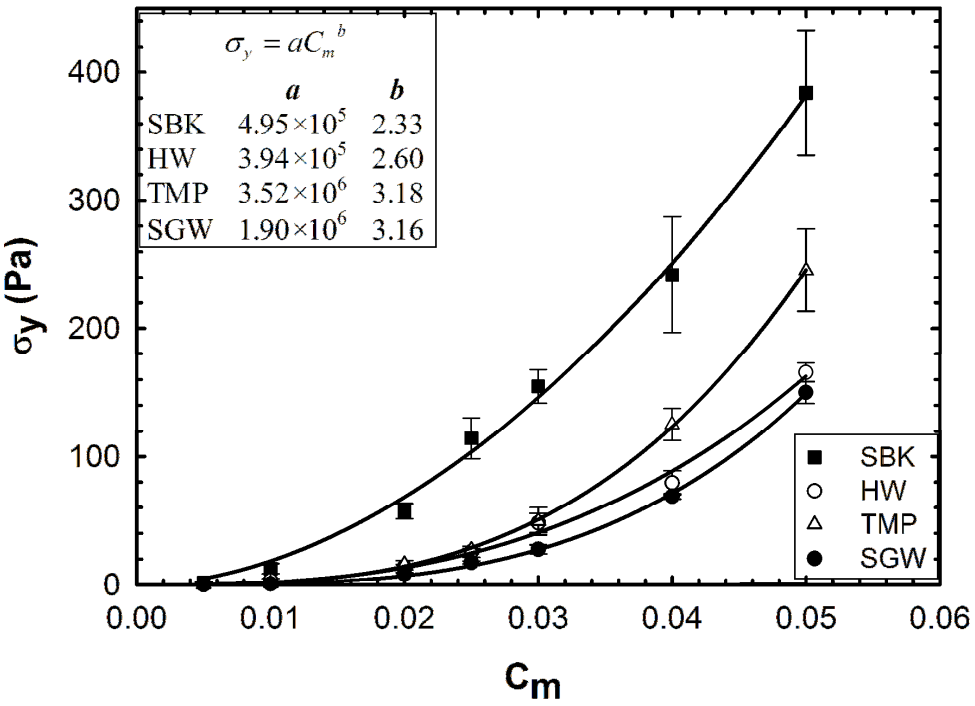

Figure 2-5: The apparent yield stress values of all tested pulp suspensions as a function of mass concentration obtained by using the shear stress ramp method at 23 °C.

The measured apparent yield stress values depend on the physical properties of the fibres. Fibres tend to form networks due to a number of attractive forces. These include colloidal, mechanical surface linkage, elastic fibre bending and surface tension, although mechanical entanglement is the greatest (Kerekes et al., 1985). Fibre properties, such as fibre length, flexibility and elastic modulus contribute to these forces and affect the apparent yield stress of the suspension. More flexible and longer fibres permit greater contact between adjacent fibres, increase the number of mechanical linkages and therefore the apparent yield stress. Due to differences in fibre length and flexibility, the apparent yield stress decreases from SBK > TMP ≅ HW > SGW at a given mass concentration. Increasing suspension concentration increases the number of fibre entanglements, the strength of the fibre network formed and hence the apparent yield stress as shown in Figure 2-5 for all the pulp suspensions tested.

2.4.2. Apparent yield stress measurement by the start-up of shear flow experiment

Apparent yield stress measurements were also performed using start-up of steady shear experiments in the Haake RV12 rheometer. Each experiment was performed five times and the apparent yield stress values were measured as the maximum shear stress achieved in the shear stress vs. time response. Typical measurements are plotted in Figure 2-6 for a 3 wt.% bleached softwood kraft pulp suspension. The apparent yield stress values obtained using this technique are listed in Table 2-4.

Generally, these values were larger than those obtained by using the previous (linear shear stress ramp) method, although the same trend as a function of fibre type and mass concentration was observed (Figure 2-7). The resulting fitted constants to power law model ($\sigma_y = aC_m^{\ b}$) are also listed in the insert of Figure 2-7.

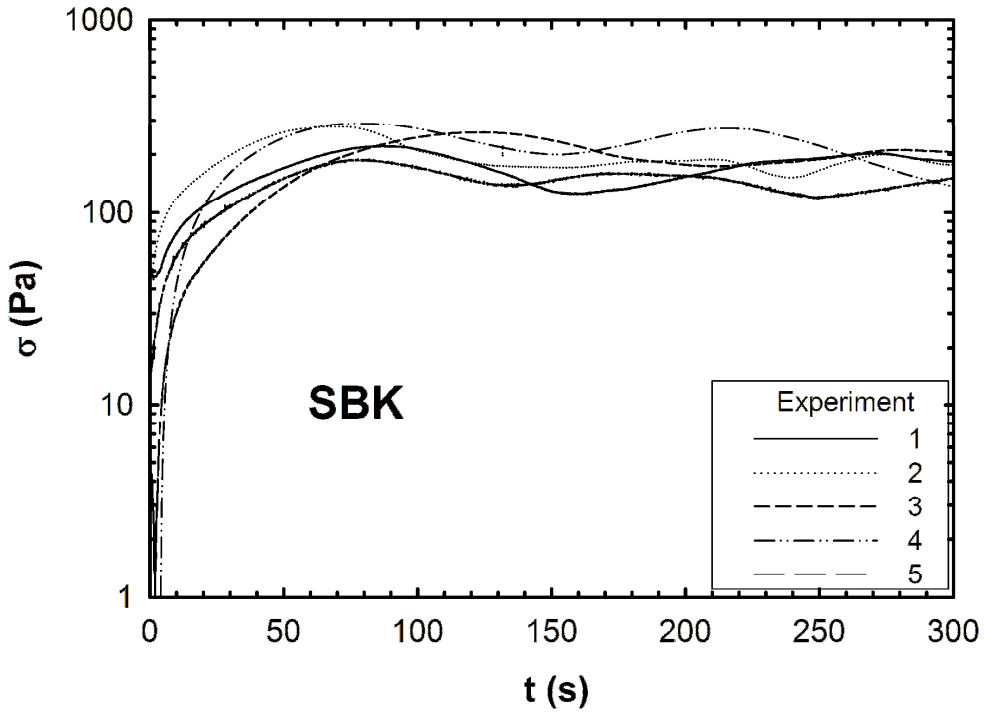

Figure 2-6: Stress response after imposition of steady shear at vane rotational rate of 8 rpm for a 3 wt.% bleached softwood kraft pulp suspension (SBK) at 23 °C. Multiple tests indicate the level of reproducibility.

Table 2-4: Apparent yield stress values obtained by using the start-up of steady shear flow experiment

C_m	*Apparent Yield Stress (Pa)-Controlled Rate-RPM=8*			
	SBK	HW	TMP	SGW
0.005	5±1.6	1.5±0.1	0.85±0.4	0.14±0.03
0.01	39±2	9±4	4±2	3±1
0.02	105 ±6	30±8	33±10	35±9
0.025	205±16	55±23	53±16	48±23
0.03	248±40	87±31	65±25	55±17
0.04	388±58	151±40	180±45	118±38
0.05	518±60	292±52	289±42	196±34

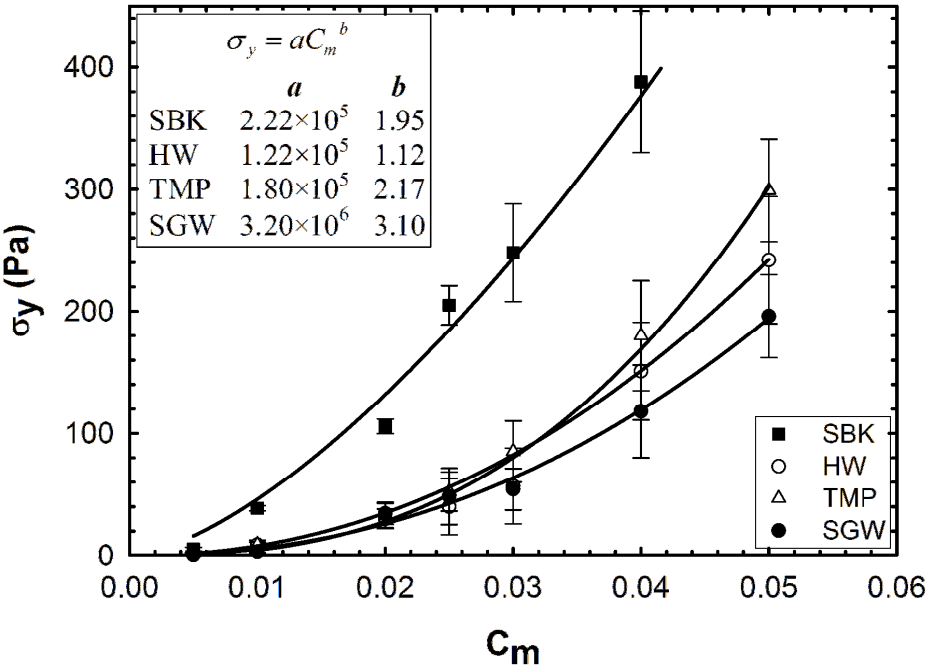

Figure 2-7: The apparent yield stress values of all tested pulp suspensions as a function of mass concentration obtained by applying the start-up of steady shear flow at 23 °C.

Under the application of constant rotational rates (constant shear rates), viscoelastic thixotropic fluids exhibit an initial stress growth that is followed by a slight stress decay to a final stead-state value. However, pulp suspensions do not attain an ultimate constant shear stress; instead they exhibit an oscillatory behaviour as shown in

Figure 2-6. This characteristic is due to the complex behaviour of fibre flocs during flow. In flow, some flocs tend to move along with the vane but slow down as the contact with the vane tip is lost. As a floc moves along with a blade, the required shear stress to maintain constant rotational rate increases. On the other hand, stress decreases when a floc loses contact with the blade tip. Due to this behaviour the shear stress does not reach a "true" steady-state value.

2.4.3. Apparent yield stress measurement by ultrasonic Doppler velocimetry (UDV)

An ultrasonic Doppler velocimeter was used to determine the velocity profile in the gap of various pulp suspensions in conjunction with torque measurements made with the Haake RV12 rotovisco viscometer. Two constant vane rotational rates of 8 and 16 rpm were used. The UDV probe was adjusted to 14° so that velocity measurements could be made at the tip of the rotating vane. Velocity profiles for different pulp suspensions at the rotational rate of 8 rpm are presented in Figures 2-8a-8d.

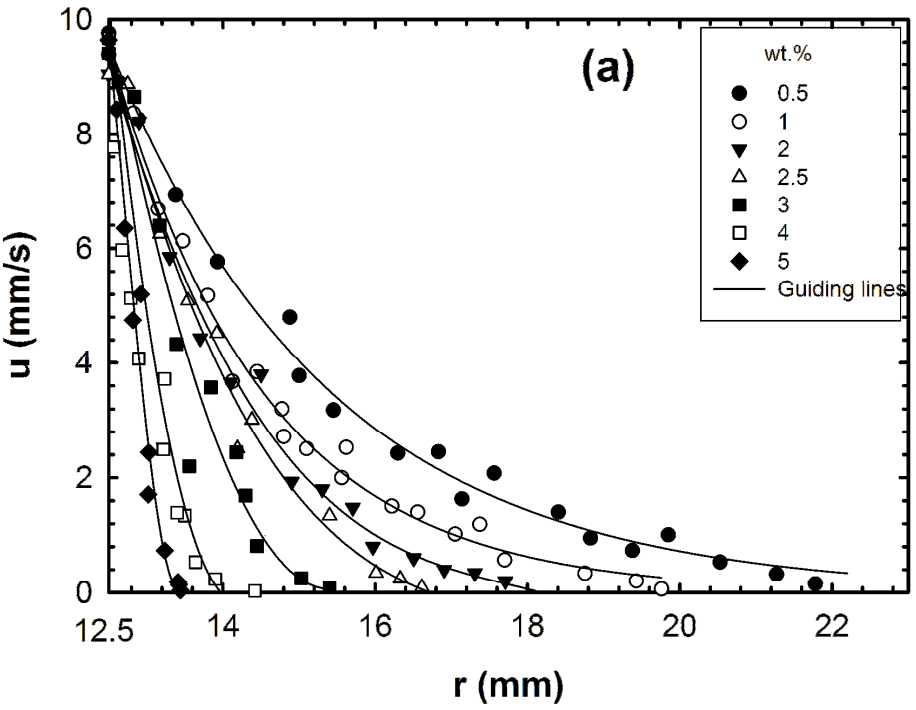

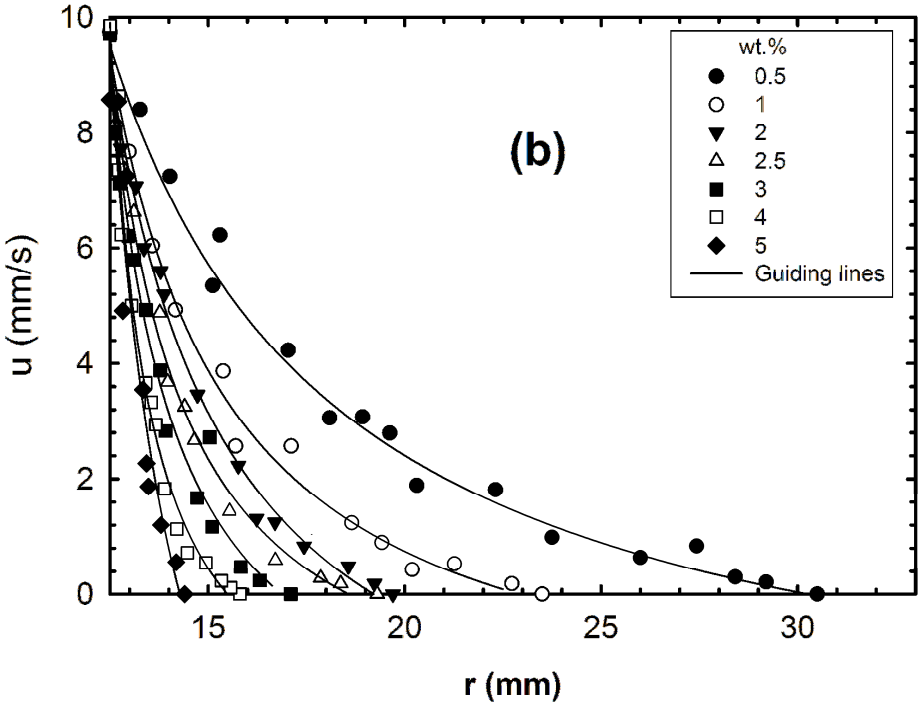
(b)
wt.%
0.5
1
2
2.5
3
4
5
Guiding lines
u (mm/s)
r (mm)
0
2
4
6
8
10
15
20
25
30

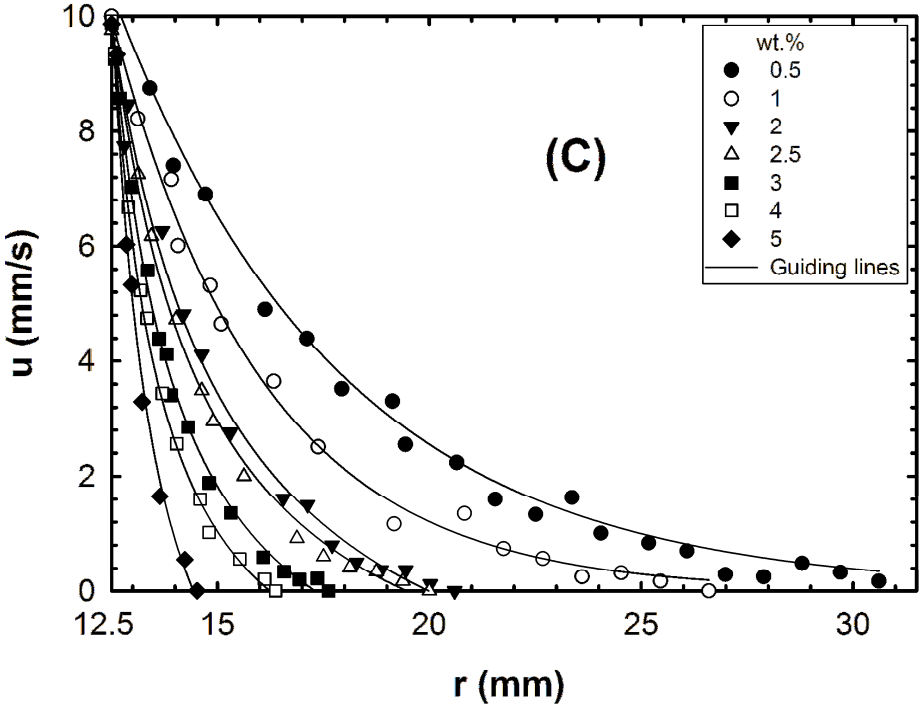
(C)
wt.%
0.5
1
2
2.5
3
4
5
Guiding lines
u (mm/s)
r (mm)
0
2
4
6
8
10
12.5
15
20
25
30

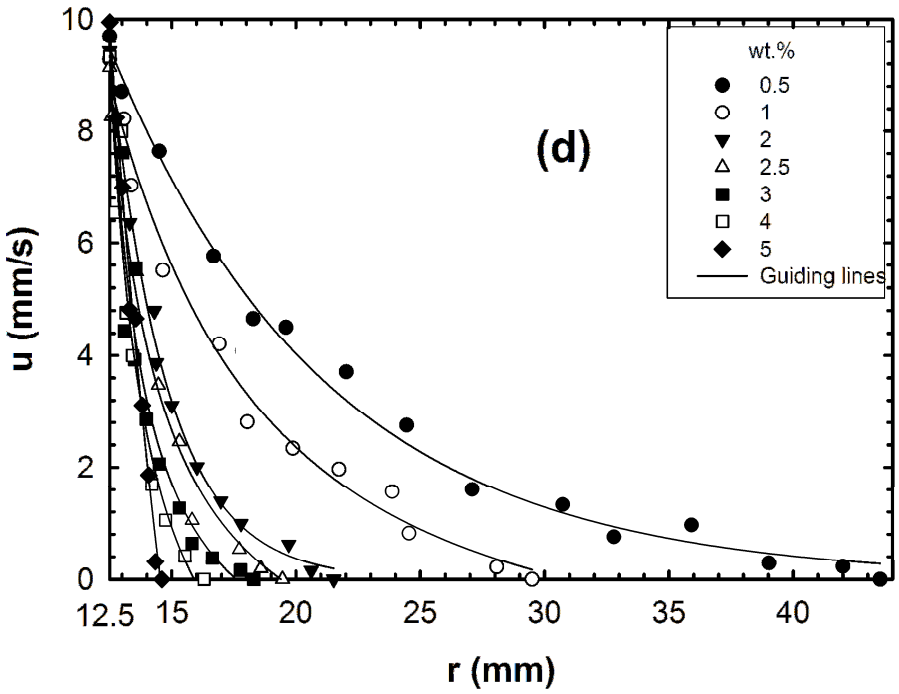

Figure 2-8: Velocity profiles across the gap for, a) SBK, b) HW, c) TMP, d) SGW pulp suspensions, at 23 °C and several mass concentrations. Note that the apparent yield stress increases nonlinearly with increase of the mass concentration and thus the yielding radius decreases.

The velocity decreases across the gap from a maximum value at the vane tip and drops to zero at a certain distance which is referred to as yielding radius R_y (Figure 2-2).

The shear stress decreases in the gap according to Eq. (2-5). The suspension contained in the region between the vane tips and the yielding radius is in flow, while the fluid beyond this region remains stationary. Increasing the mass concentration of pulp suspension increases the apparent yield stress and decreases the yielding radius, while the velocity profiles tend to move closer to linearity (Figures 2-8a-8d).

The yielding radius and the steady-state shear stress at the vane were used to calculate the apparent yield stress of suspensions by using Eq. (2-7). The results are summarized in Table 2-5 and depicted in Figure 2-9 with power-law fits to the data.

Table 2-5: Apparent yield stress obtained using UDV coupled with a rate-controlled viscometer

C_m	Apparent Yield Stress (Pa)-Velocity Profile Determination Technique			
	SBK	HW	TMP	SGW
0.005	1±0.6	0.2±0.1	0.24±0.05	0.08±0.03
0.01	11±2.5	3±1.5	1.7±0.6	0.47±0.1
0.02	46±11	11±2.4	14±3	8±1
0.025	105±21	20±5.3	25±5	15±3
0.03	137±18	40±12	45±11	23±4
0.04	221±45	71±54	118±21	56±13
0.05	358±49	181±62	238±54	127±35

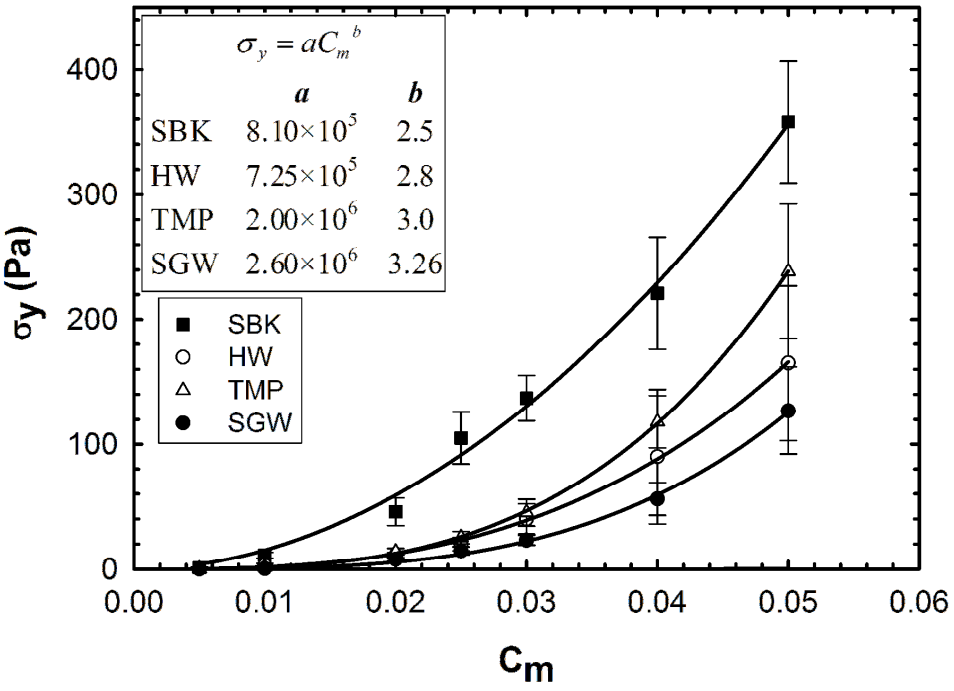

Figure 2-9: The apparent yield stress values of all tested pulp suspensions as a function of mass concentration obtained using local velocity profile measurements at 23 °C, at a constant rotational rate of 8 rpm, at pulsed repetition frequency of 8000 Hz and incident angle of 14°.

In an ideal yield stress fluid, the shear rate and thus the mean velocity must decrease gradually from a maximum value at the tip of the vane towards zero at the yielding radius. As seen in Figures 2-8a-8d, in pulp suspensions of higher mass concentrations depending on the pulp fibre properties (flexibility, size, etc.) the mean

velocity decreases from a maximum at the tip of the vane and suddenly drops to zero at the yielding radius resulting a discontinuity in the velocity profiles during the transition from the yielded to the un-yielded region. This behaviour has also been observed in concentrated colloidal suspensions, referred to as shear-banding or shear-localization effect which results from yielding and the thixotropic characteristics of the fluid. In this case, rheological models such as Bingham, Casson and Herschel-Bulkley do not predict the velocity profiles accurately and the apparent yield stress of the fluid depends on the procedure for determining it (Coussot et al., 2002a).

Pulp suspensions are heterogeneous systems containing millimetre-sized fibres and centimetre-sized fibre flocs. The discontinuity in the velocity profiles at the transition from the yielded to the un-yielded zone can also be due to the existence of large moving flocs in the layer next to the un-yielded zone. In this case, UDV identifies finite velocities for the moving fibre flocs dropping to zero in the next layer. Therefore, at this point it is not clear, whether pulp suspensions display shear localization or banding as they go through the yielding transition. Shear-Banding in concentrated pulp fibre suspensions is studied in detail in chapter 4.

2.4.4. Comparison of the different apparent yield stress measurement methods

A comparison of the apparent yield stress values determined using each method is given in Figures 2-10a-10d for the pulp suspensions studied with the constants fitted to the power law model summarized in Table 2-6. There is satisfactory agreement between the apparent yield stress values obtained using the linear shear stress ramp and the velocity measurement techniques, while the apparent yield stress values obtained using start-up of shear flow method have considerably larger values.

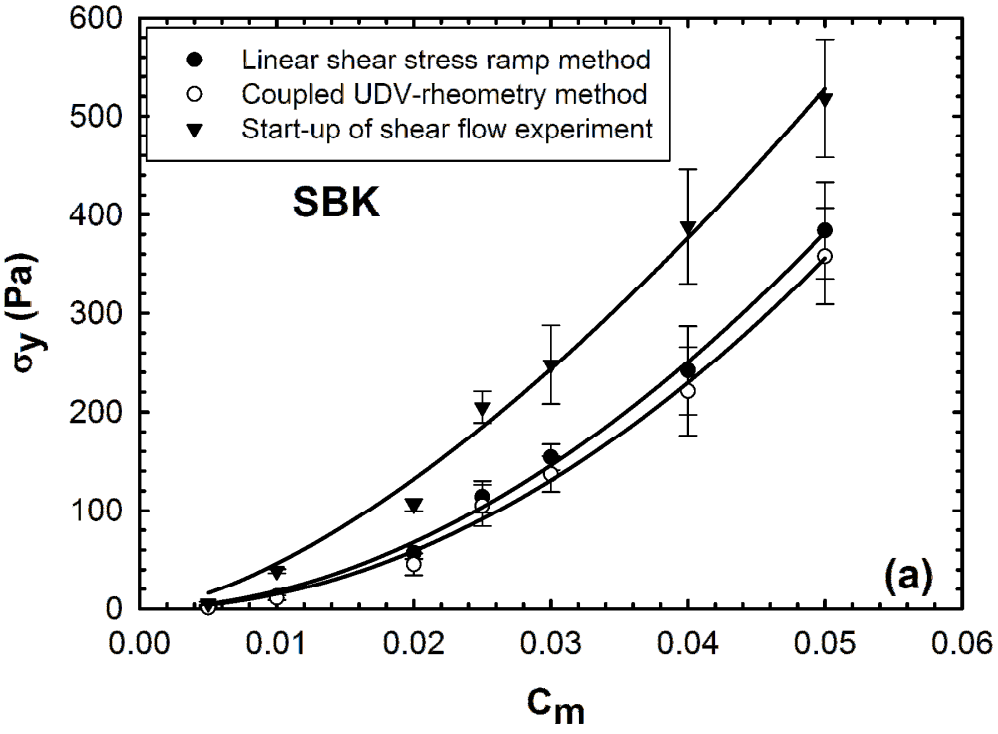
Linear shear stress ramp method
Coupled UDV-rheometry method
Start-up of shear flow experiment
SBK
(a)
σy (Pa)
cm
0
100
200
300
400
500
600
0.00
0.01
0.02
0.03
0.04
0.05
0.06

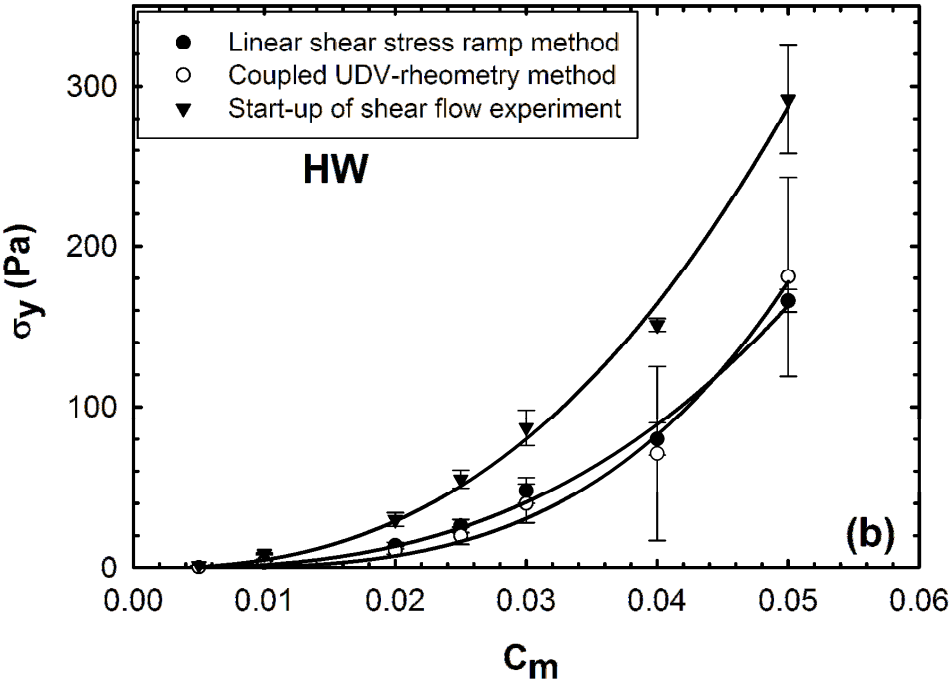
Linear shear stress ramp method
Coupled UDV-rheometry method
Start-up of shear flow experiment
HW
(b)
σy (Pa)
cm
0
100
200
300
0.00
0.01
0.02
0.03
0.04
0.05
0.06

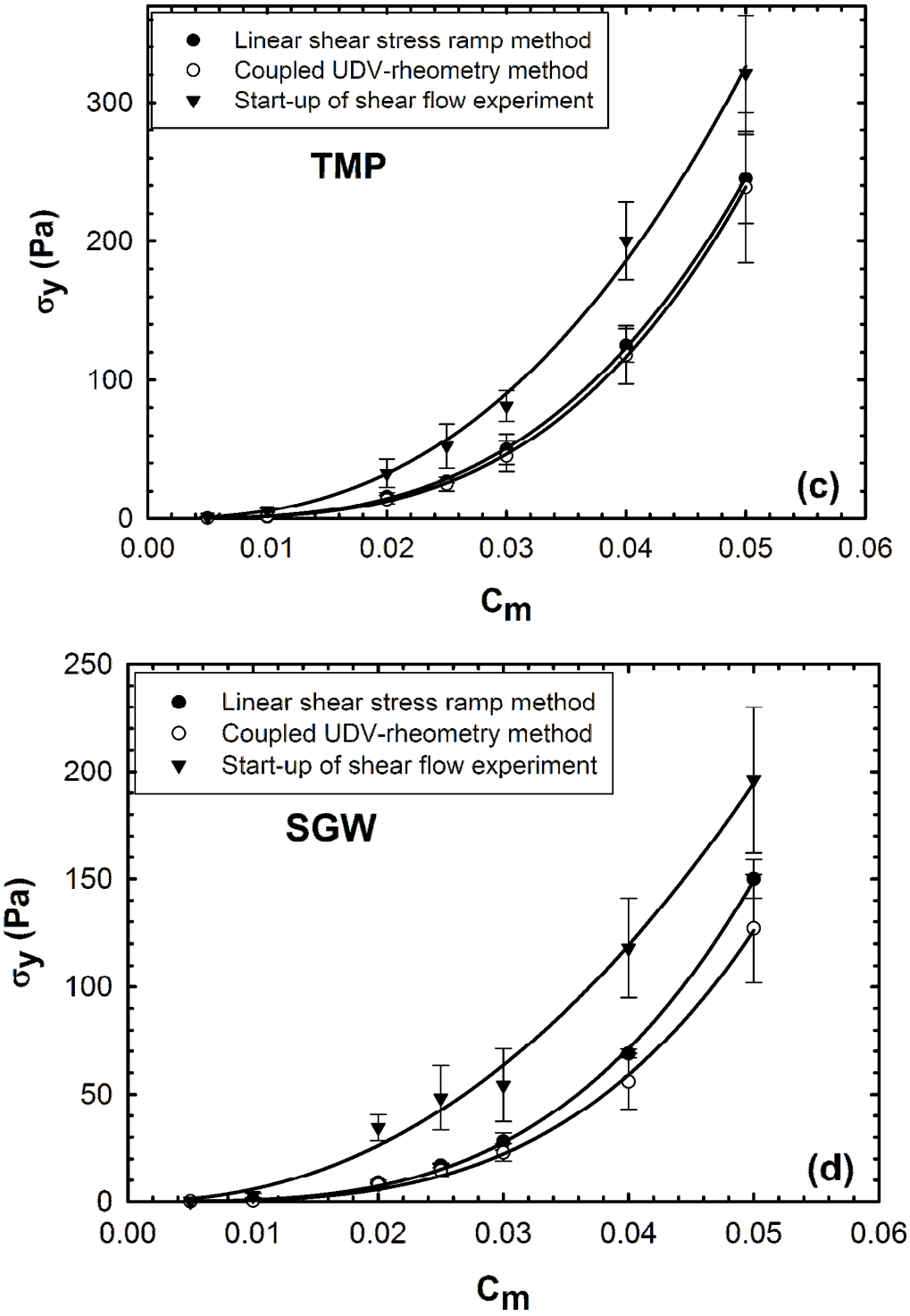

Figure 2-10: Comparison of the apparent yield stress values obtained using three different methods for a) SBK, b) HW, c) TMP, d) SGW pulp suspensions, at 23 °C and several mass concentrations. Note that the apparent yield stress values obtained by using the linear shear stress ramp and the velocity profile determination techniques are in good agreement.

Fibre networks consist of large flocs attached to each other by weaker fibre networks. Application of a constant shear stress in pulp breaks the weaker bonds in between different flocs and the suspension's behaviour deviates from that of an elastic solid (departure from linearity in the shear stress-time data). This deviation possibly occurs at a shear stress where the instantaneous viscosity is maximum. This regime which occurs at low shear stresses is referred to as the macro-scale deformation regime (Wikström, 2002). The critical shear stresses for the onset of deviation from the linearity in the shear stress-time data would have resulted in values closer to those determined by the shear stress ramp. However, it is difficult to accurately establish such critical stresses experimentally; this is the reason why these values are not reported in the present work.

With further increase in the shear stress, the yielded area increases and weaker fibre flocs possibly begin to rupture (Steen, 1990). This regime is referred to as the micro-scale deformation regime (Wikström, 2002). Beyond a specific shear stress (equivalent to the maximum shear stress in the start-up of shear experiment), most of the fibre flocs move freely in the suspension. This results in higher values of the apparent yield stresses compared with those obtained by the other methods.

As the velocity profile measurement technique uniquely identifies the velocity distribution and yielding radius in the gap, this technique gives a more accurate determination of the apparent yield stress. However, this technique is time consuming and not convenient compared with macroscopic rheometry as the application of equations must be made to infer the rheological properties from the velocity profiles. When applying a constant shear rate, the shear stress increases rapidly which ruptures the fibre network abruptly. Therefore, the accuracy of the apparent yield determination decreases.

However, by increasing the shear stress or the shear rate slowly, the fibre network ruptures gradually making it easier to determine the shear stress at which flow begins. Since the apparent yield stress values obtained using the linear shear stress ramp method are in good agreement with those obtained by the velocity measurement technique, applying linear shear stress ramps by using a stress controlled rheometer is an easy and reliable alternative for apparent yield stress measurements.

Table 2-6: Summary of fitted constants to the power-law model ($\sigma_y = aC_m^{\ b}$) for all tests

Pulp Type	*Mass Fraction Range Used*	*Linear Shear Stress Ramp Method*			*Constant Shear Rate Method*			*Velocity Profile Determination Method*		
		$a\times10^{-5}$	b	Goodness of Fit	$a\times10^{-5}$	b	Goodness of Fit	$a\times10^{-5}$	b	Goodness of Fit
SBK	$0.005\leq C_m\leq0.05$	4.95±0.20	2.33±0.10	0.99	2.22±0.15	1.95±0.11	0.98	8.10±0.50	2.50±0.13	0.98
HW	$0.005\leq C_m\leq0.05$	3.94±0.23	2.60±0.21	0.98	1.22±0.10	1.12±0.10	0.98	7.25±0.70	2.80±0.21	0.98
TMP	$0.005\leq C_m\leq0.05$	35.2±2.22	3.18±0.25	0.99	1.80±0.15	2.17±0.20	0.97	20.0±0.18	3.00±0.25	0.97
SGW	$0.005\leq C_m\leq0.05$	19.0±0.96	3.16±0.16	0.96	32.0±1.9	3.10±0.15	0.96	26.0±0.13	3.26±0.13	0.98

2.5. Summary

Pulp fibre suspensions are composed of fibre networks and flocs which possess measureable apparent yield stress. The two most widely used apparent yield stress measurement methods are linear shear stress ramps and start-up of steady shear flow experiments. These were used in this study to measure the apparent yield stress of different pulp fibre suspensions at low fibre mass concentrations up to 5 wt.%. Results obtained using these techniques differed significantly from each other. To determine the most reliable technique, an ultrasonic Doppler velocimeter (UDV) was coupled with a rate-controlled rheometer to provide a robust device and reliable method which can be used to measure the apparent yield stress. By explicitly determining the velocity profiles, the results from this technique were found to be in agreement with those obtained from the linear shear stress ramp method. Therefore, this technique can be used to obtain experimental data safely and efficiently.

3. Rheology of Pulp Suspensions Using Ultrasonic Doppler Velocimetry[3]

3.1. Introduction

Complex materials such as colloidal suspensions, foams, emulsions, fibre suspensions and gels are widely used materials in many industrial applications (Bennington et al., 1990; Bergenholtz et al., 2002; Stickel et al., 2009). These materials are composed of particles/fibres, which interact with each other physically and/or chemically while dispersed in a continuous aqueous medium. Due to these interactions they often exhibit unusual rheological behaviour, which makes their rheological study a nontrivial task (Larson, 1998).

Pulp fiber suspensions fall into the category of complex fluids described above. Pulp fibre suspension flows, despite their extensive importance, have received limited attention due to the difficulties associated with appropriate experimental measurements, their heterogeneous nature and the lack of a general standard experimental procedure (Bennington et al., 1990; Swerin et al., 1993; Wikström et al., 1998).

Previous studies on pulp suspension rheology are mostly limited to apparent yield stress measurements (Gullichsen and Harkonen, 1981; Bennington et al., 1990; Swerin, 1993; Wikström et al., 1998), viscoelasticity studies (Damani et al., 1993; Swerin, 1993; Swerin et al., 1998) and pressure-driven pipe flow experiments (Lee and Duffy, 1976; Logdill et al., 1988; Ogawa et al., 1990; Li et al., 1995b; Duffy and Abdullah, 2003; Duffy et al., 2004). The behavior of pulp suspensions beyond apparent yield stress has received little attention in the literature. However, this behavior is of great importance since all processes in the pulp and paper industry occur at high shear stresses. Having consistent rheological data, i.e., complete flow curves, more practical, precise and reliable rheological models can be proposed.

[3] A version of this chapter has been published. Derakhshandeh, B., Hatzikiriakos, S.G., Bennington, C.P.J., 2010. Rheology of pulp fibre suspensions using ultrasonic Doppler velocimetry. Rheologica Acta 49(11-12): 1127-1140.

Wood fibres are held tightly together by a chemical substance referred to as lignin. Wood chips are processed in order to liberate the wood fibres from lignin during pulping process so they can be used to make paper products. Breaking down the wood into fibres can be accomplished by mechanical or chemical processes or combinations of both. These treatments alter the fibre properties, the fibre lignin content and the fibre geometric dimensions such as the diameter, length and fibre wall thickness (Smook, 1992; Biermann, 1996; Gullichsen and Fogelholm, 1999). These changes in fibre properties in turn affect the flow behaviour of pulp suspensions. To optimize various processes and process equipment in the pulp industry, it is necessary to understand the effects of such parameters on the rheology of fibre suspensions.

This chapter demonstrates that conventional rheological measurement techniques fail when used to study complex fluids such as pulp fibre suspensions. In addition, it is shown that the velocity profile determination techniques, when coupled with conventional rheometry, make a robust apparatus to investigate the rheological properties of such complex fluids.

We first study the steady-state flow curves of different types of pulp suspensions over a wide range of fibre mass concentration using conventional rheometry techniques. Next, ultrasonic Doppler velocimetry (UDV) is coupled with conventional rheometry to study the same suspensions. The effective rheological behavior of pulp suspensions are then inferred from these local measurements and compared with those deduced from conventional experiments. A Herschel-Bulkley model is used to fit both the velocity profiles obtained by coupled UDV-rheometry technique and the steady-state flow curves obtained by conventional rheometry. Finally, the effect of pH and lignin content (important parameters during the process of pulp fibre production) on the final rheological behavior of pulp fibre suspensions at different fibre mass concentrations are studied. Two types of pulp suspensions, one without lignin (softwood bleached kraft) and the other with lignin (thermal-mechanical pulp) at different fibre mass concentrations and pH levels are examined.

3.2. Materials and Experimental Testing

Pulp fibre suspensions were prepared at fibre mass concentrations of 1 to 5 wt.% using the procedure explained in section 2.3 of chapter 2. Hydrochloric acid and sodium hydroxide solutions of 0.1N were used to adjust the pH of 1, 3 and 5 wt.% SBK and TMP pulp suspensions at 4, 6, 8 and 10. Pulp suspensions were kept at these pH levels for 24 hours prior to the experimental testing.

To obtain the steady-state flow curves of pulp suspensions, conventional rheometrical tests were carried out with a stress-controlled Kinexus rotational rheometer (Malvern instruments Ltd, UK). Constant shear stress values were applied on the suspensions and the steady-state shear rate values were obtained. The flow curves were then constructed using data points obtained by the creep tests from a similar vane in large cup geometry to that described in chapter 2.

A Haake RV12 viscometer was coupled with a pulsed ultrasonic Doppler velocimeter (Model DOP2000, Signal Processing, Switzerland) to measure locally the velocity and the shear stress distribution across the gap simultaneously. Three rotational speeds of 2, 8 and 16 rpm were applied to assure the consistency of the data for all fibre suspensions of various mass concentrations. A Herschel-Bulkley (HB) constitutive model was used to fit the velocity profiles and to predict the measured steady-state flow curves obtained by conventional rheometry.

3.3. Results and Discussion

3.3.1. Conventional rheometry analysis

After pre-shearing all suspensions at conditions summarized in Table 2-2, different shear stress values were applied and the resulting steady-state shear rates were obtained. The steady-state flow curves were then constructed using all data points generated with this procedure. Figure 3-1 illustrates the results obtained for 2.5 wt.% pulp suspensions.

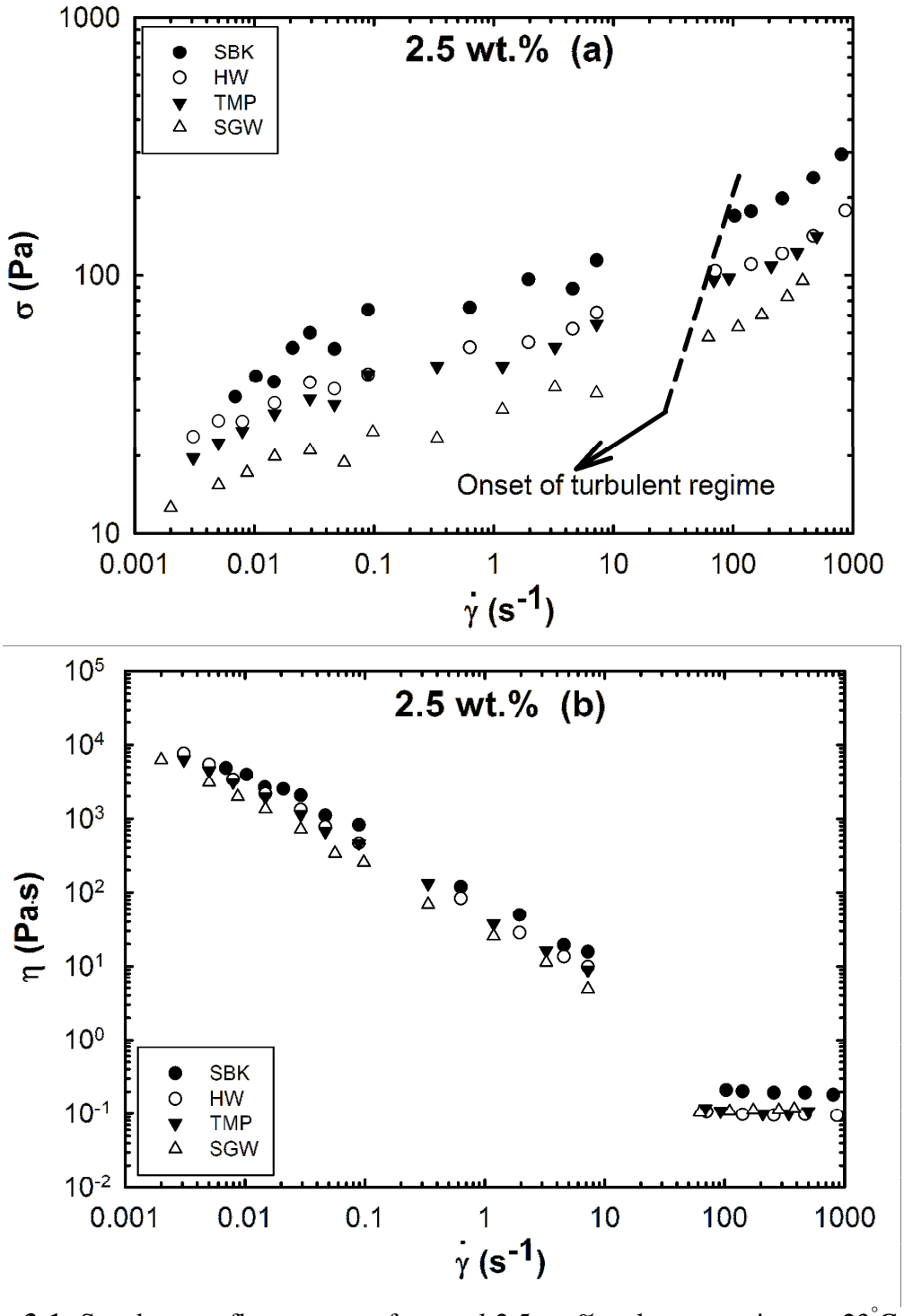

Figure 3-1: Steady-state flow curves of several 2.5 wt.% pulp suspensions at 23°C. Note that there is no sign of yield stress over the range of shear rates used.

Pulp suspensions are highly shear-thinning fluids above the apparent yield stress. By increasing the shear rate, fibre networks and fibre flocs rupture and the suspension flows more readily. This causes the shear-thinning behaviour of pulp suspensions over a wide range of shear rate, as can be seen from Figure 3-1b where the viscosity for all the 2.5 wt.% pulp suspensions is plotted as a function of the shear rate (essentially the data of Figure 3-1a).

However, reaching a certain high shear stress, pulp suspensions exhibit a Newtonian flow regime, which is referred to as the turbulent or fluidized regime (Kerekes, 1983; Bennington et al., 1991; Hietaniemi and Gullichsen, 1996). At this critical shear stress, pulp suspensions rupture at the edge of the vane resulting in a dramatic change in the measured shear rate. This can be clearly observed as a gap in the measured shear rate values in Figure 3-1a ($\dot{\gamma}\approx$10-50 s^{-1}) over which no measurements can be made. Entering this regime, a pulp suspension is sheared strongly along the axial and radial directions and individual fibres and different fibre flocs move separately in a random manner, while fluidized in the suspension (Bennington et al., 1991; Hietaniemi and Gullichsen, 1996; Chen, 1997). The shear stress at which pulp fibre suspensions begin to fluidize is referred to as the critical shear stress for the onset of turbulence or fluidization (Bennington et al., 1991; Chen, 1997). This critical shear stress, denoted by σ_d, is an important operational parameter in the pulp and paper industry as pulp suspensions are typically processed in the fluidized state to reduce the energy consumptions and the associated investment costs (Chen, 1997).

The critical shear stress values are extracted from the steady-state flow curves as the values at which Newtonian flow behaviour begins. These are listed in Table 3-1 and plotted in Figure 3-2 as a function of fibre mass concentration.

The dependency of the critical shear stress values on fibre mass concentration has been correlated using a power-law model ($\sigma_d = aC_m^{\ b}$). The resulting fitted constants are listed as an insert in Figure 3-2. It should be noted that similar correlations were derived for the apparent yield stress of these pulp suspensions, as described in chapter 2.

Table 3-1: Critical shear stress for the onset of turbulence or fluidization of pulp suspensions

	σ_d (Pa)			
C_m	SBK	HW	TMP	SGW
0.01	62	55	51	39
0.02	151	96	114	63
0.025	256	134	150	88
0.03	311	175	175	132
0.04	448	222	266	176
0.05	663	336	412	257

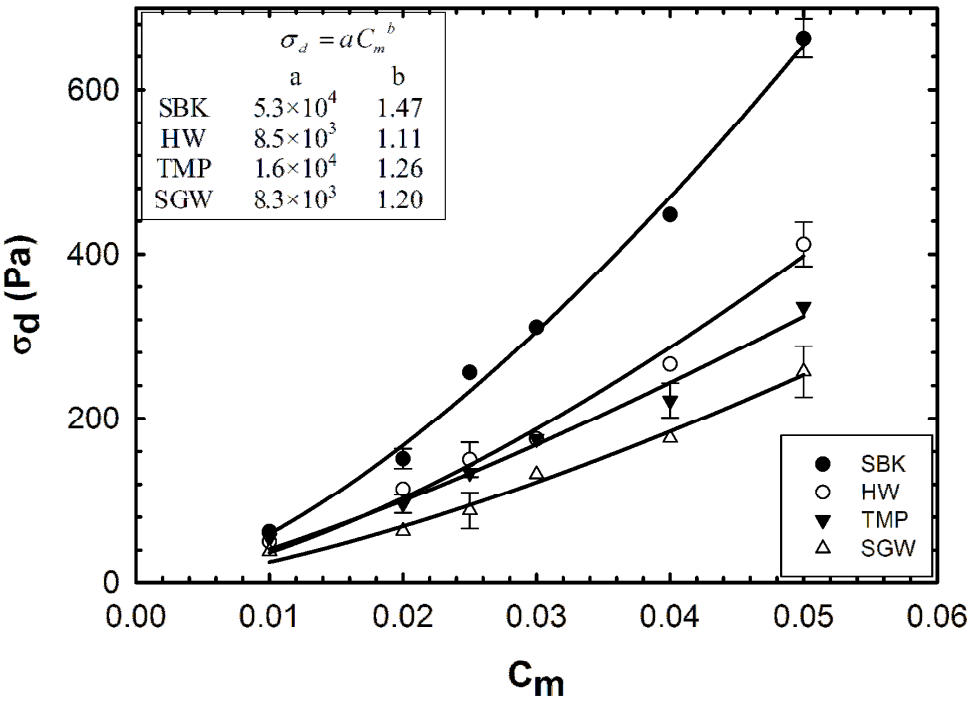

Figure 3-2: The critical shear stress values for the onset of turbulence or fluidization of several pulp suspensions as a function of fibre mass concentration. Solid lines are power-law fits with constants shown in the insert.

Pulp fibre suspensions exhibit yielding behaviour (Gullichsen and Harkonen, 1981; Bennington et al., 1990; Swerin et al., 1993; Wikström et al., 1998). However, the steady-state flow curves obtained using a conventional rheometrical technique exhibit apparent yield stress values which are significantly lower than those reported in chapter 2 and in some cases even show no sign of a yield stress, at least in the investigated range of shear stress values. The reasons for such a rheological behaviour are discussed in the next section where the local velocity profiles are obtained and used to study the rheology of such materials.

3.3.2. Velocity profile measurements

In this section the measured steady-state flow curves from conventional macroscopic rheological measurements (presented above) are compared with those deduced from the coupled UDV-rheometry technique. As discussed above an ultrasonic Doppler velocimeter was used to determine local velocity profiles of various pulp suspensions in conjunction with torque measurements with the Haake R12 rotovisco viscometer. A Herschel–Bulkley (HB) model (Eq. 3-1) was used along with Eqs. (2-5) and (2-6) to calculate the velocity profile across the gap of the rheometer (Eq. 3-2).

$$\sigma = \sigma_y + K\dot{\gamma}^n \tag{3-1}$$

$$u(r) = r\int_{r}^{R_y}\left(\frac{\mathrm{T}}{2\pi hr^2} - \sigma_y}{K}\right)^{\frac{1}{n}}\frac{dr}{r} \tag{3-2}$$

where σ_y, K and n are HB parameters and R_1 and R_y are the vane and the yielding radii while $R_1 \le r \le R_y$.

The integral expression of Eq. (3-2) was solved for all types of pulp suspensions at all investigated rotational rates in order to determine the HB constants, σ_y, K and n. The HB constants obtained from Eq. (3-2) were then used to describe the flow curves of pulp suspensions obtained by the conventional rheometry. Figures 3-3a-3d illustrate typical experimentally determined velocity profiles and their comparison with those determined numerically by using Eq. (3-2), for 3 wt.% pulp suspensions at three different rotational rates.

The velocity decreases across the gap, starting from a maximum at the vane tip and falling to zero at a certain distance referred to as the yielding radius R_y (Figure 2-1). The shear stress decreases in the gap according to Eq. (2-5). The suspension contained in the region between the vane tips and the yielding radius is in flow, while the fluid beyond this region remains stationary.

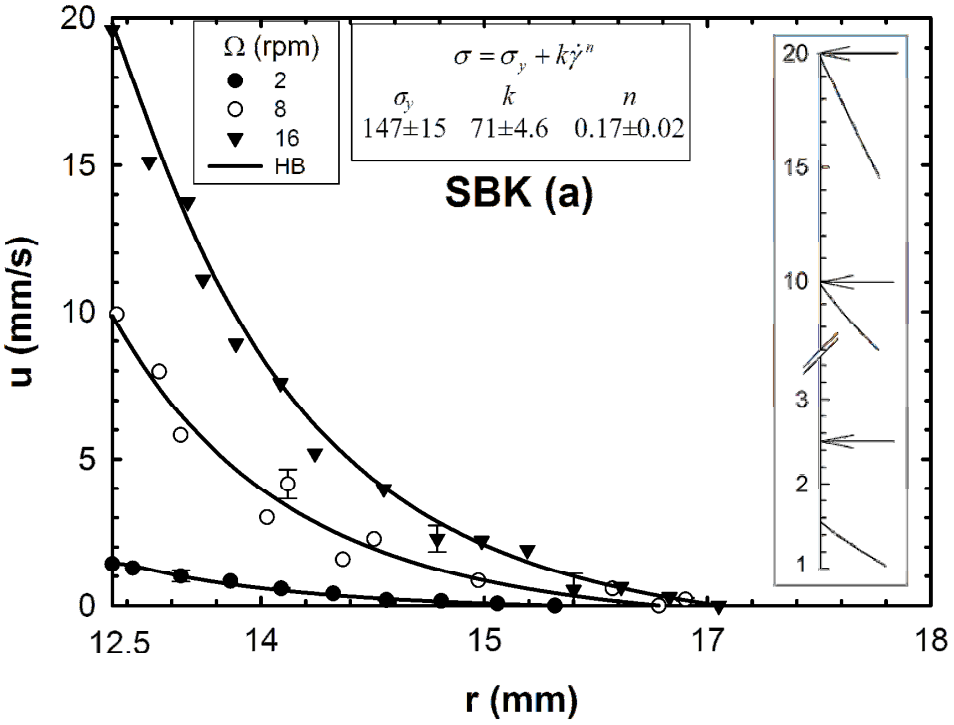
Ω (rpm)
2
8
16
HB
$\sigma = \sigma_y + k\dot{\gamma}^n$
σ_y k n
147±15 71±4.6 0.17±0.02
SBK (a)
u (mm/s)
r (mm)
0
5
10
15
20
12.5
14
15
17
18
1
2
3

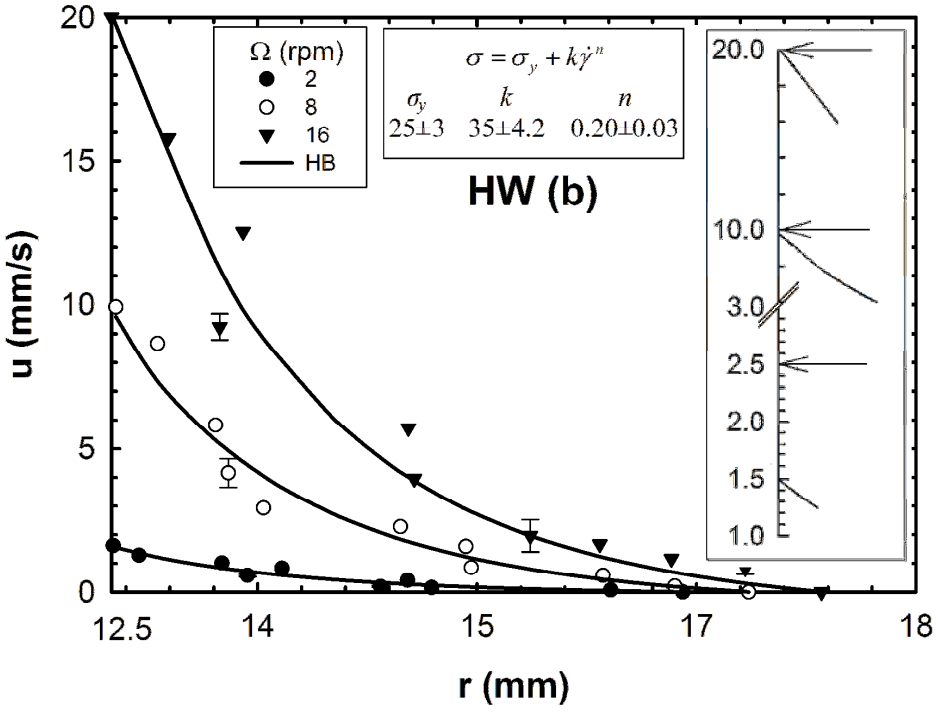
Ω (rpm)
2
8
16
HB
$\sigma = \sigma_y + k\dot{\gamma}^n$
σ_y k n
25±3 35±4.2 0.20±0.03
HW (b)
u (mm/s)
r (mm)
0
5
10
15
20
12.5
14
15
17
18
1.0
1.5
2.0
2.5
3.0
10.0
20.0

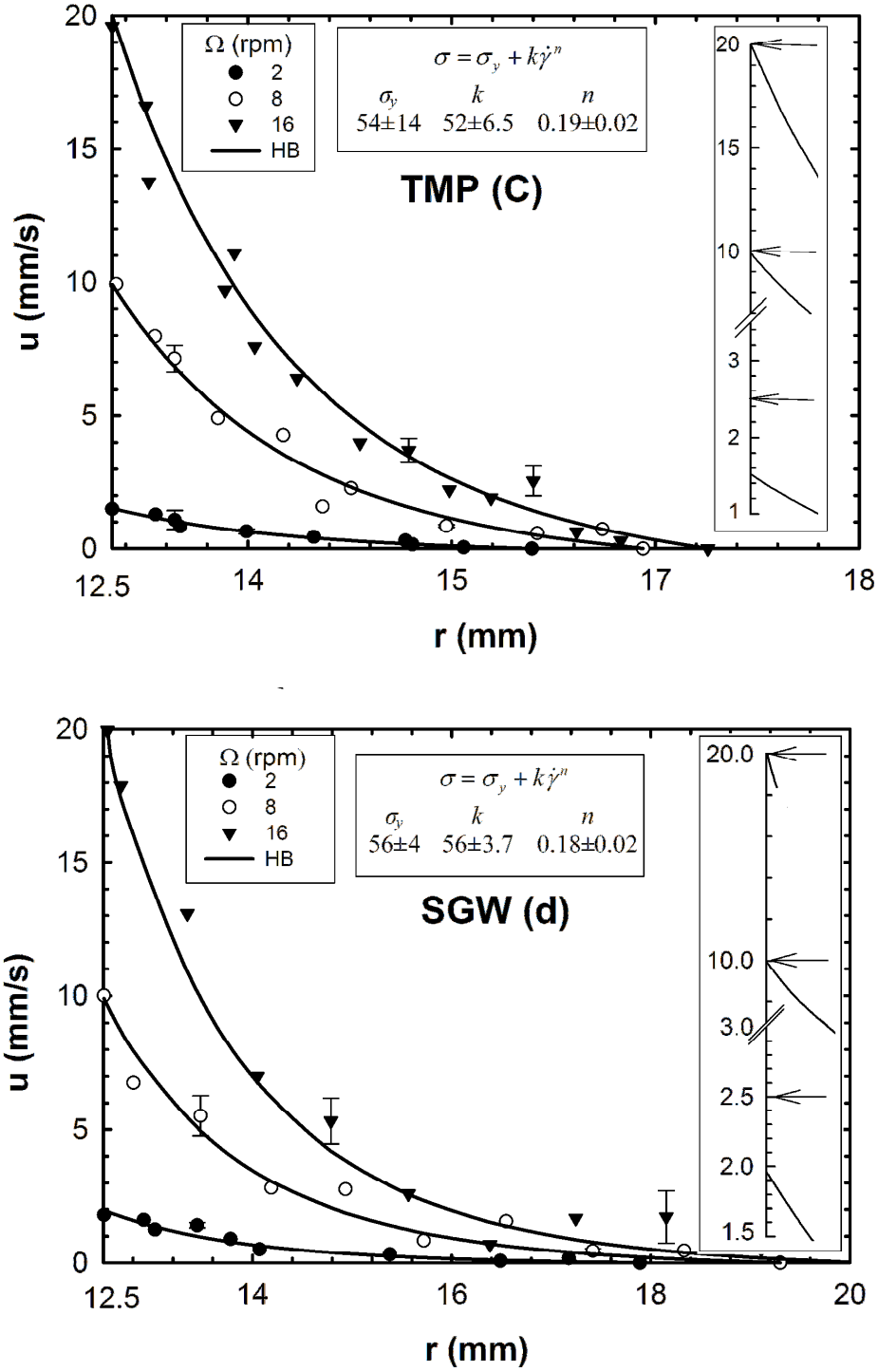

Figure 3-3: Velocity profiles across the gap for 3 wt.% suspensions of a) SBK, b) HW, c) TMP, d) SGW fibres at 23°C and three rotational speeds, namely 2, 8 and 16 rpm. The solid lines are fits of the Herschel-Bulkley model. Arrows in the insert indicate the nominal wall velocity which at low rotational speeds is lower due to the wall slippage. Error bars indicate the 95% confidence interval of the mean.

As referred to above, the solid lines in Figs. 3-3a-3d are the predictions of the HB model, in fact Eq. (3-2). The overall agreement between the HB model calculations and the experimentally measured velocity profiles is satisfactory. It is noted that the HB model with the same constants adequately predicts the velocity profiles obtained at different rotational rates.

Coupled UDV-rheometry technique revealed convincingly the yielding behavior in pulp suspensions and the apparent yield stress values predicted by the HB model are in agreement with those reported in chapter 2. Nevertheless, conventional rheometry is not always capable of detecting yielding behavior. This is due to apparent wall slippage that occurs at small rotational speeds as shown as an insert in Figs. 3-3a-3d, where the arrows indicate the linear speed at the vane surface based on the nominal rotational speed. While there is practically no apparent wall slippage (no difference between the nominal and actual linear speeds) at higher rotational rates (8 and 16 rpm), all types of pulp suspensions exhibit an apparent wall slip of around 20% at the lower vane rotational rate of 2 rpm. This behavior was also previously observed for nonadhesive concentrated emulsions (Bécu et al., 2006) and pastes of microgel particles (Meeker et al., 2004a).

In such cases, using local velocity measurement techniques to study the rheological behavior of complex fluids has many advantages over the conventional techniques. One of which is that the wall slip does not affect the experimental data. These techniques measure the actual bulk shear rates and calculate the shear stress using the basic momentum balance equations and the interpretation of the experimental data does not depend on any wall artefacts (Bécu et al., 2006).

The UDV-rheometry technique was also used to measure the local velocity profiles across the gap in the cup-and-vane geometry for pulp suspensions of different fibre mass concentrations. Figures 3-4a-4d illustrate the obtained velocity profiles and the calculations based on the HB model for all types of pulp suspensions.

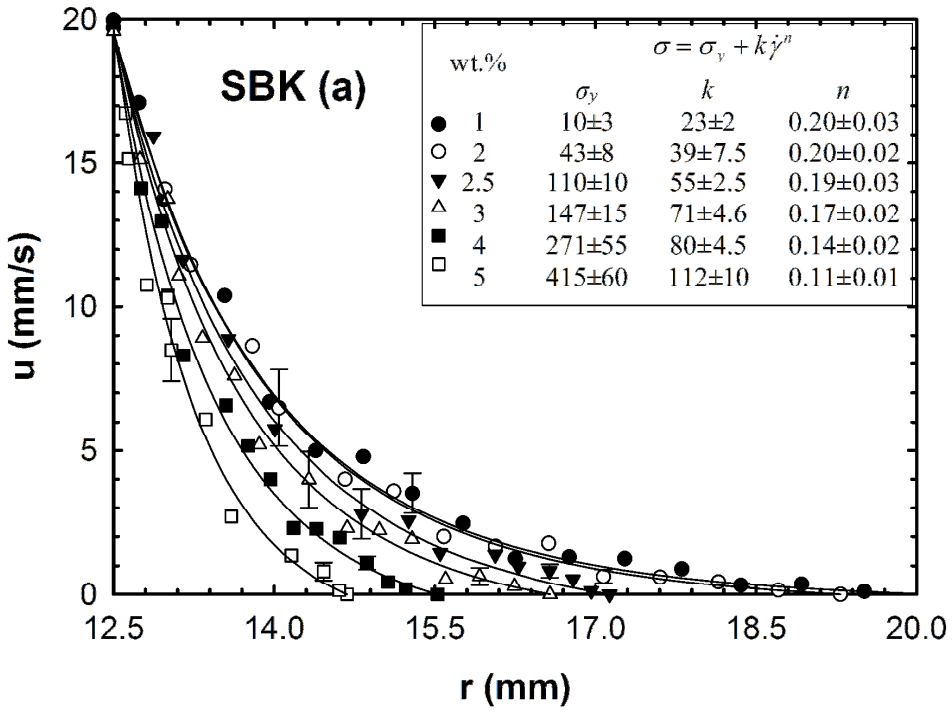
SBK (a)
$\sigma = \sigma_y + k\dot{\gamma}^n$
wt.% σ_y k n
1 10±3 23±2 0.20±0.03
2 43±8 39±7.5 0.20±0.02
2.5 110±10 55±2.5 0.19±0.03
3 147±15 71±4.6 0.17±0.02
4 271±55 80±4.5 0.14±0.02
5 415±60 112±10 0.11±0.01
u (mm/s)
r (mm)
0
5
10
15
20
12.5
14.0
15.5
17.0
18.5
20.0

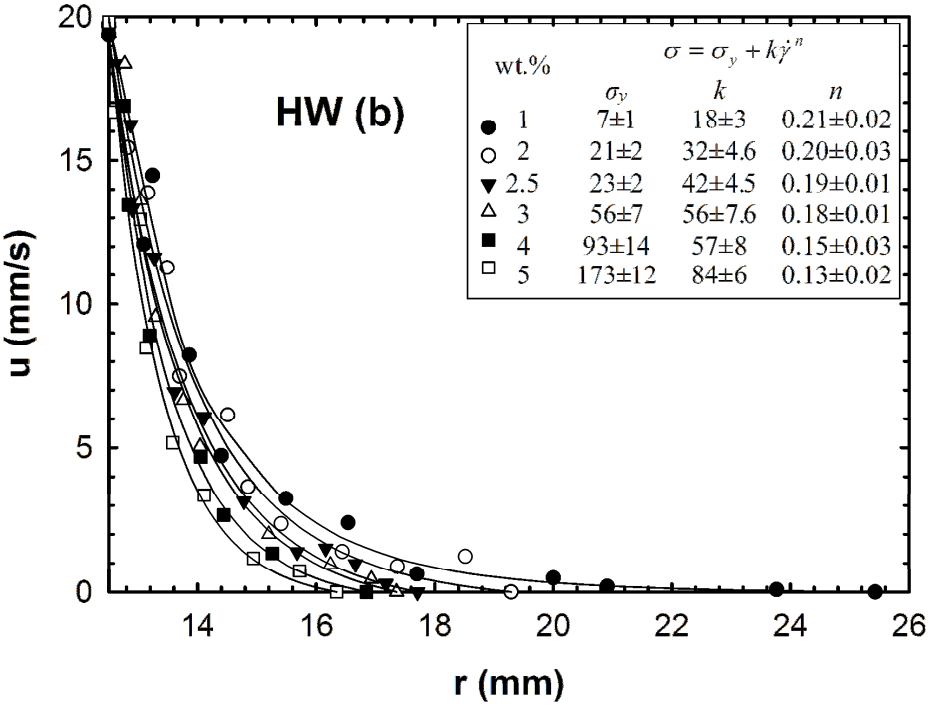
HW (b)
$\sigma = \sigma_y + k\dot{\gamma}^n$
wt.% σ_y k n
1 7±1 18±3 0.21±0.02
2 21±2 32±4.6 0.20±0.03
2.5 23±2 42±4.5 0.19±0.01
3 56±7 56±7.6 0.18±0.01
4 93±14 57±8 0.15±0.03
5 173±12 84±6 0.13±0.02
u (mm/s)
r (mm)
0
5
10
15
20
14
16
18
20
22
24
26

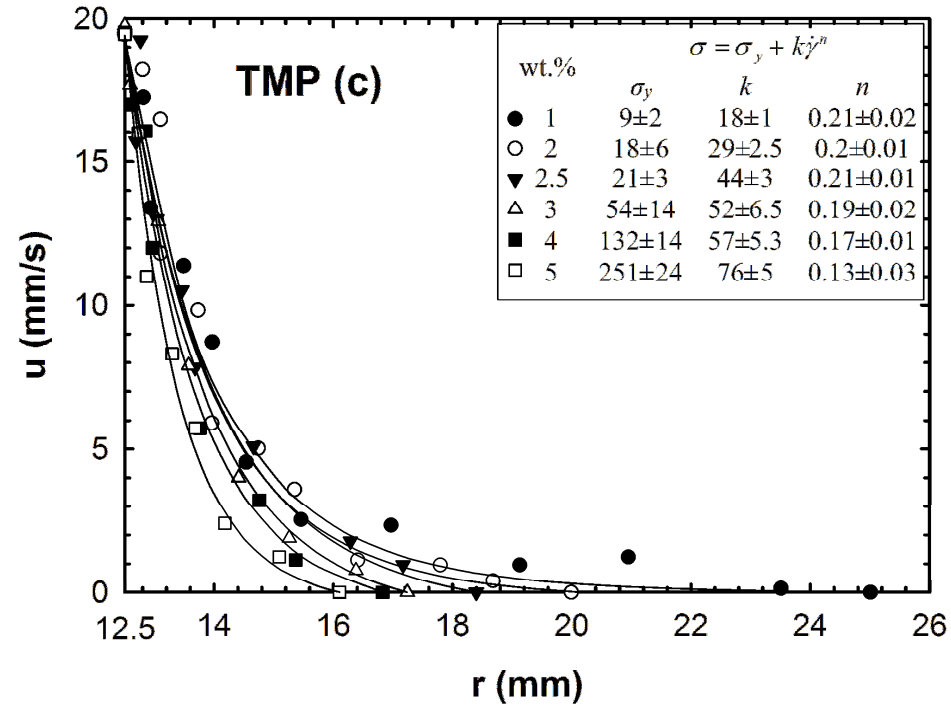

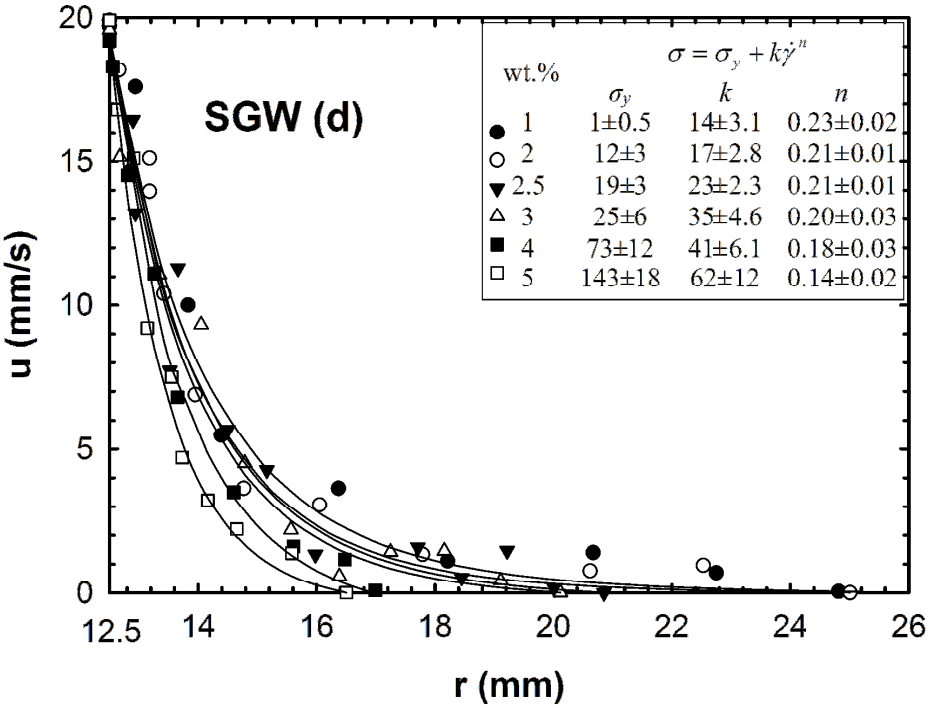

Figure 3-4: Velocity profiles across the gap for, a) SBK, b) HW, c) TMP, d) SGW pulp suspensions at 23°C, vane rotational rate of 16 rpm and several mass concentrations. Solid lines are the best fits to the data by the Herschel-Bulkley model with constants listed in the insert. Error bars indicate the 95% confidence interval of the mean.

Again, the HB model with the same constants accurately describes the experimentally measured data for different vane rotational velocities (three in total). However, as it was observed before in chapter 2, pulp suspensions at higher fibre concentrations exhibit a discontinuous transition through the yielding radius. This behaviour is studied in more detail in chapter 4. The resulting fitted HB constants are summarized in Table 3-2a-2d for all the investigated pulp suspensions and fibre mass concentrations.

The rheological behaviour of pulp suspensions depends on the physical properties of the fibres. Fibres tend to form networks due to a number of attractive forces, including colloidal, mechanical surface linkage, elastic fibre bending and surface tension, although mechanical entanglement is the greatest (Kerekes et al. 1983). Fibre properties, such as fibre length, flexibility and elastic modulus contribute to these forces and affect the rheological behaviour of the suspension.

More flexible and longer fibres permit greater contact between adjacent fibres, increasing mechanical linkages and therefore the apparent yield stress. Due to differences in fibre length and flexibility, the apparent yield stress and the flow curves decreases from SBK > TMP $\cong$ HW > SGW at a given mass concentration. Increasing suspension concentration increases the number of fibre entanglements, the strength of the fibre network formed and hence increases the apparent yield stress and the consistency index (K) while decreases the shear-thinning index (n) in the HB model (Table 3-2).

Table 3-2: Herschel–Bulkley constants for a) SBK b) HW c) TMP and d) SGW pulp suspensions as functions of the fibre mass concentration

a) SBK	$\sigma = \sigma_y + K\dot{\gamma}^n$		
	σ_y	K	n
0.01	10±3	23±2	0.20±0.03
0.02	43±8	39±7.5	0.20±0.02
0.025	110±10	55±2.5	0.19±0.03
0.03	147±15	71±4.6	0.17±0.02
0.04	271±55	80±4.5	0.14±0.02
0.05	415±60	112±10	0.11±0.01

b) HW	$\sigma = \sigma_y + K\dot{\gamma}^n$		
	σ_y	K	n
0.01	7±1	18±3	0.21±0.02
0.02	21±2	32±4.6	0.20±0.03
0.025	23±2	42±4.5	0.19±0.01
0.03	56±7	56±7.6	0.18±0.01
0.04	93±14	57±8	0.15±0.03
0.05	173±12	84±6	0.13±0.02

c) TMP	$\sigma = \sigma_y + K\dot{\gamma}^n$		
	σ_y	K	n
0.01	9±2	18±1	0.21±0.02
0.02	18±6	29±2.5	0.2±0.01
0.025	21±3	44±3	0.21±0.01
0.03	54±14	52±6.5	0.19±0.02
0.04	132±14	57±5.3	0.17±0.01
0.05	251±24	76±5	0.13±0.03

d) SGW	$\sigma = \sigma_y + K\dot{\gamma}^n$		
	σ_y	K	n
0.01	1±0.5	14±3.1	0.23±0.02
0.02	12±3	17±2.8	0.21±0.01
0.025	19±3	23±2.3	0.21±0.01
0.03	25±6	35±4.6	0.20±0.03
0.04	73±12	41±6.1	0.18±0.03
0.05	143±18	62±12	0.14±0.02

3.3.3. Comparison of the conventional rheometry and the UDV techniques

Figures 3-5a-5d compare the HB model predictions where constants were obtained from local velocity profile measurements (solid lines) with experimental data obtained from conventional rheometry. The HB model agrees well with the experimentally measured flow curves up to the onset of the turbulent regime. It should be noted that the term "turbulent" used here and in many other pulp and paper scientific journals should not be confused by the "turbulent" regime defined by the *Re* number (See chapter 1). At shear stress values close to the apparent yield stress, the data obtained by the conventional rheometry technique are all lower than those predicted by HB model and those obtained by velocimetry technique. This is clearly due to wall slip.

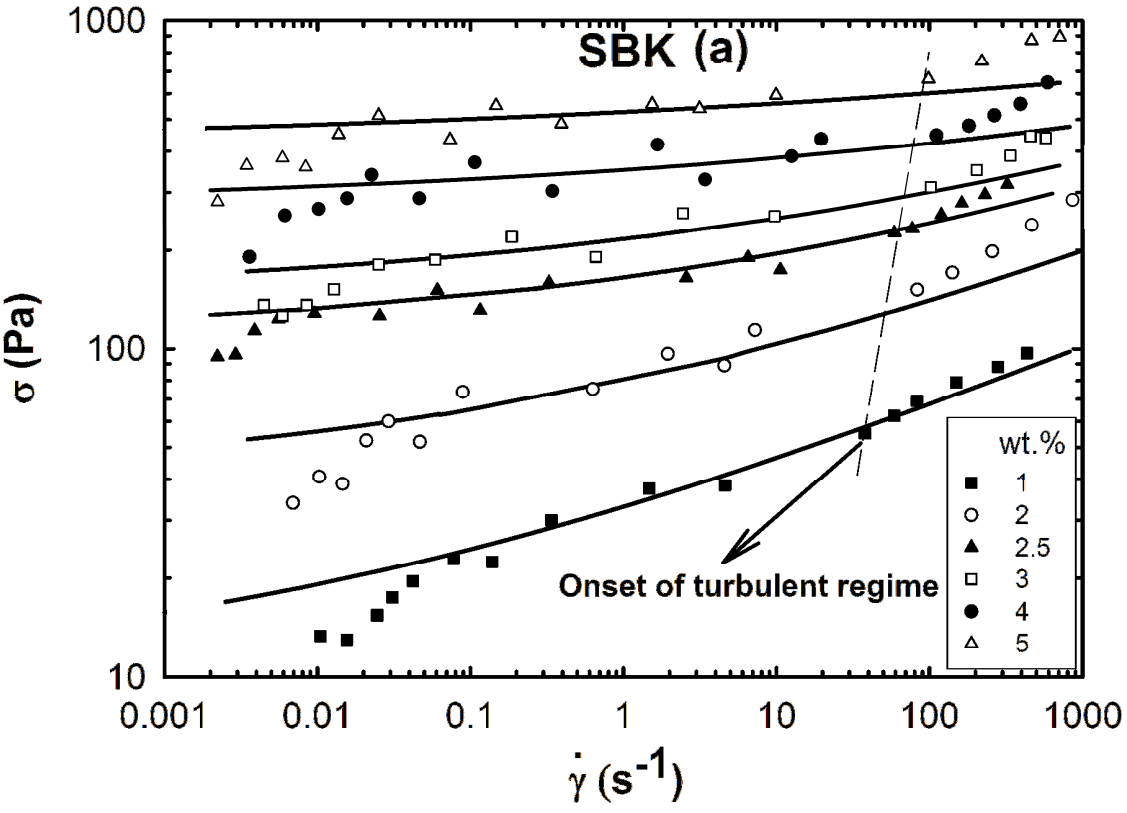

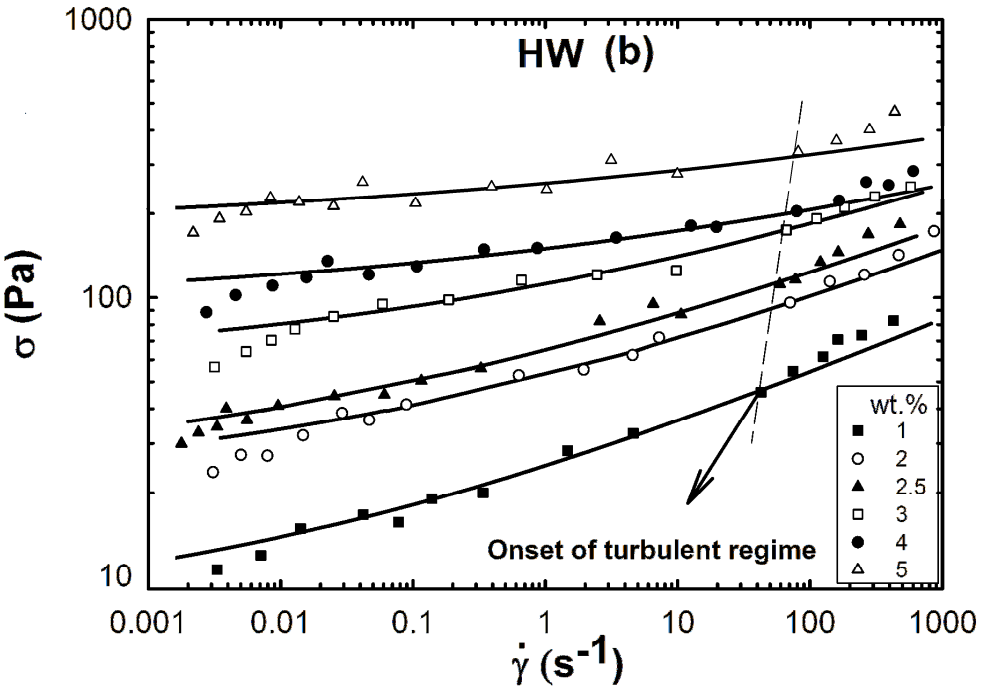
HW (b)
1000
100
10
σ (Pa)
0.001
0.01
0.1
1
10
100
1000
γ̇ (s-1)
wt.%
1
2
2.5
3
4
5
Onset of turbulent regime

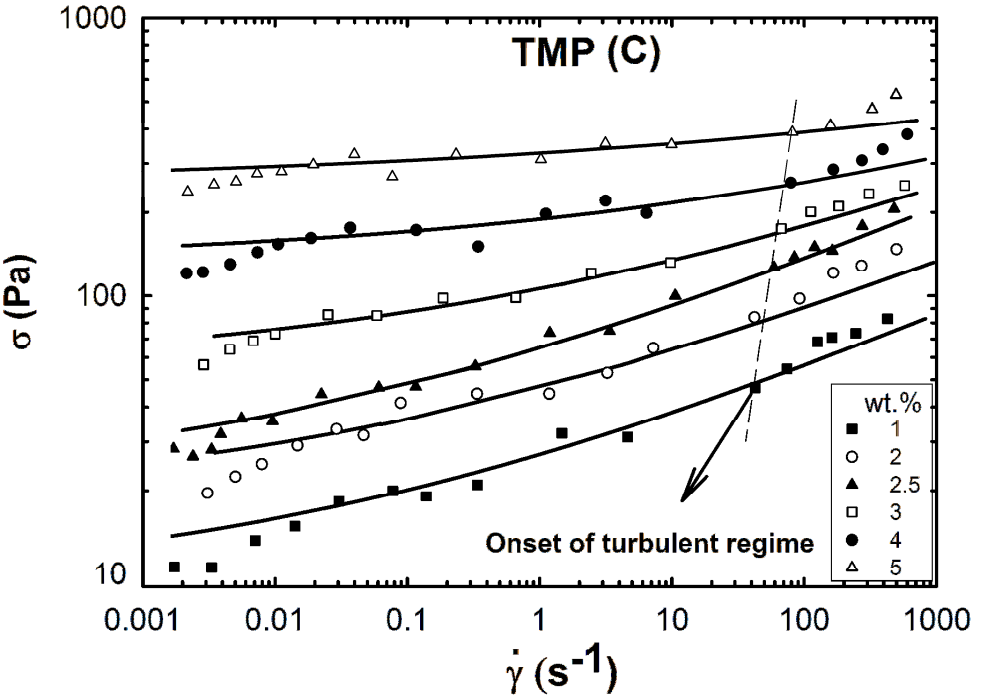
TMP (C)
1000
100
10
σ (Pa)
0.001
0.01
0.1
1
10
100
1000
γ̇ (s-1)
wt.%
1
2
2.5
3
4
5
Onset of turbulent regime

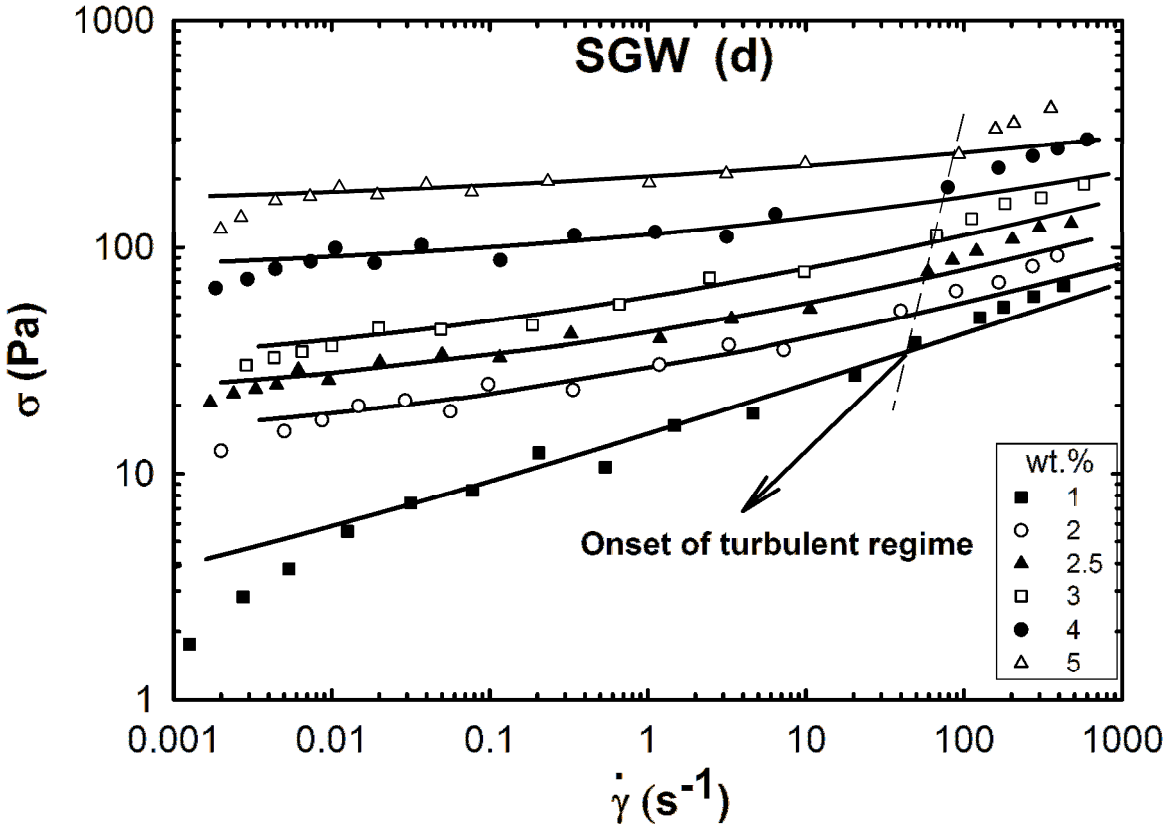

Figure 3-5: Steady-state flow curves for, a) SBK, b) HW, c) TMP, d) SGW pulp suspensions at 23°C and several mass concentrations. Solid lines are the predictions of the Herschel-Bulkley model with constants obtained from the fits to the local velocity profiles (see Figure 3-4). Note that there is a deviance from the Herschel-Bulkley model at low shear rates due to wall slippage.

During the flow of suspensions, particles/fibres cannot efficiently attach to the wall physically. This leads to the formation of a thin layer of fluid adjacent to the wall referred to as the "apparent slip layer" which has been observed in different types of suspensions and gels (Bramhall and Hutton, 1960; Vinogradov et al., 1975 and 1978; Coussot et al., 1993; Jana et al., 1995; Cloitre, 2000; Bertola et al., 2003; Meeker et al., 2004a,b; Kalyon, 2005). The influence of such a slip layer is more pronounced at low shear rates and is reduced as the shear rate increases.

Pulp suspensions are composed of large fibre flocs which make it difficult for them to sufficiently occupy the space adjacent to the vane. Therefore, a slip layer forms around the vane. Increasing the shear rate, some fibre flocs rupture into smaller flocs and into individual fibres. Fibres redistribute more evenly around the vane and thus wall

slippage is diminished since better contact between the vane and fibres is achieved. Due to the presence of wall slippage and the fact that the flow curves obtained by conventional rheometry technique are estimated from the wall velocity (arrows in the insert of Figs. 3-3a-3d), conventional rheometry results a different shear rate from the actual shear rate imposed to the fluid.

3.3.4. Effect of pH and lignin on the rheology of SBK and TMP suspensions

Fibre volume concentration and physical properties of fibres significantly influence the apparent yield stress of pulp fibre suspensions (Bennington et al., 1990). More specifically, increasing the fibre elasticity and/or the fibre aspect ratio enhances the fibre entanglement and the apparent yield stress of suspensions according to Eq. (1-7).

Coupled UDV-rheometry technique was used to obtain the velocity profiles of 1, 3 and 5 wt.% suspensions of SBK (without lignin) and TMP of the same fibre mass concentrations (with lignin) at vane rotational rates of 8 and 16 rpm. To examine the effect of pH, suspensions were prepared at fixed pH values ranging from 4-10 covering both acidic and alkaline regions. A Herschel-Bulkley rheological model was used to fit the obtained velocity profiles and the rheological parameters were then obtained as illustrated in Figures 3-6a,b and 3-7a,b for SBK and TMP suspensions respectively.

Generally, no significant change was observed in the rheological behaviour of suspensions over the acidic region. However, entering the alkaline region, the apparent yield stress σ_y and the HB consistency index K increased as a function of pH (see Figures 3-6a,b and 3-7a,b).

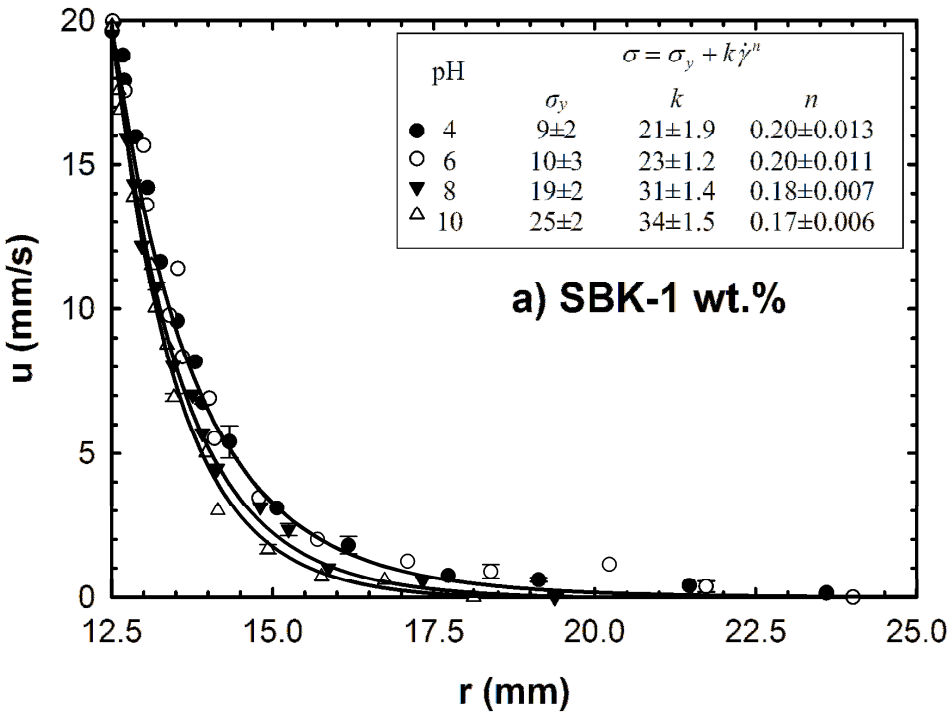

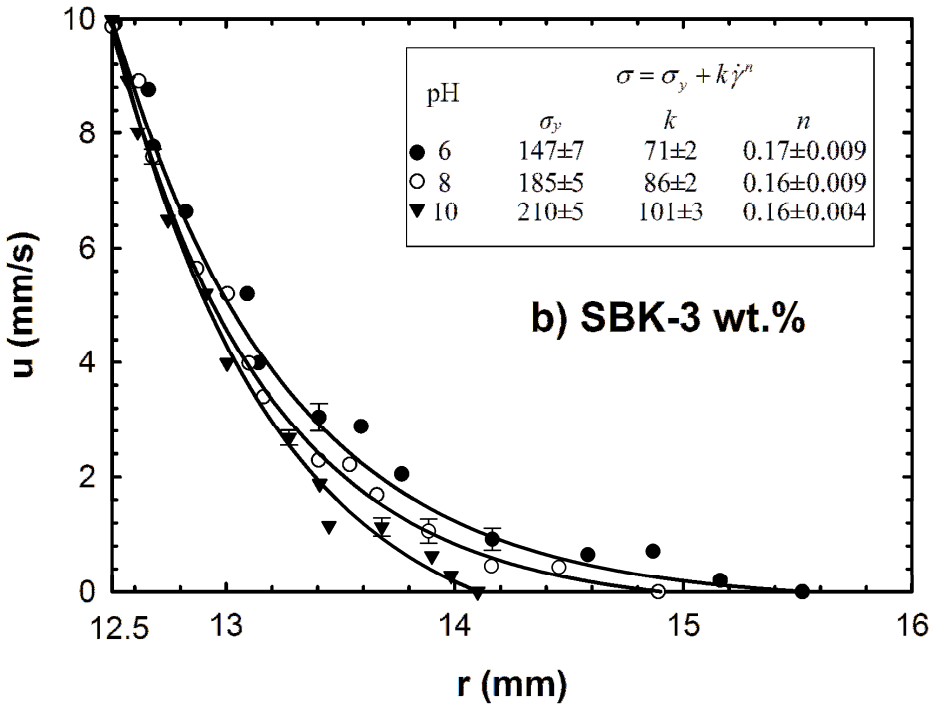

Figure 3-6: Velocity profiles across the gap for SBK at vane rotational rate of 16 rpm at a) 1 wt.%, b) 3 wt.%, pulp suspensions at 23°C and pH=4,6, 8 and 10. Solid lines are the best fits to the data by the Herschel-Bulkley model with constants listed in the insert. Error bars indicate the 95% confidence interval of the mean.

This behaviour is due to two reasons. First, as pH increases over the alkaline region, fibres swell and more flexible fibres are produced. The increased fibre flexibility promotes conformability, thus allowing the fibres to form more fibre-fibre contacts and to achieve stronger fibre networks (Toven, 2000). This in turn increases the suspension apparent yield stress and the HB consistency index. Second, the swollen fibres occupy a larger volume in the suspension; this results in higher fibre volume concentrations C_v hence increase the suspension apparent yield stress according to Eq. (1-7).

The percentage increase in the apparent yield stress σ_y and consistency index K of pulp suspensions at pH=6, 8 and 10 compared with those at pH=4 has been summarized in Table 3-3 for SBK and TMP suspensions. The dependency of the apparent yield stress on the pH of the suspension is more pronounced at lower fibre mass concentrations. This is due to the availability of more space between individual fibres which facilitates the fibre swelling process.

Pulp suspensions exhibit a considerable change in the rheological properties when pH increases from 6 to 8. However, further increase in pH from 8 to 10 does not affect the rheological properties significantly. This is probably due to the fact that fibres can only swell up to a maximum level regardless of the pH.

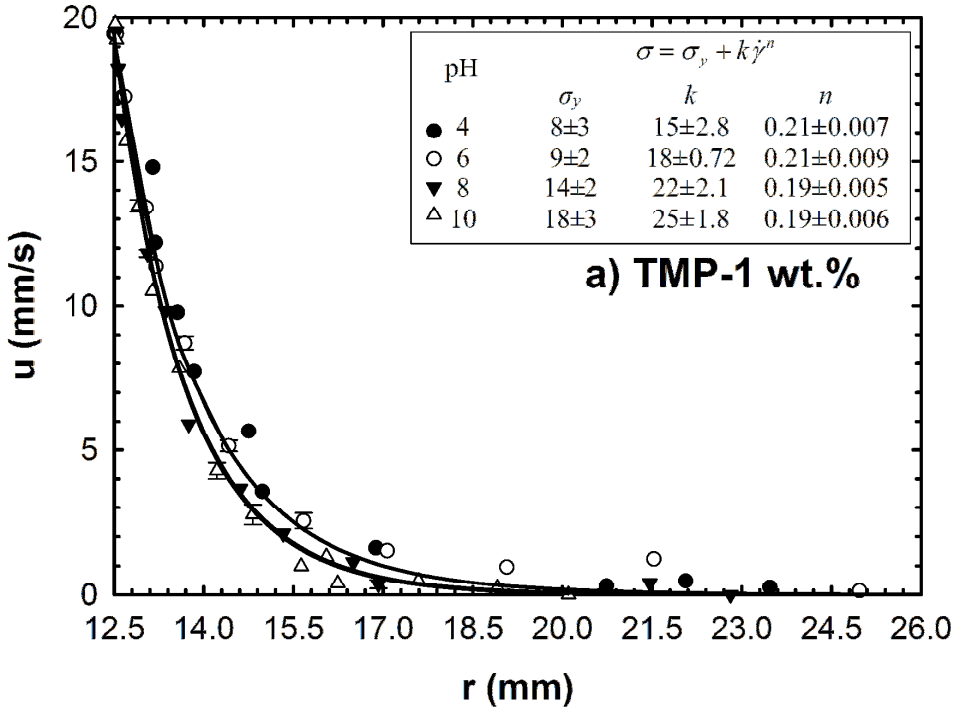

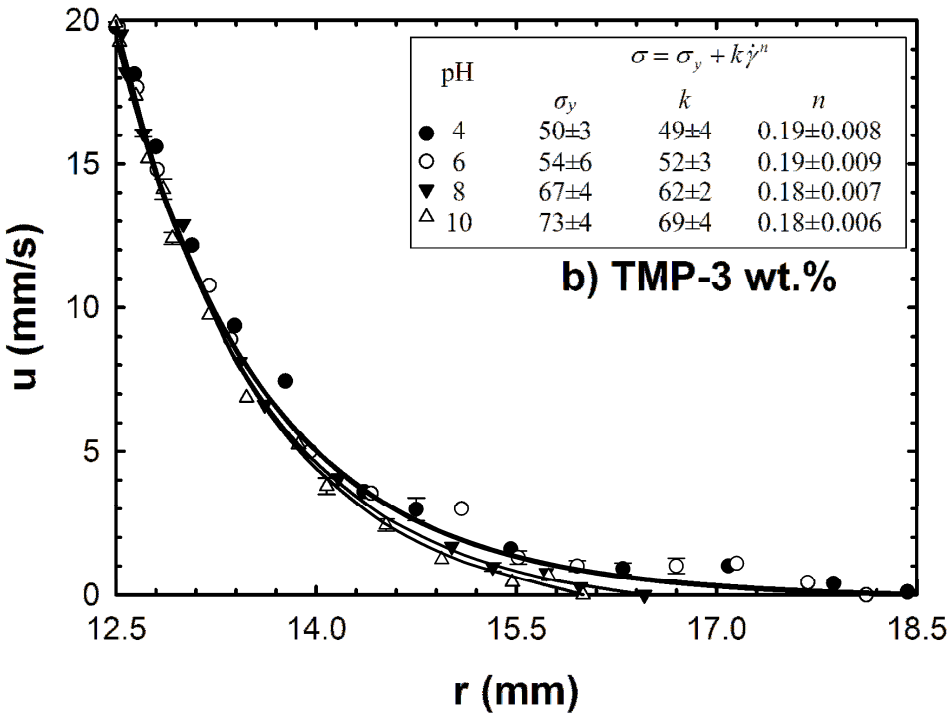

Figure 3-7: Velocity profiles across the gap for TMP at vane rotational rate of 16 rpm at a) 1 wt.%, b) 3 wt.%, pulp suspensions at 23°C and pH=6, 8 and 10. Solid lines are the best fits to the data by the Herschel-Bulkley model with constants listed in the insert.

Table 3-3: Percentage increase of the apparent yield stress and consistency index of a) SBK and b) TMP pulp suspensions compared with those at pH=4

a) SBK	*% increase compared with pH=4*					
	pH=6		pH=8		pH=10	
	σ_y	K	σ_y	K	σ_y	K
0.01	11	9.5	111	48	177	62
0.03	3.5	3	30	25	48	47
0.05	3.75	3.7	26.5	21	32	34

b) TMP	*% increase compared with pH=4*					
	pH=6		pH=8		pH=10	
	σ_y	K	σ_y	K	σ_y	K
0.01	12.5	20	75	46	125	66
0.03	8	6	34	27	46	41
0.05	4.8	5	75	7.5	86	19

Wood fibre is composed of various constituents one of which is lignin. Lignin is an amorphous, highly branched, three dimensional phenolic polymer, which lends rigidity and cohesiveness to the wood tissue (Biermann, 1996). Lignin serves as a glue to keep

fibres together in the wood matrix and maintains the rigidity of fibres. Due to these functions lignin removal enhances fibre swelling (Stone et al., 1968; Ahlgren, 1970; Lindstrom et al., 1980; Westman et al., 1981; Ehrnrooth, 1982). As seen in Table 3-3, the percentage increase in the apparent yield stress and the HB consistency index of TMP pulp suspensions are lower than those of SBK pulp suspensions at the same pH values. This is clearly due to the higher lignin content of the TMP fibres which makes them less susceptible to swelling.

These observations explain the importance of studying the rheological properties of pulp fibre suspensions under controlled experimental conditions. Differences in the suspension pH values and pulp fibre properties lead to different final rheological properties.

3.4. Summary

The rheological properties of pulp fibre suspensions using conventional rheometry and an ultrasonic Doppler velocimetry technique were studied. Increasing the fibre mass concentration, pulp suspensions were found to exhibit higher apparent yield stress and shear-thinning behaviour. More specifically, increasing the fibre mass concentration, the apparent yield stress and the consistency index in the HB model (K) were found to increase, while the power-law index in the HB model (n) was found to decrease.

Pulp suspensions were found to exhibit a Newtonian behaviour beyond a certain shear stress. The critical shear stress values required to begin the Newtonian regime were measured for several pulp fibre suspensions. The critical shear stress was found to depend on fibre mass concentration following a power-law dependence with exponents in the range of 1.1 to 1.47.

Data obtained by using conventional rheometry techniques (macroscopic measurements) suffer from wall artefacts despite the use of a vane in large cup geometry that is known to minimize wall slippage. Velocity profile measurements through the use of an ultrasonic Doppler velocimetry technique on the other hand, uniquely identify the real velocity distribution and yielding radius in the gap. This technique measures the actual bulk shear rate imposed on the fluid and calculates the shear stress using the basic

momentum balance equations, thus eliminating wall slip effects. Hence, this technique gives an accurate determination of the flow curves of complex fluids such as pulp suspensions. The velocity profile determination technique is useful to study other types of complex fluids such as biomass slurries and other types of fibre suspensions the rheology of which is not simple to be studied by conventional rheometry.

Apparent yield stress and HB consistency index were found to increase as pH increased over the alkaline region in both SBK and TMP pulp suspensions. This behaviour is attributed to the increase in the flexibility of pulp fibres as pH increases. The more flexible fibres make stronger fibre networks and produce higher fibre volume concentrations hence increase the apparent yield stress. Fibres with less lignin content are more susceptible to swelling, and as a result the rheological properties of fibre suspensions with less lignin content, exhibit stronger dependency on the suspension pH.

4. Thixotropy, Yielding and Ultrasonic Doppler Velocimetry in Pulp Fibre Suspensions[4]

4.1. Introduction

Thixotropy is the decrease of viscosity with time when a sample is sheared from rest and its subsequent recovery when flow stops (Schalek and Szegvari, 1923; Mewis and Wagner, 2009). Extensive studies of thixotropy have taken place and been reported in the scientific literature for various systems. Some noteworthy publications include the reviews of the field by Mewis (1979), Barnes (1997), and Mewis and Wagner (2009).

Due to the presence of microstructure within the sample, thixotropic materials often exhibit an apparent yield stress i.e. a minimum shear stress is required to rupture the structures and to initiate flow (Mewis and Wagner, 2009; Ovarlez et al., 2009). In other words, unless the apparent yield stress is exceeded, flow does not take place. In an ideal yield-stress fluid, the shear rate is constant or exhibits a continuous spatial profile and models such as Herschel-Bulkley, Casson or Bingham precisely predict the velocity profiles in a given geometry (Bonn and Denn, 2009).

However, most of the concentrated suspensions do not conform to this definition of apparent yield stress (Raynaud et al., 2002; Bonn et al., 2002; Baudez et al., 2004; Jarny et al., 2005). The presence of thixotropy and yielding is often associated with shear-banding. In this case, the shear rate profile exhibits an apparent discontinuity, i.e., the shear rate takes two significantly different values for the same shear stress (Coussot et al., 1993; Mas and Magnin, 1994; Pignon et al., 1996; Ovarlez, 2006). This can also be viewed as a pseudo phase separation, where the flowing complex fluid is spatially split into two regions bearing the same shear stress, one being the low-shear-rate and the other the high-shear-rate region. This is the banding instability that gives rise to a

[4] A version of this chapter has been published. Derakhshandeh, B., Vlassopoulos, D., Hatzikiriakos, S.G., 2011. Thixotropy, yielding and ultrasonic Doppler velocimetry in pulp fibre suspensions. Rheologica Acta doi:10.1007/s00397-011-0577-7.

discontinuous velocity profile (Olmsted, 2008; Dhont and Briels, 2008). Typically, this translates into a stress plateau region in the flow curve (Coussot et al., 1993). However, the inverse is not always true, i.e. the appearance of stress plateau in the flow curve does not necessarily mean that there is shear banding (Meeker et al., 2004a,b). Note also that often a thin slip layer is observed with slip velocities being a weak (power-law) function of the shear stress and it is unclear if banding occurs or not (Becu et al., 2006; Erwin et al., 2010; Coussot and Ovarlez, 2010). Wormlike micelles represent the most extensively studied and best understood shear-banding experimental system, which exhibits a strong shear thinning but typically no yield stress (Cates and Fielding, 2009). From the above it is evident that the field is very rich and there are different macroscopic reflections of shear banding, although the origin always appears to be the coupling of the system's order parameter to the flow field. A further remark is that there is often a distinction made between shear banding and shear stress localization. Whereas both reflect discontinuous velocity and discontinuous shear rate, the former is associated with the steady thinning flow curve and finite velocities in the two bands; on the other hand, the latter is the pseudo phase separation situation with a nearly zero or unsteady velocity branch and a finite velocity branch (Coussot, 2007). For the present purposes we shall call the velocity discontinuity banding, but note that it reflects coexistence behaviour.

Concentrated suspensions and pastes such as paint, mud and cement are known to be yielding and often thixotropic materials (Barnes, 1997; Raynaud et al., 2002). Shear-banding is often observed in these systems and, given the complex flow behaviour, a number of studies have been devoted to develop appropriate techniques to study their rheology. It is now well-known that velocimetry techniques such as magnetic resonance imaging (MRI), particle image velocimetry (PIV) and ultrasonic Doppler velocimetry (UDV) can be successfully implemented to study thixotropic systems (Raynaud et al., 2002), and shear-banding (Mas and Magnin, 1994; Callaghan, 2008; Manneville, 2008).

Generally, models such as Herschel-Bulkley (HB) have been used to represent the flow behaviour of pulp fibre suspensions at different fibre mass concentrations (Pettersson, 2004; Ventura et al., 2007). Chapter 3 of this thesis also indicates that the HB model adequately describes the velocity profiles and the flow behaviour of pulp suspensions. However, in some cases at higher fibre mass concentrations, the obtained

velocity profiles exhibited a discontinuous change in the slope at the interface between the yielded and un-yielded regions. This is typical behaviour of materials which exhibit shear banding (Olmsted, 2008).

As discussed in the previous chapters, pulp suspensions are heterogeneous systems containing millimetre-sized fibres and centimetre-sized fibre flocs. The discontinuity in the velocity profiles at the transition from the yielded to the un-yielded zone can also be due to the presence of large moving flocs in the layer next to the un-yielded region. In this case, UDV probes finite velocities for the moving fibre flocs and drops to zero in the next layer. Therefore, at this point it is not clear, whether pulp suspensions display shear banding as they go through yielding transition.

The literature review presented in chapter 1 indicates that past works have generally focused on the apparent yield stress measurement, post-yield flow behaviour and some particular aspects of pulping or papermaking. One aspect that has not been addressed to date is measurement and analysis of thixotropy and possible shear-banding effects in pulp suspensions, particularly the more concentrated ones.

This chapter addresses the time-dependent rheology of concentrated pulp suspensions with emphasis on thixotropy, viscosity bifurcation and shear-banding. Ultrasonic Doppler velocimetry (UDV) is used to explore the velocity profiles across the gap of a vane in large cup geometry in order to study the yielding transition in pulp suspensions. The velocity profiles are then used to propose a model to describe the behaviour of pulp sheared in the yielded region. In this chapter, we study a 6 wt.% pulp fibre suspension higher than those used in the previous chapters since the phenomena of thixotropy and shear banding are more dominant at high mass concentrations.

4.2. Materials and Experimental Testing

Pulp fibre suspensions of 6 wt.% were prepared from stone-ground wood (SGW; Paprican, Pointe-Claire, QC) using the procedure explained in section 2.3 of chapter 2. The pulp fibre properties are also summarized in Table 2-1. Having shortest fibres and

least extent of flocculation amongst commercially available pulp fibres, SGW pulp suspension is an ideal candidate for this study.

A stress-controlled Kinexus rotational rheometer (Malvern instruments Ltd, UK) was used to perform all the rheological experiments with a vane in large cup geometry similar to that described in chapter 2. As we make use of a wide gap Couette geometry, different sets of torque-rotation velocity are required to calculate the shear rate within the gap using Eq. (4-1) (Coussot, 2005):

$$\dot{\gamma}(\sigma_1, t) = 2\mathrm{T}\left(\frac{\partial \Omega}{\partial \mathrm{T}}\right)_t \tag{4-1}$$

where T is the applied torque on the vane corresponding to shear stress σ_1 and Ω is the vane rotational velocity at time t.

We are limited to such a more complicated approach as simpler common geometries such as parallel-plate and cone-plate geometries fail when used to study pulp suspensions as discussed before. Rheological experiments include hysteresis loops, apparent flow curves by applying shear stress ramps, transient experiments by changing the shear stress in a stepwise manner and creep experiments.

In order to measure the local velocities within the suspension, a rate-controlled Haake RV12 viscometer equipped with a vane geometry (see details in section 2.2 of chapter 2) was coupled with a pulsed ultrasonic Doppler velocimeter (Model DOP2000, Signal Processing, Switzerland). As discussed in chapter 3 at low rotational rates of less than 2 rpm wall slippage occurs at the tip of the vane. On the other hand, at high rotational rates the pulp becomes fully fluidized, and it becomes difficult to obtain accurate velocities as the data become noisy. Therefore, to prevent these two effects, vane rotational speeds of 8, 16 and 32 rpm were selected to examine the behaviour of the samples. These were found to be appropriate rates based on the signals obtained from UDV and the rheological response of pulp suspensions. Applying these rotational rates, the velocity profiles were measured at both steady-state and transient conditions.

4.3. Results and Discussion

4.3.1. Hysteresis loops

A typical experiment to study thixotropy is the measurement of the hysteresis loop. In this measurement, the shear stress or shear rate is increased and then decreased continuously or in small steps. A thixotropic material exhibits a hysteresis loop as shown in Figure 4-1 for a 6 wt.% pulp fibre suspension. In the hysteresis experiment, the flow time induced by the rheometer should be shorter than that required for structure build-up (Beris et al., 2008; Coussot and Ovarlez, 2010). In our measurement, the shear stress was increased linearly from 50 Pa to 350 Pa with a ramp rate of 1 Pa/s to ensure flow times shorter than the time required to build-up structures within the sample. This will be confirmed later by the results obtained from transient experiments.

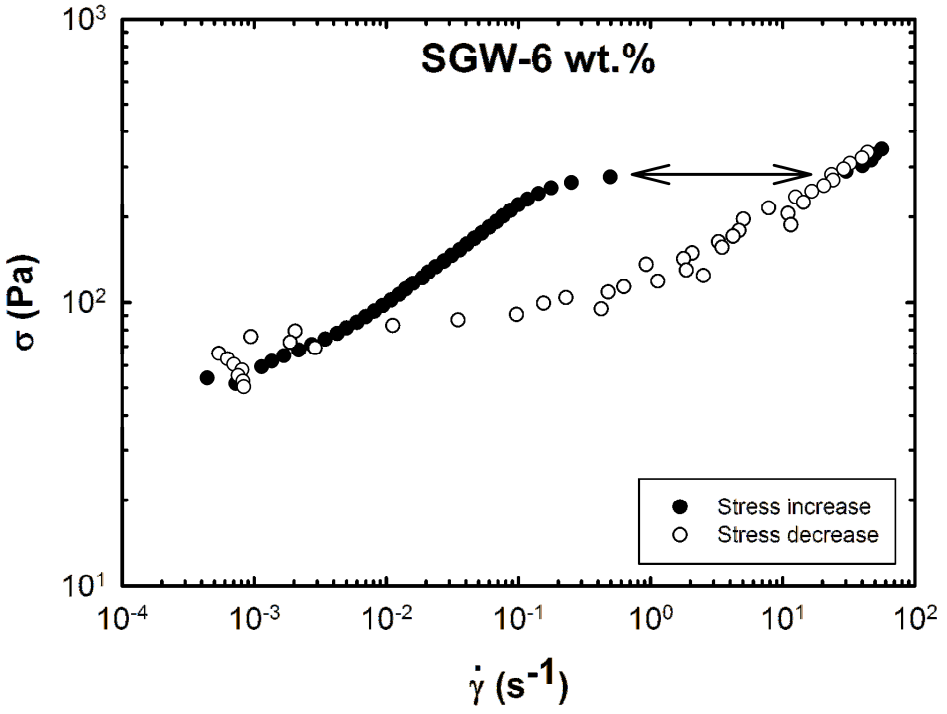

Figure 4-1: Hysteresis loop for 6 wt.% pulp fibre suspension. Sample was pre-sheared at 350 Pa for 2 minutes followed by 20 minutes rest. Shear stress increased from 50-350 Pa in 300 s and decreased over the same time frame. The arrow indicates the plateau in the flow curve from 6 to about 18 s^{-1}.

A limitation of hysteresis experiment is that it is not possible to differentiate the effects of time and shear rate as both contribute in the experimental testing (Bird and Marsh, 1968; Mewis and Wagner, 2009). Therefore, other characterization tools are required to confirm thixotropy. Nevertheless, there are two interesting observations in the hysteresis loop of pulp suspension plotted in Figure 4-1. First, at a shear stress of ~278 Pa the shear rate jumps from about 6 to about 18 s^{-1} generating a plateau in the flow curve (the arrow in Figure 4-1). The presence of a plateau in the flow curve is known to be due to either wall slip (Hatzikiriakos and Dealy, 1992) or shear-banding (Coussot, 2005; Olmsted, 2008), an effect which has also been observed in many pasty materials (Coussot et al. 1993, 2010). This is examined in more detail later.

Secondly, based on the shape of the hysteresis loop (Figure 4-1) at low shear rates it can be concluded that low shear rates induce structure formation within the pulp suspension (Kanai and Amari, 1995). The hypothesis is that at lower shear rates the deformation is not large enough to either break-down or align the fiber domains. Instead, smaller fibre flocs merge to make structures (domains) of larger dimensions and individual fibres collide to make and/or be incorporated into the fibre flocs. In contrast, at high shear rates the upward and downward flow curves overlap as pulp adopts the same state of structures.

Next, the effect of rest time (before measurement) on the rheological behaviour of pulp suspension is investigated. In the field of glassy suspensions (a particular, much-studied class of structured systems) this time is called waiting time. Samples were pre-sheared with a shear stress of 350 Pa for 2 minutes and then left to rest for different time periods of 2, 5, 10 and 20 minutes prior to be subjected to a shear stress ramp to obtain the flow curves. It should be noted that the pre-shearing stress of 350 Pa is in the thinning regime (Figure 4-1) where the sample is fully fluidized to ensure rupturing of the structures within the sample. In the case of pulp fibre suspensions, it is not feasible to estimate the relaxation times by means of linear viscoelasticity studies due to the limitations associated with sample loading into the rheometer as discussed above. Nevertheless, it is suggestive that relaxation times are ultra-long, as expected in pasty materials and suspensions (Coussot et al., 2005). Therefore, to appropriately select different rest times, the first two time periods (2 and 5 min) were selected close to each

other to check reproducibility of the time effects, while the other two time periods were chosen to be further apart to provide more information on the time-dependent rheology of pulp taking into account proper experimental conditions (e.g. not too long in order to avoid evaporation problems).

The results (various flow curves corresponding to various rest times) are plotted in Figure 4-2. As the rest time increases, the flow curves shift upward, i.e. the viscosity increases with rest time, presumably reflecting structure build-up. Pre-shearing the suspension ruptures the structures within the sample and makes the fibres to orient. However, left at rest for sufficient period of time, fibres settle, but given their vast polydispersity, they form a 3D network which is swollen with water throughout the sample. In this case, the sample should be very shear-thinning as shown in chapter 3. This also explains the increase in the viscosity of the suspension with rest time. Here again, there exists a plateau in the flow curves of pulp suspension the level of which strongly depends on the shear history and particularly on the rest time prior to the measurement. Moreover, flow curves overlap at high shear rates as the fibre structures in the suspension are ruptured and/or aligned, at least partially, to the same extent.

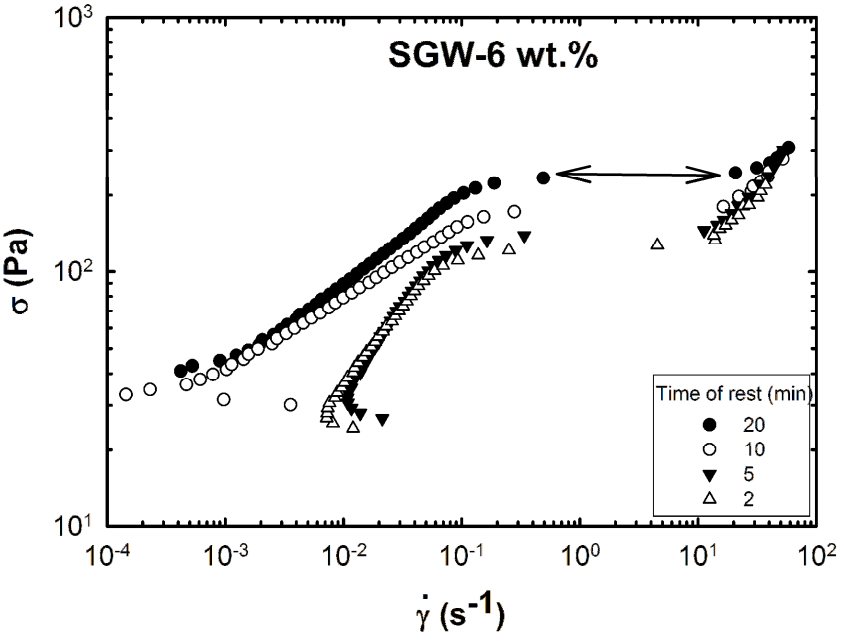

Figure 4-2: Apparent flow curves of pulp fibre suspension. Samples were pre-sheared at 350 Pa for 2 minutes followed by 2, 5, 10 and 20 minutes rest. The arrow indicates the plateau in the flow curve.

4.3.2. Transient behaviour during shear flow

To independently study the effect of time and shear history on the behaviour of pulp suspension, a preferred experiment is to apply step changes in the shear stress/shear rate and measure the transient change of the shear rate/shear stress until a steady-state is reached. Therefore, here in contrast to the hysteresis loop technique, the relative effects of time and shear can be easily decoupled and resolved. This is typical of the approach followed in thixotropic suspensions (Erwin et al., 2010).

4.3.2.1. Build-Up Behaviour

Pulp suspension was first sheared at initial shear stress values of σ_i=350 and 370 Pa (both in the thinning regime of Figure 4-1) until steady-state shear rates were achieved. This ensures the well-defined initial state of the sample prior to any further experimental testing. To study the kinetics of structural growth during shear, shear stress was then suddenly reduced to σ_e=280, 285, 290 and 300 Pa and the evolution of viscosity with time was followed as shown in Figures 4-3a and 4-3b for σ_e=280 and 300 Pa respectively. During the decrease of the shear stress from σ_i to σ_e, the viscosity increased to a new steady-state as microstructures evolved in the suspension. It should be noted that a pulp suspension, regardless of the magnitude of the initial applied shear stress σ_i, adopts the same final steady state viscosity (Figure 4-3a and 4-3b). This clearly shows the reversibility of the process, an essential element of thixotropy. These observations indicate that the pulp fibre suspension is a thixotropic material. It is presumed that increasing the fibre concentration, fibre size and flexibility increase the extent of thixotropy in pulp suspension, although these have not been examined here.

In such a flocculated system, the final equilibrium state is governed by a number of parameters which facilitate structuring and/or destructuring. These parameters are in principle of two kinds: hydrodynamic shear stresses which pull the structures apart, but also occasionally collide them, and Brownian motions (Mewis and Wagner, 2009). These parameters are often incorporated into the constitutive equations to model thixotropy by means of a variable structure parameter. The variable structure parameter depends on the

actual state of the structure, evolves with the flow history and is often described with the help of a kinetic equation (Coussot, 2007, and references therein).

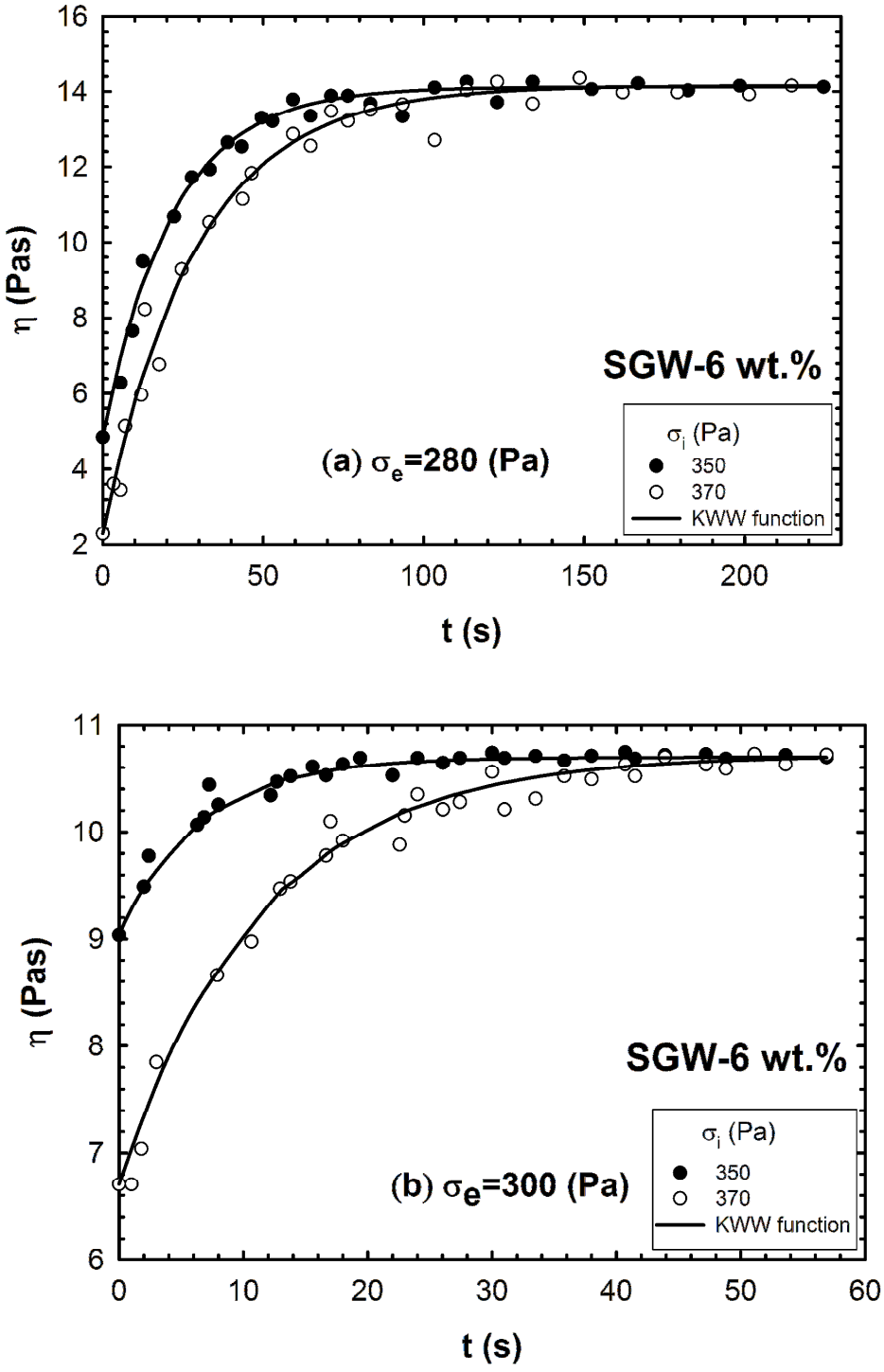

Figure 4-3: Structure build-up in pulp suspensions from initial shear stresses of σ_i=350 and 370 Pa to (a) Sudden decrease of the shear stress to σ_e=280 Pa (b) σ_e=300 Pa. Solid lines show the fits of a KWW function.

The contribution of the Brownian motions relative to the hydrodynamic forces in a dilute system can be expressed by the Peclet number:

$$Pe = \frac{\dot{\gamma}}{D_r} \tag{4-2}$$

where D_r is the rotary diffusion coefficient for a fibre given (Macosko, 1994) by:

$$D_r = \frac{3k_B T\left(\ln 2\frac{l}{d} - 0.5\right)}{8\pi\eta_s l^3} \tag{4-3}$$

where k_B is the Boltztmann constant, T is the absolute temperature, η_s is the medium viscosity, l and d are the fibre length and diameter respectively. We have calculated this number for the pulp suspension to evaluate the extent of the Brownian motions although the pulp suspension used in this study is a concentrated system. The contribution of the Brownian motions to structure build-up in pulp is negligible as Pe number will be in the order of 10^9 for the smallest particles i.e. l=0.07 mm (Table 2-1). Therefore, the transient response of pulp suspension to a sudden change in the shear stress is expected to be mainly governed by the strain-induced rearrangements. This will be studied in more detail as we try to quantify the transient behaviour.

In order to quantify thixotropy, the transient response of the sample (Figures 4-3a and 4-3b) was fitted to a stretched exponential or Kohlrausch-Williams-Watts (KWW) function (Eq. 4-4):

$$\eta = \eta_0 + (\eta_\infty - \eta_0)\left(1 - e^{-\left(\frac{t}{\tau}\right)^\beta}\right) \tag{4-4}$$

where η_0 and η_∞ are the suspension viscosity prior and after shearing while τ and β (often assumed to be equal to 1) are constants (Barnes, 1997).

The KWW function was found to adequately describe the structural growth of pulp suspension during shear as shown by the solid lines in Figures 4-3a and 4-3b. The corresponding characteristic times (τ) obtained from Eq. (4-4) are summarized in Table 4-1 for samples at different initial and final flow conditions.

Table 4-1: Thixotropic time constants for build-up

Build-up			
Initial shear stress, σ_i=350 (Pa)		Initial shear stress, σ_i=370 (Pa)	
Final shear stress, σ_e (Pa)	Thixotropic time constant, τ (s)	Final shear stress, σ_e (Pa)	Thixotropic time constant, τ (s)
280	21.6	280	28.8
285	19.8	285	23.7
290	12.0	290	17.4
300	5.8	300	11.4

In samples sheared at the same initial shear stress, σ_i, the corresponding characteristic time (τ) decreases linearly as the final shear stress σ_e increases. This again indicates that the structure build-up in pulp suspension is governed by shear-induced collisions. The same dependency between the characteristic times and the magnitudes of the final shear stress was observed before for bentonite dispersions (Mylius and Reher, 1972), thixotropic fumed silica dispersions (Dullaert and Mewis, 2005) and layered-silicate montmorillonite suspensions (Mobuchon et al., 2007). It should be noted that the stretching exponent β in Eq. (4-4) was independent of the flow history and remained constant close to 1 for all measurements. In other words the structure build-up in pulp fibre suspensions is a single exponential process and can be characterized by one characteristic time. This indicates that pulp fibre flocs have a narrow size distribution in the suspension.

Figures 4-3a, 4-3b and Table 4-1 show that pulps which were initially sheared at a lower shear stress of σ_i=350 Pa evolve faster with shorter characteristic times compared with those sheared at σ_i=370 Pa. Suspensions pre-sheared at lower shear stress include more developed structures and thus respond faster during the structure growth process. Next we study the structure breakdown in pulp suspensions.

4.3.2.2. Structure Breakdown

A similar procedure as above was followed to study the flow induced breakdown of structures in pulp suspensions. Samples were pre-sheared at two different initial shear stress values of σ_i=100 and 200 Pa until a steady-state shear rate was achieved. Shear

stress was then suddenly increased to σ_e=280, 300, 320 and 350 Pa and the transient change in the viscosity with time was followed.

Figure 4-4 reports the transient change in pulp viscosity for jumps from σ_i=100 Pa to different final shear stress values. Here again the same empirical KWW functions of Eq. (4-4) were fitted to the data (solid lines in Figure 4-4) with constants given in Table 4-2. This model adequately describes the kinetics of the structure breakdown with stretching exponents of close to 1.

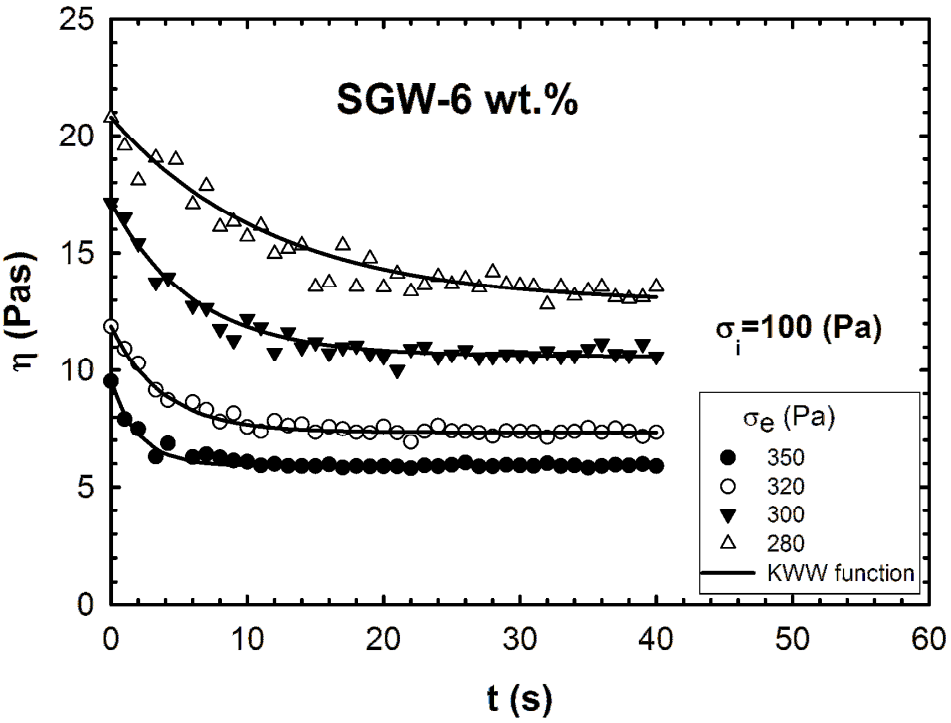

Figure 4-4: Structure breakdown in pulp suspensions from an initial shear stress of σ_i=100 Pa to 280, 300, 320 and 350 Pa. Solid lines show the fits of a KWW function.

Generally, the characteristic times obtained for the structure breakdown are shorter than those of structure build-up. Furthermore, the characteristic times obtained for the structure breakdown exhibit less dependency on the initial shear history. This indicates that the structure breakdown is mostly governed by the magnitude of the final applied shear stress, and that shear history does not play a major role in the structure breakdown process.

Table 4-2: Thixotropic time constants for breakdown

Breakdown			
Initial shear stress, σ_i=100 (Pa)		Initial shear stress, σ_i=200 (Pa)	
Final shear stress, σ_e (Pa)	Thixotropic time constant, τ (s)	Final shear stress, σ_e (Pa)	Thixotropic time constant, τ (s)
280	9.8	280	9.4
300	7.1	300	6.9
320	5.9	320	6.1
350	3.8	350	3.5

4.3.3. Viscosity bifurcation

To study in greater detail the flow of suspension over the observed plateau in the flow curves plotted in Figures 4-1 and 4-2, and associated yielding behaviour, creep experiments were performed at various shear stress values over sufficiently long times. The samples were pre-sheared prior to the experiments at a shear stress of 350 Pa for 2 minutes then left to rest for 20 minutes before further testing.

A range of shear stress values was applied and the shear rate was measured with time as depicted in Figure 4-5a. At shear stresses above a critical value ($\sigma_c \cong 279$ Pa), the shear rate increases rapidly to a steady-state value indicating flow. However, below this critical shear stress, which corresponds to a critical shear rate, $\dot{\gamma}_c$, the shear rate decreases with time until ultimately flow stops. This corresponds to a discontinuous shear rate profile as will be shown in the next section by the local measurement of the velocity profile across the gap of the rheometer. In other words, there is no stable flow below a critical shear rate, an effect referred to as viscosity bifurcation, as shown in Figure 4-5b, where the viscosity is plotted as a function of time. This has been proposed as an absolute measure of apparent yield stress (Da Cruz et al., 2002; Coussot et al., 2002b). It should be noted that it is difficult to measure the very exact value of the critical shear stress in pulp, although it was found to be in the range of $\sigma_c \cong 278 - 280$ Pa.

In an "ideal" yield stress fluid, as discussed before, flow stops at $\dot{\gamma}_c = 0$. However, this is not the case for the concentrated pulp suspension studied here neither for many pasty materials due to continuous internal rearrangements and local stresses (Coussot et al., 2002c; Bertola et al., 2003; Jarny et al., 2005).

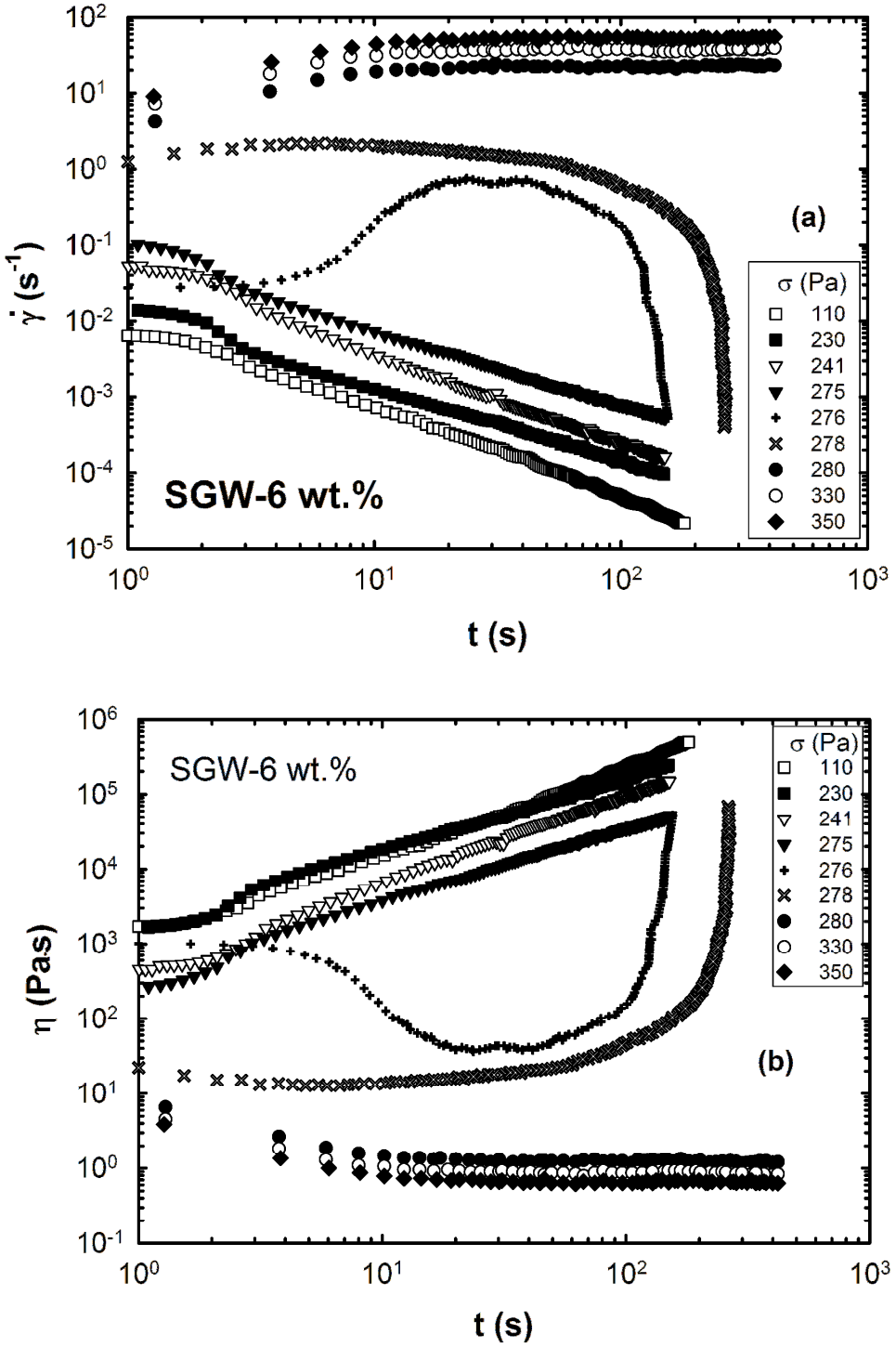

Figure 4-5: (a) Creep tests and (b) the change in viscosity in time showing viscosity bifurcation. Pulp suspensions were pre-sheared at 350 Pa for 2 minutes followed by rest for 20 minutes.

In the next section, the ultrasonic Doppler velocimeter is used in conjunction with a rate-controlled rheometer to investigate thixotropy and possible shear banding and to study the transient flow of pulp suspensions.

4.3.4. Local velocity profiles

The discontinuity of the shear rate profile discussed above would be more clearly shown by local velocity measurements. Figure 4-6 depicts the steady-state velocity profile obtained at a vane rotational rate of 16 rpm which corresponds to a nominal shear rate of ~20 s^{-1}. Velocity is at maximum at the tip of the vane (r=12.5 mm) and decreases across the gap until the flow stops at a radius referred to as the yielding radius (R_y).

We then measured the velocity profile across the gap of the rheometer and solved a Herschel-Bulkley model (Eq. 2-9) using the "least squares" method to find the best fits of the HB model to the data as shown in Figure (4-6). The best fit of the HB model to the velocity profile was obtained by constants of σ_0=261 Pa, K=71 and n=0.2 as shown as solid line in Figure (4-6). The measured velocity profile exhibits a discontinuous transition from yielded to the un-yielded region (see Figure 2-2) and the prediction of a Herschel-Bulkley model does not quite agree with the experimentally obtained velocity profiles (Figure 4-6). In an ideal yield stress fluid the velocity profile progressively decreases from a maximum at the vane to zero at the yielding radius. However, as observed from Figure 4-6, the HB models (with different parameters) do not completely predict the transition through yielding radius. This is due to the discontinuous change in the slope of the velocity profile which is incompatible with predictions of velocity profile by means of a HB model. The discontinuity in the velocity profile may come from two possible sources, shear-banding and/or slippage. It should be noted that the HB model was previously found to adequately predict the velocity profiles of pulp fibre suspensions at lower fibre concentrations as discussed in chapter 3.

Pulp is a suspension of fibres and fibre flocs in water. Water is a low viscousity fluid and thus fibres and fibre flocs are able to move easily in the suspension given enough spatial freedom. Therefore, in the very last layer of the suspension in the yielded region, fibres and flocs might slip over the ones in the first layer of the un-yielded region

and this might lead to such a discontinuity in the velocity profiles. Furthermore, a layer of water may also be formed in the transition from yielded to the un-yielded region which in turn can develop such discontinuous velocity profiles. Nevertheless, regardless of the origin of such behaviour, pulp suspension at this concentration cannot be modeled as an ideal yield stress fluid as all models describing apparent yield stress predict a continuous change of the velocity through yielding radius.

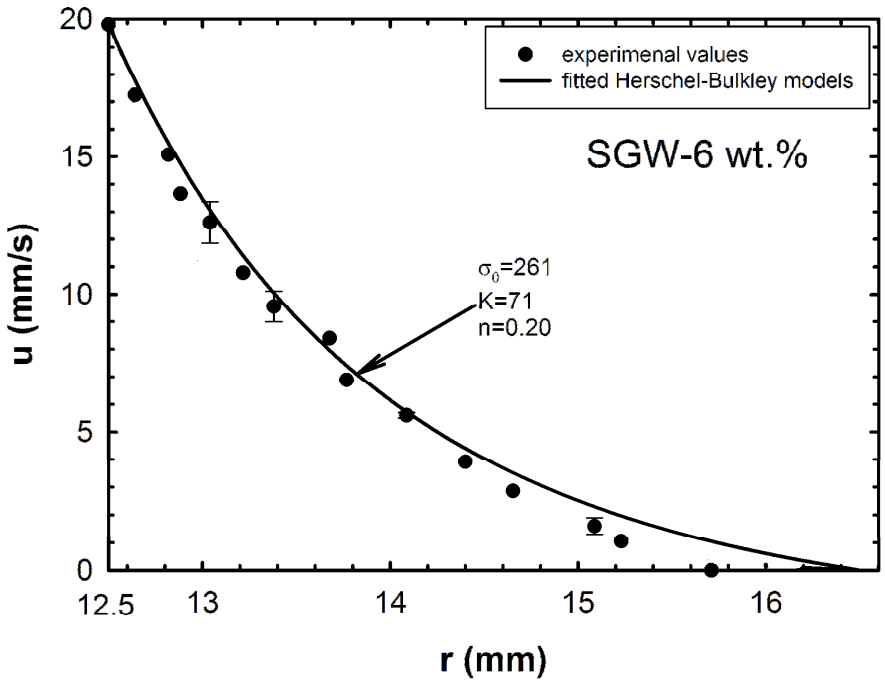

Figure 4-6: Steady-state velocity profile of pulp suspension at a vane rotational rate of 16 rpm. Pulp was pre-sheared at 350 Pa for 2 minutes with no time of rest after. Solid line is the best fit by a Herschel-Bulkley model. Error bars indicate the 95% confidence interval of the mean. Note that the HB model fails to predict the velocity profile due to the discontinuous change in the slope of velocity profile through yielding.

As discussed above, the rest time prior to the experimental testing affects its rheology. It is worthwhile to examine the corresponding changes in the velocity profiles of the suspension as well. Pulp was pre-sheared at 350 Pa for 2 minutes and left at rest for various time periods prior to the measurement of the velocity profiles, i.e. similar experiments with those plotted in Figure 4-2. A vane rotational rate of 16 rpm was suddenly applied and the variation of torque with time was followed using the rheometer. While steady-state toque was attained, the velocity profile measurement was commenced

and 15 profiles were averaged. Figure 4-7 depicts the steady-state velocity profiles in the suspensions left at rest for 0, 60 and 120 minutes. As implied from Figure 4-7 the un-yielded region (or zero velocity) increased with the time of rest. This is more clearly shown in Figure 4-8 where the yielding radius (R_y) decreases with the time of rest to a constant final value.

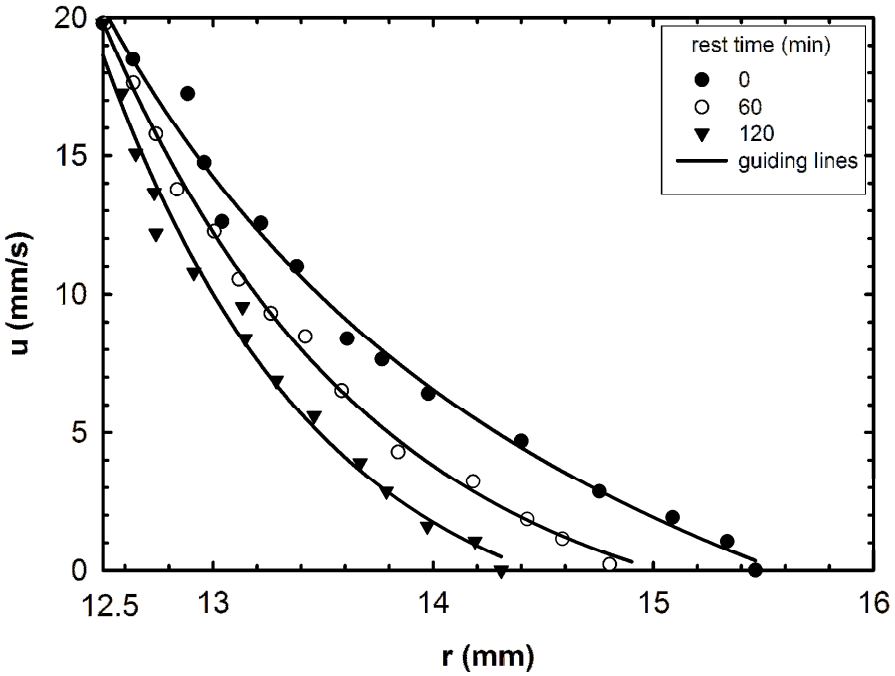

Figure 4-7: Steady-state velocity profiles of pulp suspension at a vane rotational rate of 16 rpm. Pulp was pre-sheared at 350 Pa for 2 minutes and left at rest for 0, 60 and 120 minutes prior to the velocity measurement. Solid lines are eye-guiding lines.

The yielding radius, R_y, can be used to estimate the critical shear stress, σ_c, or, in the case of an ideal yield stress fluid the apparent yield stress using Eq. (4-5):

$$\sigma_c = \frac{\mathrm{T}}{2\pi h R_y^{\,2}} \tag{4-5}$$

where T is the steady-state torque from the rheometer and h is the height of the vane. The critical shear stress values obtained from the steady-state velocity profiles are plotted against the time of rest inside Figure 4-8.

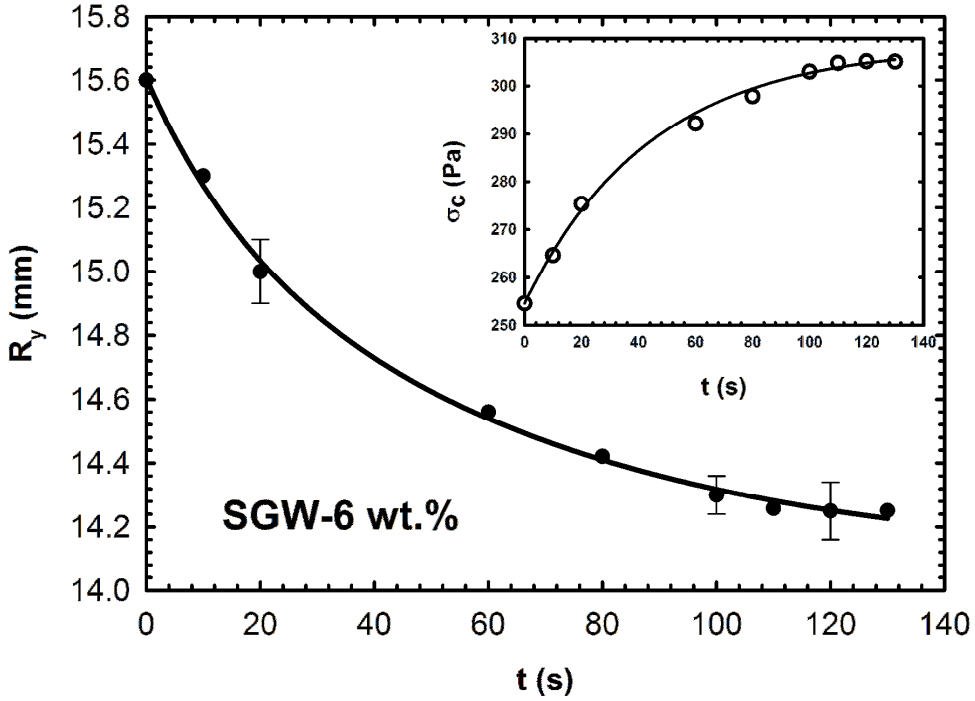

Figure 4-8: Yielding radius as a function of the rest time deduced from the steady-state velocity profiles. There is no significant change in yielding radius after ~100 min. Inset: evolution of the critical shear stress with time of rest.

The critical shear stress of the pulp rested for 20 minutes was found to be ~275 Pa, which is in agreement with that of Figure 4-1 obtained by rheometry. Figure 4-8 indicates that the critical shear stress required to initiate a stable flow in the suspension increases with the time of rest. This again reflects the time-dependency of the rheology of pulp suspension.

Next, the evolution of the velocity profiles is studied during a transient test. Pulp was pre-sheared at 350 Pa for 2 minutes followed by a 5 minutes rest time. The vane was then suddenly fixed to rotate at 16 rpm and the velocity profiles were measured every 5 seconds until steady-state was achieved. Figure 4-9 illustrates the temporal change in the velocity profiles of the suspension.

As the yielding radius increases with time, the velocity profiles become less abrupt although they all exhibit the discontinuous change of the velocity in transition to the un-yielded region. The yielding radius increases nearly exponentially with time until

steady-state is achieved as shown inside Figure 4-9. This functionality has been observed before in pasty materials (Raynaud et al., 2002).

The velocity profiles obtained by the above procedures can be used to propose a rheological model to describe the flow of pulp in the yielded region of the rheometer. This will be discussed in the next section.

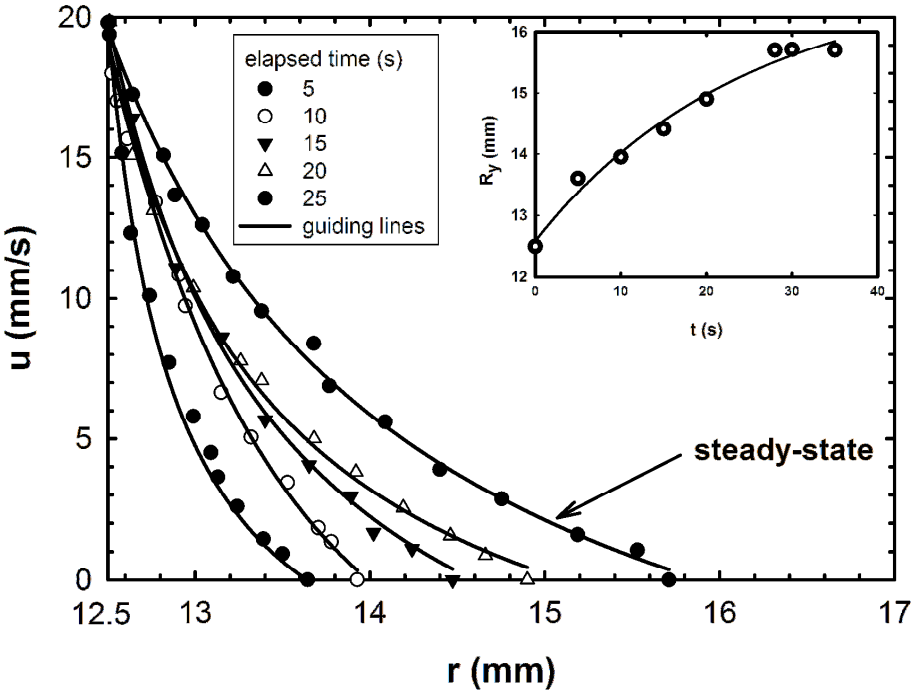

Figure 4-9: Transient velocity profiles of pulp suspension when the vane rotational rate was suddenly increased to 16 rpm. Pulp was pre-sheared at 350 Pa for 2 minutes and left at rest for 5 minutes prior to the velocity measurement. Solid lines are the eye-guiding lines. Inset: The evolution of the yielding radius with time fitted to an exponential function.

4.3.5. Rheological interpretation of the velocity profiles

As discussed before, in the case of concentrated pulp suspensions, there is a critical shear stress σ_c which defines a limit between no-shear and significant shear. This critical shear stress which is given by Eq. (4-5) remains constant at different velocities as long as pulps experience the same shear history.

Coussot (2005) has suggested that the steady-state velocity profiles obtained at different vane rotational rates to be analyzed together. This makes it possible to assess the rheological behaviour of the sample over a wide range of shear rates. To do so, the velocity profiles should be scaled with a velocity or distance to construct a master curve. Here we adopt the same concept and scale the obtained velocity profiles with the yielding radius R_y. Figure 4-10 reports the steady-state velocity profiles obtained at vane rotational rates of 8, 16 and 32 rpm.

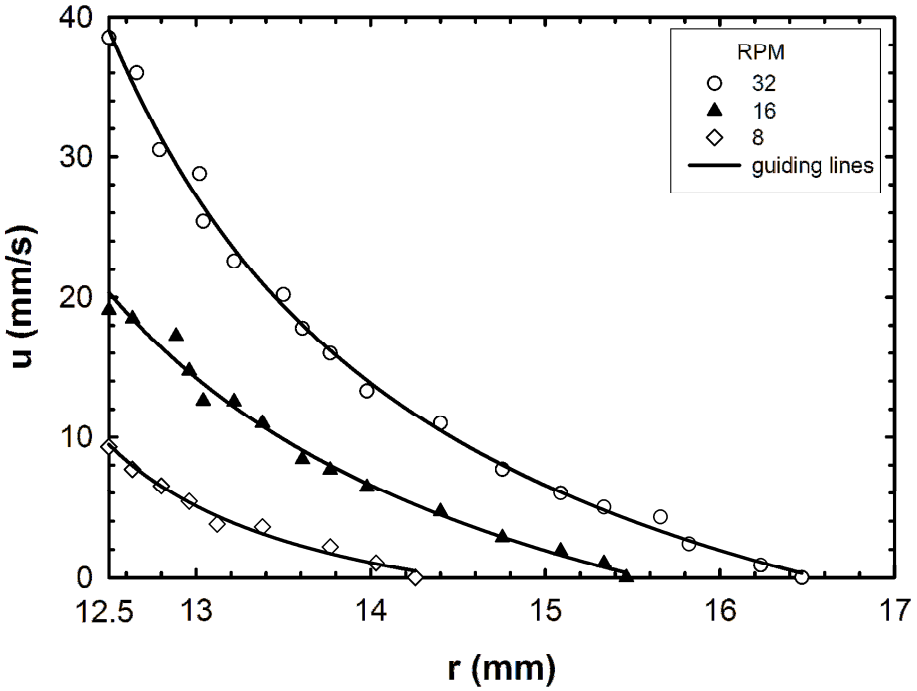

Figure 4-10: Steady-state velocity profiles at vane rotational rates of 8, 16 and 32 rpm. Solid lines are eye-guiding lines. Note that no slippage was found at the tip of the vane.

Scaling the local radius within the gap of the Couette geometry by the yielding radius R_y gives:

$$R = \frac{r}{R_y} \tag{4-6}$$

The local velocity at the dimensionless radius R then becomes:

$$U = \frac{u}{R_y} \tag{4-7}$$

where u (mm/s) is the local velocity across the gap and U is the scaled velocity (s^{-1}). Accordingly, the shear rate and the shear stress distributions across the gap of the Couette geometry become:

$$\dot{\gamma}(R) = \left| R \frac{\partial\left(U/R\right)}{\partial R} \right| \tag{4-8}$$

$$\sigma(r) = \sigma_c \left(\frac{R_y}{r} \right)^2 = \frac{\sigma_c}{R^2} = \sigma(R) \tag{4-9}$$

Figure 4-11 depicts the velocity profiles measured at vane rotational rates of 8, 16 and 32 rpm, all falling along a single master curve quite well. Once a master curve is obtained for the velocity profiles, various models can be fitted to the data to calculate the shear rate distribution by using Eq. (4-8).

It should be noted that for a single material the shear rate distribution should be the same regardless of the type of the model fitted to the master curve. Here, we fit a model of the form Eq. (4-10) (solid lines in Figure 4-11) which was previously used successfully for bentonite suspensions by Raynaud et al. (2002).

$$U(R) = \alpha\left(R^{-m} - R\right) \tag{4-10}$$

Using Eqs. (4-8) and (4-10), the shear rate distribution across the gap becomes:

$$\dot{\gamma} = \alpha(m+1)R^{-(m+1)} \tag{4-11}$$

where α and m are constants. The constitutive equation in steady-state for pulp suspension in the yielded region can then be derived by using Eqs. (4-8), (4-9) and (4-11):

$$\sigma = A\dot{\gamma}^{\frac{2}{m+1}} \tag{4-12}$$

and

$$A = \frac{\sigma_c}{\left[\alpha(m+1)\right]^{\frac{2}{m+1}}} \tag{4-13}$$

Eq. (4-13) is the constitutive equation which describes the behaviour of pulp suspension at shear stresses above the critical shear stress (σ_c~278 Pa). The constants of this model were found to be α=0.295 and m=7.95 for the 6 wt.% SGW pulp fibre suspensions examined here.

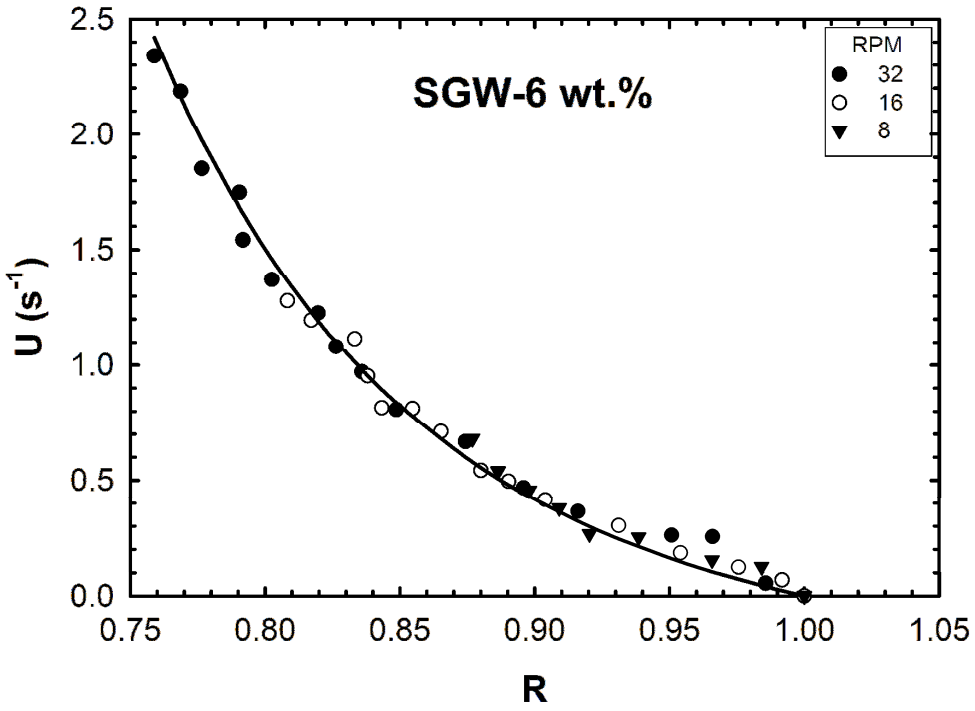

Figure 4-11: Master curve obtained from steady-state velocity profiles of Figure 4-10. Solid line is the fit of Eq. (4-11) to the data with α=0.295 and m=7.95.

4.4. Summary

Rheological experiments with concentrated pulp suspensions showed that they exhibit many of the hallmarks of glassy colloids and pasty materials, namely strong dependence of rheology on the rest time, thixotropy and yielding. Their thixotropic response was marked by a fast characteristic time in response to sudden changes of shear stress. In contrast to the structure breakdown, kinetics of structure build-up found to be dependant on the previous shear history. The transient response of pulp to step changes in the stress level was described adequately by KWW functions from which single characteristic times for build-up and breakdown processes were obtained.

The flow curves of these dense pulp suspensions were found to exhibit a plateau where a slight change of the applied shear stress led to a dramatic change in the corresponding shear rates. The direct implication of such a plateau in practice is that there is no stable flow below a critical shear stress due to viscosity bifurcation. This in turn results in a discontinuity in the slope of the velocity profiles in the vicinity of the yielding radius where the Herschel-Bulkley model fails to predict the flow. This study demonstrates that pulp viscosity and the critical shear stress increase with the time of rest, while the discontinuity in the velocity profiles becomes more pronounced.

The velocity profiles obtained for pulp suspensions at different vane rotational speeds were found to fall along a single master curve. This master curve was then used to propose a constitutive rheological model to describe the flow behaviour of pulp at shear stresses above the critical shear stress.

In summary, this study shows that dense pulp fibre suspensions beyond a critical fibre concentration taking into account the fibre size and flexibility are thixotropic yielding materials and are prone to exhibit shear-banding. The discontinuous change in the slope of the velocity profiles in the vicinity of the yielding radius suggests either shear-banding or slippage of fibre flocs over each other. These must be distinguished in the future in order to obtain a clear picture and develop design criteria for the processing of these systems.

5. Conclusions, Contributions to the Knowledge and Recommendations

5.1. Conclusions

The rheology of commercial pulp fibre suspensions was studied at fibre mass concentrations of 0.5-6 wt.% using conventional rheometry and coupled UDV-rheometry technique. Conventional rheometry was found to fail when used to study the rheology of pulp fibre suspensions at low shear rates due to the presence of wall slip. On the other hand, the coupled UDV-rheometry technique has shown good suitability for the task, since it allowed the measurement of local velocities within the gap of the rheometer regardless of any existing wall artefacts.

The coupled UDV-rheometry technique was used to measure the apparent yield stress of pulp fibre suspensions through the measurement of the steady-state velocity profiles across the gap of the rheometer. The apparent yield stress values obtained by this technique were in good agreement with those obtained by applying linear shear stress ramps using a stress-controlled rheometer. However, these measurements resulted in significantly different values compared with those obtained from a rate-controlled rheometer by applying constant shear rates. The results obtained by the three measurement techniques examined in this study were compared, and models were proposed to predict the apparent yield stress as a function of fibre mass concentration. It was shown that the coupled UDV-rheometry technique is most reliable to measure apparent yield stress values to be used in designing mixing operations due to geometrical similarities and the measurement of the velocities within the yielded region of the rheometer. The measurement technique developed in this study can be used not only for pulp fibre suspensions, but also for any visco-plastic material exhibiting complex rheological behaviour.

Conventional rheometry and coupled UDV-rheometry were further used to study the post-yield flow behaviour of pulp fibre suspensions. Pulp fibre suspensions were found to be shear-thinning materials up to a critical shear stress, after which Newtonian behaviour prevailed. The velocity profiles were fitted with a Herschel-Bulkley model to

obtain the model parameters. These parameters were then used to describe the flow curves obtained by conventional rheometry. Herschel-Bulkley model was found to adequately describe the flow behaviour up to the critical shear stress required to commence the Newtonian regime. However, a discrepancy was found between the model predictions and the flow curves obtained by the conventional rheometry at low shear rates. Further analysis of the velocity profiles proved the presence of wall slip at low shear rates, which was found to be the reason for the discrepancy observed in the results.

The UDV-rheometry technique was also used to study the effect of important process parameters such as pH and lignin content on the rheology of pulp fibre suspensions. Increasing pH over the alkaline region increased the viscosity and apparent yield stress of pulp fibre suspensions as the fibre volume fraction increased due to fibre swelling. The effect of pH on the rheology was less significant as the lignin content was increased in the TMP fibre suspensions. Lignin serves as a glue to keep fibres together and prevent them from swelling. This study showed that conventional rheometry fails at low shear rates when used to study complex pulp fibre suspensions. Additionally, velocimetry techniques such as UDV are useful to explore and correct the effects of experimental perturbations such as wall slip.

The velocity profiles measured for pulp fibre suspensions exhibited a progressive decrease in transition from yielded to un-yielded region up to a certain fibre mass concentration. At higher concentrations the velocity profiles exhibited an abrupt change in the slope in transition to the un-yielded region, implying the presence of shear banding. Therefore to study this phenomena and effects such as thixotropy in more detail pulp fibre suspensions at 6 wt.% were studied by means of conventional rheometry and coupled UDV-rheometry techniques. Pulp suspensions were found to exhibit thixotropy based on the measurements of the hysteresis loops and step changes in the applied shear stress. Structure break-down and build-up were studied by means of appropriate experimental protocols, and characteristic time scales of the process were obtained by means of a stretched exponential function. It was shown that structure break-down and build-up in pulp suspensions are basically governed by the shear-induced collisions.

The flow curves obtained for 6 wt.% pulp fibre suspensions exhibited a plateau over which no measurements could be made. This plateau was found to correspond to the viscosity bifurcation effect, implying the presence of instability below a critical shear rate. The direct implication of such a plateau was found to be an abrupt change in the slope of the velocity profiles in transition to the un-yielded region within the gap of the rheometer. The Herschel-Bulkley model failed to describe the velocity profiles. To propose a constitutive rheological model to describe the flow behaviour of the concentrated pulp suspensions in the sheared region of the rheometer, the velocity profiles obtained at different vane rotational rates were used to construct a master curve. This master curve was then used to propose a constitutive model for pulps which cannot be modeled as ideal yield stress fluids. This study shows that pulp fibre suspensions exhibit a change in rheological behaviour as the fibre mass concentration, increases beyond a critical concentration taking into account the fibre size and flexibility.

5.2. Contributions to the Knowledge

The contributions to knowledge that have been resulted from this research work are identified as follows:

1. Conventional rheometry fails to study the rheology of pulp fibre suspensions at low shear rates due to the presence of wall slip. However, conventional rheometers can be efficiently modified with velocimetry techniques such as ultrasonic Doppler velocimetry to become powerful tools to study complex systems such as pulp fibre suspensions. The main advantage of the latter is the measurement of the actual velocity profiles across the gap of the rheometer regardless of the presence of any wall artefacts.
2. Based on the above mentioned coupled UDV-rheometry technique the apparent yield stress of pulp fibre suspensions was measured using the radius of shearing and the torque distribution in the gap of the rheometer. This method of measuring the apparent yield stress is the most reliable when used with complex suspensions such as pulp fibre suspensions to provide raw data for mixing operation applications. This velocimetry-based apparent yield

stress measurement technique can be used in suspensions with complex rheological behaviour, particularly those with large particles.

3. The thixotropy and shear banding effects in concentrated pulp fibre suspensions were studied for the first time in the literature. It is reported that pulp fibre suspensions at high fibre mass concentrations are thixotropic materials exhibiting shear banding instability. It was found that constitutive rheological models such as Herschel-Bulkley are not adequate to describe the rheology of concentrated pulp fibre suspensions.

4. The transient response of pulp to step changes in the stress was studied. In contrast to the structure breakdown, kinetics of structure build-up was found to be dependant on the previous shear history. The transient behaviour was described by KWW functions from which single characteristic times for both build-up and breakdown were obtained. This is the first time that the kinetics of structure break-down and build-up is studied in the literature for pulp fibre suspensions.

5.3. Recommendations for Future Work

Several important aspects of pulp fibre suspension rheology are yet to be studied. These are recommended below for possible future work.

1. This study reports that different apparent yield stress measurement techniques and definitions may result in different values. It is worthwhile to study the apparent yield stress both in macroscopic and microscopic scales. At macroscopic scale apparent yield stress can be measured by means of conventional rheometry and/or coupled velocimetry-rheometry techniques, while at a microscopic scale it can be measured by techniques such as light scattering echo. This will shed insight into the yielding transition and may clarify the existing ambiguity.

2. The apparent yield stress measurement technique developed in this study by means of coupled velocimetry-rheometry technique should be further established

by measuring the apparent yield stress of different systems other than pulp suspensions including ideal yield stress fluids and those which exhibit shear banding.

3. Pulp fibre suspensions were found to exhibit wall slip at low shear rates. However, the governing microscopic mechanisms are not well-known. Although of limited practical significance, it is worthwhile to study and further examine the phenomena of wall slip in these systems at low shear rates.

4. Pulp fibre suspensions were found to exhibit a change in the rheological behaviour from an ideal yield stress fluid to a suspension with shear banding as the fibre mass concentration increases. However, the exact mechanisms for such a change in behaviour are not yet known. Factors such as fibre flexibility, length and size distribution that may play a role in these phenomena should be examined in more detail in the future.

5. Concentrated pulp fibre suspensions were found to exhibit thixotropy and shear banding instability. These should be modeled by means of constitutive models which include a structure parameter which evolves with time and depends on the flow kinematics.

Bibliography

Ahlgren, P.A.V., 1970. Chlorite delignification of spruce wood. Ph.D. Thesis, McGill Univ., Montreal.

Ankerfors, M., Lindström, T., 2010. The starting material-MFC. SustainComp Conference, Trondheim, October 26-27.

Archer, L.A., 2005. Polymer processing instabilities. Marcel Dekker, New York, Chapter four: 73-120.

Bachelet, C., Dantan, P.h., Flaud, P., 2004. Indirect on-line determination of the rheological behavior of a power law fluid based on numerical flow simulations. Eur. Phys. J. Appl. Phys. 25: 209-217.

Baravian, C., Lalante, A., Parker, A., 2002. Vane rheometry with a large finite gap. Applied Rheology 12: 81–87.

Barnes, H.A., Walters, K., 1985. The yield stress myth? Rheologica Acta 24(4): 323-326.

Barnes, H.A., Carnali, J.O., 1990. The vane-in-cup as a novel rheometer geometry for shear thinning and thixotropic materials. Journal of Rheology 34(6): 841–866.

Barnes, H.A., 1995. A review of slip (wall depletion) of polymer solutions, emulsions and particle suspensions in viscometers: its cause, character and cure. J. Non-Newtonian fluid Mech. 56: 221-251.

Barnes, H.A., 1997. Thixotropy-a review. J. of non-Newtonian Fluid Mechanics 70(1-2): 1–33.

Barnes, H.A., Nguyen, Q.D., 2001. Rotating vane rheometry - a review. Journal of Non-Newtonian Fluid Mechanics 98(1): 1-14.

Baudez, J., Rodts, S., Chateau, X., Coussot, P., 2004. New technique for reconstructing instantaneous profiles from viscometric tests: Application to pasty materials. J. Rheol. 48: 69–82.

Be´cu, L., Manneville, S., Colin, A., 2006. Yielding and Flow in Adhesive and Nonadhesive Concentrated Emulsions. Physical Review Letters 96: 138302.

Bécu, L., Grondin, P., Colin, A., Manneville, S., 2004. How does a concentrated emulsion flow? Yielding, local rheology and wall slip. Colloids and surfaces A: physicochem. Eng Aspects 263:146–152.

Bennington, C.P.J., Kerekes, R.J., Grace, J.R., 1990. The yield stress of fibre suspensions. Canadian Journal of Chemical Engineering 68(10): 748-757.

Bennington, C.P.J., Kerekes, R.J., Grace, J.R., 1991. Motion of pulp fibre suspensions in rotary devices. Canadian Journal of Chemical Engineering 69(1): 251–258.

Bennington, C.P.J., Azevedo, G., John, D.A., Birt, S.M., Wolgast, B.H., 1995. The yield stress of medium and high consistency mechanical pulp fibre suspensions at high gas contents. Journal of Pulp and Paper Science 21(4): 111-118.

Bennington, C.P.J., Kerekes, R.J., 1996. Power requirements for pulp suspension fluidization. Tappi Journal 79(2): 253-258.

Bergenholtz, J., Brady, J.F., Vicic, M., 2002. The non-Newtonian rheology of dilute colloidal suspensions J. Fluid Mech. 456: 239–75.

Beris, A.N., Stiakakis, E., Vlassopoulos, D., 2008. A thermodynamically consistent model for the thixotropic behaviour of concentrated star polymer suspensions. J. Non-Newtonian Fluid Mech. 152:76-85.

Bertola, V., Bertrand, F., Tabuteau, H., Bonn, D., Coussot, P., 2003. Wall slip and yielding in pasty materials. Journal of Rheology 47(5): 1211–1226.

Bird, R.B., Marsh, B.D., 1968. Viscoelastic Hysteresis. I. Model predictions. Trans. Soc. Rheol. 12: 479–488.

Bird, R.B., Stewart, W.E., Lightfoot, E.N., 2001. Transport Phenomena. Second Edition, John Wiley & Sons.

Biermann, C.J., 1993. Handbook of Pulping and Papermaking. San Diego, Academic Press.

Blakeney, W.R., 1966. The viscosity of suspensions of straight rigid rods. Journal of Colloid and Interface Science 22(4): 324–330.

Bowles, J.E., 1977. Foundation Analysis and Design. Second edition. McGraw Hill.

Bonn, D., Coussot, P., Huynh, H.T., Bertrand, F., Debrégeas, G., 2002. Rheology of soft-glassy materials. Europhysics Letters 59:786-792.

Bonn, D., Denn, M.M., 2009. Yield stress fluids slowly yield to analysis. Science 324:1401-1402.

Bramhall, A.D., Hutton, J.F., 1960. Wall effect in the flow of lubricating greases in plunger viscometers. Br. J. Appl. Phys. 11: 363.

Brenner, H., 1974. Rheology of a dilute suspension of axisymmetric Brownian particles. International Journal of Multiphase Flow 1(2): 195-341.

Brummer, R., 2005. Rheology essentials of cosmetic and food emulsions. Springer-Verlag Berlin Heidelberg.

Cadling, L., Odenstad, S., 1950. The Vane Borer. Proceedings of the Royal Swedish Geotechnical Institute No. 2: 1-87.

Callaghan, P.T., 2008. Rheo NMR and shear banding. Rheol. Acta 47:243-255.

Celzard, A., Fierro, V., Kerekes, R.J., 2009. Flocculation of cellulose fibres: new comparison of crowding factor with percolation and effective-medium theories. Cellulose, 16(6): 983-987.

Chase, W.C., Donatelli, A.A., Walkinshaw, J.W., 1989. Effects of freeness and consistency on the viscosity of hardwood and softwood pulp suspensions. Tappi Journal 72(5): 199-204.

Chaouche, M., Koch, D.L., 2001. Rheology of non-Brownian rigid fibre suspensions with adhesive contacts. Journal of Rheology 45(2): 369-383.

Chen, K.F., Chen, S.M., 1997. Fluidization properties of high-consistency fibre suspensions. Experimental Thermal and Fluid Science 14(2):149-159.

Chen, B., Tatsumi, D., Matsumoto, T., 2003. Fiber orientation and flow properties of pulp fiber suspensions under shear flow conditions. Textile Research Journal 59(12): 471-478.

Cheng, D., 1986. Yield stress: A time-dependent property and how to measure it. Rheologica Acta 25(5): 542-554.

Cloitre, M., Borrega, R., Leibler, L., 2000. Rheological aging and rejuvenation in microgel pastes. Phys. Rev. Lett. 85: 4819–4822.

Coussot, P., Leonov, A.I., Piau, J.M., 1993. Rheology of concentrated dispersed systems in low molecular weight matrix. J. Non-Newtonian Fluid Mech. 46: 179–217.

Coussot, P., Piau, J., 1995. large-scale field coaxial cylinder rheometer for the study of the rheology of natural coarse suspensions. J. Rheol. 39 (1): 104-123.

Coussot, P., Nguyen, Q.D., Huynh, H.T., Bonn, D., 2002a. Avalanche behavior in yield stress fluids. Phys Rev Lett 88:175501.

Coussot, P., Nguyen, D.Q., Huynh, H.T., Bonn, D., 2002b. Viscosity bifurcation in thixotropic, yielding fluids. Journal of Rheology 46(3): 573–589.

Coussot, P., Raynaud, J.S., Bertrand, F., Moucheront, P., Guilbaud, J.P., Huynh, H.T., Jarny, S., Lesueur, D., 2002c. Coexistence of liquid and solid phases in flowing soft-glassy materials. Physical Review Letters 88(21): 218301-1.

Coussot, P., 2005. Rheometry of pastes, suspensions and granular materials. John Wiley and sons.

Coussot, P., 2007. Rheophysics of pastes: a review of microscopic modelling approaches. Soft Matter 3:528-540.

Coussot, P., Tocquer, L., Lanos, C., Ovarlez, G., 2009. Macroscopic vs local rheology of yield stress fluids. J Non-Newton Fluid Mech. 158: 85-90.

Coussot, P., Ovarlez, G., 2010. Physical origin of shear-banding in jammed systems. European Physical J. 33(3): 183-188.

Cui, H., Grace, J.R., 2007. Flow of pulp fibre suspension and slurries: A review. International Journal of Multiphase flow. 33(9): 921-934.

Cullen, P.J., O'Donnel, C.P., Houska, M., 2003. Rotational rheometry using complex geometries—A review. Journal of Texture Studies 34: 1–20.

Da Cruz, F., Chevoir, F., Bonn, D., Coussot, P., 2002. Viscosity bifurcation in granular materials, foams, and emulsions. Physical Review E 66(5):051305.

Daily, J.W., Bugliarello, G., 1961. Basic data for dilute fibre suspensions in uniform flow with shear. TAPPI 44(7): 497–512.

Dalpke, B., Kerekes, R.J., 2005. The influence of fibre properties on the apparent yield stress of flocculated pulp suspensions. Journal of Pulp and Paper Science 31(1): 39-43.

Damani, R., Powell, R.L., Hagen, N., 1993. Viscoelastic characterization of medium consistency pulp suspensions. Canadian Journal of Chemical Engineering 71(5): 676–685.

Dealy, J.M., Wissbrun, K.F., 1990. Melt rheology and its role in plastics processing: theory and applications. VNR, NewYork.

Dhont, J.K.G., Briels, W.J., 2008. Gradient and vorticity banding. Rheol. Acta 47: 257-281.

Dong, X.M., Revol, J.F., Gray, D.G., 1998. Effect of microcrystallite preparation conditions on the formation of colloid crystals of cellulose. Cellulose 5(1): 19-32.

Donald, I.B., Jordan, D.O., Parker, R.J., Toh, C.T., 1977. 9th International Conference on Soil Mechanics and Foundation Engineering 1: 81.

Duffy, G.G., Titchener, A.L., 1975. The disruptive shear stress of pulp networks. Svensk Papperstidning 78(13): 474-479.

Duffy, G.G., 1978. Pipe friction pressure loss of pulp suspensions: literature review and evaluation of data and design methods. Tappi press TIS 0410-12.

Duffy, G.G., 1995. Flow of medium consistency wood pulp fibre suspensions. Appita Journal 48(1): 51-55.

Duffy, G.G., 2003. The significance of mechanistic-based models in fibre suspension flow. Nordic Pulp and Paper Research Journal 18 (1): 74-80.

Duffy, G.G., Abdullah, L., 2003. Fibre suspension flow in small diameter pipes. Appita J. 56: 290–295.

Duffy, G.G., Ramachandra, S., Xu, J.Q., 2004. Developments in processing fibre suspensions. In: Proceedings of the Fifth-eighth Appita Annual Conference and Exhibition. 2: 433–442.

Duffy, G.G., 2006. Measurements, mechanisms, models: some important insights into the mechanisms of flow of fibre suspensions, Annual Transactions of The Nordic Rheology Society 14: 19-31.

Dullaert, K., Mewis, J., 2005. Thixotropy:Build-up and breakdown curves during flow. Journal of Rheology 49(6): 1213-1231.

Eberle, A.P.R., Baird, D., Wapperom, P., 2008. Rheology of non-Newtonian fluids containing glass fibres: A review of experimental literature." Industrial and Engineering Chemistry Research 47(10): 3470-3488.

Ein-Mozaffari, F., Bennington, C.P.J., Dumont, G.A., 2005. Suspension yield stress and the dynamic response of agitated pulp chests, Chemical Engineering Science 60(8-9): 2399-2408.

Ehrnrooth, E.M.L., 1982. Softening and mechanical behaviour of single wood pulp fibres-the influence of matrix composition and chemical and physical characteristics. Ph.D. dissertation Univ. Helsinki.

Erwin, B.M., Vlassopoulos, D., Cloitre, M., 2010. Rheological fingerprinting of an aging soft colloidal glass. Journal of Rheology 54(4): 915-939.

Fielding, S.M., Cates, M.E., Sollich, P., 2009. Shear banding, aging and noise dynamics in soft glassy materials. Soft Matter 5(12): 2378-2382.

Fisher, D.T., Clayton, S.A., Boger, D.V., Scales, P.J., 2007. The bucket rheometer for shear stress-shear rate measurement of industrial suspensions. J. Rheol. 51(5): 821-831.

Ganani, E., Powell, R.L., 1985. Suspensions of rodlike particles—literature review and data correlations. Journal of Composite Materials 19(3): 194–215.

Ganani, E., Powell, R.L., 1986. Rheological properties of rodlike particles in a Newtonian and a non-Newtonian fluid. Journal of Rheology 30(5): 995–101.

Gullichsen, J., Harkonen, E., 1981. Medium consistency technology. II. Storage dischargers and centrifugal pumps. Tappi Journal 64 (6): 69-72.

Gullichsen, J., Fogelholm, C., 1999. Papermaking Science and Technology: Chemical Pulping. Book 6A. Fapet Oy, Helsinki.

Guthrie, W.E., 1959. An apparent viscosity for use in the application of Reynolds number to the flow of dilute pulp suspensions. Tappi Journal 42(3): 232-235.

Hatzikiriakos, S.G., Dealy, J.M., 1991. Wall slip of molten high density polyethylenes. I. Sliding plate rheometer studies. J Rheol 35:497–523.

Hatzikiriakos, S.G., Dealy, J.M., 1992. Role of Slip and Fracture in the Oscillating Flow of HDPE in a Capillary. J. Rheology, 36: 845-884.

Head, V. P., 1952. A Shear Criterion for the Hydraulic Behaviour of Paper Stocks in Pumps, Pipes, Valves and Flow meters. Tappi Journal 35(6): 260-266.

Head, V.P., Durst R.E., 1957. Stock slurry hydraulics. Tappi Journal 40(12): 931-936.

Hein, I.A., O'Brien, W.D., 1993. Current time-domain methods for assessing tissue motion by analysis from reflected ultrasound echoes—A review. IEEE Transactions on Ultrasonics, Ferroelectrics, and Frequency Control 40: 84–102.

Hietaniemi, J., Gullichsen, J., 1996. Flow properties of medium consistency fibre suspensions. Journal of Pulp and Paper Science 22(12): 469-474.

Horie, M., Pinder, K.L., 1979. Time-dependent shear flow of artificial slurries in coaxial cylinder viscometer with a wide gap. The Canadian Journal of Chemical Engineering 57(2): 125-134.

Hubbe, M.A., 2007. Flocculation and redispersion of cellulose fiber suspensions: A review of effects of hydrodynamic shear and polyelectrolytes. BioResources 2(2): 296-331.

Jana, S., Kapoor, B., Acrivos, A., 1995. Apparent wall-slip velocity coefficients in concentrated suspensions of noncolloidal particles. J. Rheol. 39: 1123–1132.

James, D.F., Yogachandran, N., Loewen, M.R., Liu, H., Davis, A.M.J., 2003. Floc rupture in extensional flow. Journal of Pulp and Paper Science 29(11): 377-382.

Jarny, S., Roussel, N., Rodts, S., Le Roy, R., Coussot, P., 2005. Rheological behavior of cement pastes from MRI velocimetry. Concrete Cement Res. 35:1873–1881.

Jastrzebski, Z.D., 1967. Entrance effects and wall effects in an extrusion rheometer during the flow of concentrated suspensions. Industrial and Engineering Chemistry Fundamentals 6: 445–453.

Kalyon, D.M., 2005. Apparent slip and viscoelasticity of concentrated suspensions. J. Rheol. 49 (3): 621-640.

Kanai, H., Amari, T., 1995. Negative thixotropy in ferric-oxide suspensions. Rheol. Acta 34: 303–310.

Kao, S.V., Mason, S.G., 1975. Dispersion of particles by shear. Nature 253(5493): 619-621.

Kerekes, R.J.E., Douglas, W.J.M., 1972. Viscosity properties of suspensions at the limiting conditions for turbulent drag reduction. The Canadian J. of Chemical Eng. 50: 228-231.

Kerekes, R.J., 1983a. Pulp floc behaviour in entry flow to constrictions. Tappi J. 66(1): 88-91.

Kerekes, R.J., 1983b. Pulp flocculation in decaying turbulence: a literature review. Journal of Pulp and Paper Science 9 (3): 86-91.

Kerekes, R.J., Soszynski, R.M., Doo, P.A.T., 1985. The flocculation of pulp fibres. 8th Fundamental Research Symposium, Mechanical Eng. Pub., Oxford, England: 265–310.

Kerekes, R.J., Schell C.J., 1992. Characterization of fibre flocculation by a crowding factor. Journal of Pulp and Paper Science 18(1): 32-38.

Kerekes, R.J., 1996. Characterizing fibre suspensions. Tappi Engineering Conference, Chicago, USA: 21-28.

Kerekes, R.J., 2006. Rheology of fibre suspensions in papermaking: an overview of recent research. Nordic Pulp and Paper Research Journal 21(5): 598–612.

Kitano, T., Kataoka, T., 1981. The rheology of suspensions of vinylon fibres in polymer liquids. I. Suspensions in silicone oil. Rheologica Acta 20(4): 390-402.

Koseli, V., Zeybek, S., Uludag, Y., 2006. Online Viscosity Measurement of Complex Solutions Using Ultrasound Doppler Velocimetry. Turkish J. of Chemistry 30: 297-305.

Larson, R.G., 1998. The Structure and Rheology of Complex Fluids. Oxford Uni. Press.

Lee, P.F.W., Duffy, G.G., 1976. An analysis of the drag reducing regime of pulp suspension flow. Tappi, 59: 119–122.

Li, T.Q., Weldon, M., Odberg, L., McCarthy, M.J., Powell, R.L., 1995a. Pipe flow behaviour of hardwood pulp suspension studied by NMRI. J. Pulp Pap. Sci. 21: 408–414.

Li, T.Q., Odberg, L., Powell, R.L., Weldon, M., McCarthy, M.J., 1995b. Flow of pulp suspension through an abrupt contraction studied by flow encoded nuclear magnetic resonance imaging. Nordic Pulp and Paper Research Journal 10(2): 133-151.

Liddell, P.V., Boger, D.V., 1996. Yield stress measurements with the vane. Journal of Non-Newtonian Fluid Mechanics 63 (2-3): 235–261.

Lindstrom, T., Westman, L., 1980. The colloidal behaviour of kraft lignin," Colloid Polym. Sci. 258(4).

Longdill, G.R., Duffy. G.G., 1988. The shear behaviour of medium concentration wood pulp suspensions. Appita 41(6): 456-461.

Luthi, O., 1987. Pulp rheology applied to medium consistency pulp flow. Tappi Engineering conference, New Orleans: 347-353.

Macosko, C.H.W., 1994. Rheology: Principles, Measurements, and Applications. Wiley-VCH.

Manneville S, Bécu L, Colin A (2004) High-frequency ultrasonic speckle velocimetry in sheared complex fluids. Eur. Phys. J. Appl. Phys. 28: 361-373.

Martin, F.L., Parker, A., Hort, J., Hollowood, T.A., Taylor, A.J., 2005. Using vane geometry for measuring the texture of stirred yogurt. J. of Texture Studies 36: 421–438.

Martínez-Padilla, L.P., Rivera-Vergas, C., 2006. Flow behaviour of Mexican sauces using a vane-in-a-large cup rheometer. Journal of Food Engineering 72: 189-196.

Martinez, D.M., Buckley, K., Jivan, S., Lindstrom, A., Thiruvengadaswamy, R., Olson, J.A., Ruth, T.J., Kerekes, R.J., 2001. Characterizing the mobility of papermaking fibres during sedimentation. Transactions of 12th fundamental research symposium, Oxford: 225-254.

Mason, S.G., 1950. The flocculation of pulp suspensions and the formation of paper. Tappi Journal 33: 440 (1950).

Mas, R., Magnin, A., 1994. Rheology of colloidal suspensions: case of lubricating greases. J. Rheology 38:889-908.

Mason, S.G., 1950. The motion of fibres in flowing fluids. Pulp and Paper Canada Magazine 51(5): 93-100.

McClements, D.J., Povery, M.J.W., Jury, M., Betsanis, E., 1990. Ultrasonic Characterization of a Food Emulsion. Ultrasonics 28: 266-272.

Meeker, S.P., Bonnecaze, R.T., Cloitre, M., 2004a. Slip and flow of soft particle Pastes. Phys. Rev. Lett. 92: 198302/1–4.

Meeker, S.P., Bonnecaze, R.T., Cloitre, M., 2004b. Slip and flow of pastes of soft particles: Direct observation and rheology. J. Rheol. 48(6): 1295–1320.

Mewis, J., 1979. Thixotropy—A general review. J. Non-Newtonian Fluid Mech. 6:1–20.

Mewis, J., Wagner, N.J., 2009. Thixotropy. Advances in Colloid and Interface Science 147-148: 214-227.

Meyer, R., Wahren, D., 1964. On the elastic properties of three-dimensional fibre networks. Svensk Papperstidning 67(10): 432-436.

Mewis, J., Metzner, A.B., 1974. The rheological properties of suspensions of fibres in Newtonian fluids subjected to extensional deformations. Journal of Fluid Mechanics 62(3): 593-600.

Mih, W., Parker, J., 1967. Velocity profile measurements and a phenomenological description of turbulent fibre suspension pipe flow. Tappi Journal 50(5): 237-246.

Milliken, W.J., Gottlieb, M., Graham, A.L., Mondy, L.A., Powell, R.L., 1989. The viscosity-volume fraction relation for suspensions of rod-like particles by falling-ball rheometry. Journal of Fluid Mechanics 202: 217-232.

Mhetar, V., Archer, L.A., 1998. Slip in entangled polymer solutions. Macromolecules 31: 6639–6649.

Møller, P.C.F., Mewis, J., Bonn, D., 2006. Yield stress and thixotropy: on the difficulty of measuring yield stresses in practice. Soft Matter 2: 274–283.

Mooney, M., 1931. Explicit formulas for slip and fluidity. J. Rheology 2: 210–222.

Mobuchon, C., Carreau, P.J., Heuzey, M-C, 2007. Effect of flow history on the structure of a non-polar polymer/clay nanocomposite model system," Rheologica Acta 46(8):1045-1056.

Mylius, E., Reher, E., 1972. Modelluntersuchungen zur Charakterisierung Thixotroper Medien un ihre Anwendung für Verfahrenstechnische Prozessberechnungen. Plaste Kautsch. 19: 420–431.

Nawab, M.A., Mason, S.G., 1958. The viscosity of dilute suspensions of thread-like particles. Journal of Physical Chemistry 62(10): 1248-1253.

Nguyen, Q.D., Boger, D.V., 1981. Proc. 2nd National Conference on Rheology, Sydney: 19-23.

Nguyen, Q.D., Boger, D.V., 1983. Yield stress measurement for concentrated suspensions. J. Rheology 27: 321–349.

Nguyen, Q.D., Boger, D.V., 1985. Direct yield stress measurement with the vane method. Journal of Rheology 29: 335–347.

Nguyen, Q.D., Boger, D.V., 1992. Measuring the flow properties of yield stress fluids. Annual Review of Fluid Mechanics 24: 47-88.

Nguyen, Q.D., Akroyd, T., De Kee, D.C., Zhu, L., 2006. Yield stress measurements in suspensions: an inter-laboratory study. Korea-Australia Rheology Journal 18(1): 15-24.

Norman, B.G., Moller, K., EK, R., Duffy, G.G., 1978. Hydrodynamics of papermaking fibres in water suspension. Transactions of 6th fundamental resource symposium, Oxford: 195-249.

Norman, B., 1990. Overview of the physics of forming. Transactions of 9th fundamental resource symposium, Cambridge, (3): 73-158.

Norman, B., Söderberg, D., 2001. Overview of the forming literature. Transactions of 12th fundamental resource symposium, Oxford, (1): 431-448.

Ogawa, K., Yoshikawa, S., Suguro, A., Ikeda, J., Ogawa, H., 1990. Flow characteristics and circular pipe flow of pulp-suspension. J. Chem. Eng. Jpn. 23: 1–6.

Olmsted, P.D., 2008. Perspectives on shear banding in complex fluids," Rheol. Acta 47:283-300.

Ooi, Y.W., Sridhar, T., 2004. Resistance to uniaxial extensional flow of fibre suspensions. Rheologica Acta 43(3): 223-231.

Ovarlez, G., Bertrand, F., Rodts, S., 2006. Local determination of the constitutive law of a dense suspension of noncolloidal particles through MRI. J. Rheol. 50:259–292.

Ovarlez, G., Rodts, S., Chateau, X., Coussot, P., 2009. Phenomenology and physical origin of shear localization and shear banding in complex fluids. Rheol. Acta 48:831–844.

Pan, J., Hammad, W., Straus, S.K., 2010. Parameters affecting he chiral nematic phase of nanocrystalline cellulose films. Macromolecules 43: 3851-3858.

Papathanasiou, P., Guell, T.D., 1997. Flow Induced Alignment in Composite Materials. 1st Ed., Woodhead Publishing Limited, Cambridge, England.

Papenhuijzen, J.M.P, 1972. The role of particle interactions in the rheology of dispersed systems. Rheologica Acta 11: 73-88.

Petrie, C.J.S., 1999. The rheology of fibre suspensions. Journal of Non-Newtonian Fluid Mechanics 87(2-3): 369-402.

Petrich, M.P., Koch, D.L., Cohen, C., 2000. An experimental determination of the stress–microstructure relationship in semi-concentrated fibre suspensions. Journal of non-Newtonian Fluid Mechanics 95(2-3): 101-133.

Pettersson, J.A., 2004. Flow and mixing of pulp suspensions. Ph.D. Thesis, Chalmers University of Technology.

Pignon, F., Magnin, A., Piau, J.M., 1996. Thixotropic colloidal suspensions and flow curves with minimum: identification of flow regimes and rheometric consequences. J. Rheology 40:573-587.

Piteira, M.F., Maia, J.M., Raymundo, A., Sousa, I., 2006. Extensional flow behaviour of natural fibre-filled dough and its relationship with structure and properties. Journal of Non-Newtonian Fluid Mechanics 137(1-3): 72-80.

Powell, R.L., Morrison, T.G., 2001. Apparent viscosity of suspensions of rods using falling ball rheometry. Physics of Fluids 13(3): 588-593.

Pryce-Jones J., 1952. Studies in Thixotropy. Kolloid-Z 129: 96-122.

Ramírez-Gilly, M., Martínez-Padilla, L.P., Manero, O., 2007. Particle image velocimetry applied to suspensions of millimetric-size particles using a vane-in-a-large-baffled-cup rheometer. J. of Food Eng. 78(4): 1117-1126.

Raynaud, J.S., Moucheront, P., Baudez, J.C., Bertrand, F., Guilbaud, J.P., Coussot, P., 2002. Direct determination by nuclear magnetic resonance of the thixotropic and yielding behaviour of suspensions. J. Rheol. 46: 709-732.

Robertson, A.A., Mason, S.G., 1957. The flow characteristics of dilute fibre suspensions. Tappi, 40(50): 326-335.

Roux, J.C., Franc, N., Duffy, G.G., Fabry, B., 2001. Shear factor: A new way to characterize fibre suspension shear. Tappi Journal 84(8): 46-63.

Ross, R., Klingenberg, D., 1998. Simulation of flowing wood fibre suspensions. Journal of Pulp Paper Science 24(12): 388-392.

Sampson, W.W., 2001. The structural characterisation of fibre networks in papermaking processes-A review. Transactions of 12th Fundamental Resource Symposium, Oxford: 1205-1288.

Scott B.G.W., 1933. The Thixotropy of Heather Honey. Journal of Physical Chemistry 39(2): 213–220.

Schalek, E., Szegvari, A., 1923. The slow coagulation of concentrated iron oxide sol to a reversible gel. Kolloid-Zeitschrift 33(6): 326-334.

Schmid, C., Klingenberg, D., 2000a. Mechanical flocculation in flowing fiber suspensions, Physical Review Letters 84(2): 290-293.

Schmid, C., Klingenberg, D., 2000b. Properties of fiber flocs with frictional and attractive interfiber forces. Journal of Colloid and Interface Science 226(1): 136-144.

Schmid, C., Switzer, L., Klingenberg, D., 2000c. Simulations of fiber flocculation effects of fiber properties and interfiber friction. Journal of Rheology 44(4): 781-809.

Smook, G.A., 1992. Handbook for Pulp and Paper Technologists. Tappi Pr, 2nd edition.

Soszynski, R.M., Kerekes, R.J., 1988a. Elastic interlocking of nylon fibres suspended in liquid, Part 1, nature of cohesion among fibres. Nordic Pulp Paper Research Journal 3(4): 172-179.

Soszynski, R.M, Kerekes, R.J, 1988b. Elastic interlocking of nylon fibres suspended in liquid, Part 2, Process of interlocking. Nordic Pulp Paper Research Journal 4: 180-184.

Steen, M., 1990. Turbulance and flocculation in fibre suspensions. Ph.D. thesis, Institutte for Teknisk Varmelaere, Trondheim.

Stockie, J.M., 1997. Analysis and computation of immersed boundaries with application to pulp fibres. Ph. D. Thesis, University of British Columbia.

Stone, I.E., Scallan, A.M., 1968. The effect of component removal upon the porous structure of the cell wall of wood. Part III. A comparison between the sutphite and kraft processes. Pulp Paper Mag. Can. 60 (12).

Swerin, A., Powell, R.L., Odberg, L., 1992. Linear and nonlinear dynamic viscoelasticity of pulp fibre suspensions. Nordic Pulp Paper Research Journal 7(3): 126–143.

Swerin, A., 1998. Rheological properties of cellulosic fibre suspensions flocculated by cationic polyacrylamides. Colloids and Surfaces A: Physicochemical and Engineering Aspects 133(3): 279-294.

Switzer, L.H., Klingenberg, D.J., 2003. Simulations of fibre floc dispersion in linear flow fields. Nordic Pulp Paper Research Journal 18: 141-144.

Stickel, J.J., Knutsen, J.S., Liberatore, M.W., Luu, W., Bousfield, D.W., Klingenberg, D.J., Scott, C.T., Root, T.W., Ehrhardt, M.R., Monz, T.O., 2009. Rheology measurements of a biomass slurry: an inter-laboratory study. Rheologica Acta 48(9): 1005–1015.

Steenberg, B., Johansson, B., 1958. Viscous properties of pulp suspension at high shear-rates. Svensk Papperstidning 61(18): 696-700.

Takeda, Y., 1986. Velocity Profile Measurement by Ultrasound Doppler Shift Method. Int. J. of Heat & Fluid Flow 7(4): 313-318.

Thalen, N., Wahren, D., 1964. A New Elastoviscometer. Svensk Papperstidn 67(6): 226-231.

Thalen, N., Wahren, D., 1964a. Shear modulus and ultimate shear strength of some paper pulp fibre networks. Svensk Papperstidning 67(7): 259-264.

Thalen, N., Wahren, D., 1964b. An experimental investigation of the shear modulus of model fibre networks. Svensk Papperstidning 67(11): 474-480.

Toven, K., 2000. Swelling and physical properties of ECF/ECF light bleached softwood kraft pulps. Inter. Pulp Bleaching Conference, Nova Scotia, Jun. 27-30.

Tucker, C.L. III, Advani, S.G., 1994. Flow and Rheology in Polymeric Composites Manufacturing. Elsevier Publishers, Amsterdam, 147-202.

Umer, R., Bickerton, S., Fernyhough, A., 2007. Modelling liquid composite moulding processes employing wood fibre mat reinforcements. Key Engineering Materials 334: 113-116.

Van den Temple, M., 1971. In Elasticity, Plasticity and structure of Matter. Cambridge University Press: 123-137.

Van de ven, T.G.M., 2006. Interactions between fibres and colloidal particles subjected to flow. Annual Transactions of the Nordic Rheology Society 14: 9-17.

Ventura C, Blanco A, Negro C, Ferreira P, Garcia F, Rasteiro M (2007) Modeling pulp fiber suspension rheology. TAPPI J 6(7):17–23.

Vinogradov, G.V., Froishteter, G.B., Trilisky, K.K., Smorodinsky, E.L., 1975. The flow of plastic disperse systems in the presence of the wall effect. Rheol. Acta, 14: 765-775.

Vinogradov, G.V., Froishteter, G.B., Trilisky, K.K., Smorodinsky, E.L., 1978. The generalized theory of flow of plastic disperse systems with account of the wall effect. Rheol. Acta, 17(2): 156-165.

Wahren, D., 1980. Fibre network structures in papermaking operations. In proceedings of the conference on paper science and technology, the cutting edge, Institute of paper science and technology, Atlanta: 112.

Walls, H.J., Caines, S.B., Sanchez, A.M., Khan, S.A., 2003. Yield stress and wall slip phenomena in colloidal silica gels. J. Rheology 47: 847–867.

Westman, L., Lindstrom, T., 1981. Swelling and mechanical properties of cellulose hydrogels. J. Appl. Polym. Sci. 26(8).

Wikström, T., Rasmuson, A., 1998. Yield stress of pulp suspensions: The influence of fibre properties and processing conditions. Nordic Pulp Paper Resource Journal 13(3): 243-250.

Wikstrom, T., Rasmuson, A., 2002. Transition modelling of pulp suspensions applied to a pressure screen. Journal of Pulp and Paper Science 28(11): 374-378.

Wikström, T., 2002. Flow and rheology of pulp suspensions at medium consistency. Ph.D. thesis, Chalmers Uni. of Technology.

Yan, H., Norman, B., Lindström, T., 2006. A flow loop system for study of fibre suspension flocculation. Nordic Pulp and Paper Research Journal 21(1): 19-23.

Yoshimura, A., Prud'homme, R.K., 1988. Wall slip corrections for Couette and parallel disk viscometers. J. Rheology 32: 53–67.

Zhang, X.D., Giles, D.W., Barocas, V.H., Yasunaga, K., Macosko, C.W., 1998. Measurement of foam modulus via a vane rheometer. J. Rheology 42(4): 871-889.

Zhao, R.H., Kerekes, R.J., 1993. The effect of suspending liquid viscosity on fibre flocculation. Tappi Journal 76(2):183-188.

Zhu, L., Sun, N., Papadopoulos, K., De Kee, D., 2001. A slotted plate device for measuring static yield stress. Journal of Rheology 45(5): 1105–1122.

Ziegel, K.D., 1970. The viscosity of suspensions of large, nonspherical particles in polymer fluids. Journal of Colloid and Interface Science 34(2): 185-196.

Appendix

Appendix A: Ultrasonic Doppler Velocimetry

In this appendix the principles of ultrasonic Doppler velocimetry, its advantages as well as limitations are reviewed. More information can be found in the user manual of the instrument (DOP2000, Signal Processing, Switzerland). Ultrasonic Doppler velocimetry was developed over 30 years ago as a diagnostic medical imaging. Over the years, this technique has found its applications to important area of fluid dynamics, for example, in areas such as product mixing, fluid transportation etc. Ultrasonic Doppler velocimetry can be performed in two modes of continuous and pulsed velocimetry. Here, we shall focus on the pulsed ultrasonic Doppler velocimetry since a pulsed ultrasound Doppler velocimeter has been used in this study.

Principles of Pulsed Ultrasound Doppler Velocimetry

In a pulsed ultrasound Doppler velocimeter (UDV), an emitter periodically sends ultrasound beams to a fluid and a receiver collects the reflected pulses by the moving particles that may be present in the path of the ultrasound beam. Often, the same transducer is used as both an emitter and a receiver. Figure A-1 shows a picture of the ultrasound Doppler velocimeter coupled with a rate-controlled rheometer used in this study.

A pulsed ultrasound Doppler velocimeter measures the velocity and the depth of the particles within a moving fluid by measuring two parameters. First, it measures the frequency of the emitted and reflected pulses resulted from motion of the particles. In addition, it measures the time required for an ultrasound beam to travel from the emitter to the particle and reflect back to the receiver. This parameter is referred to as the time delay. By measuring these two parameters, the depth of the moving particle can be measured by Eq. (A-1):

$$y = \frac{c.T_f}{2} \tag{A-1}$$

where c is the velocity of sound in the medium and T_f is the time delay between an emitted burst and the echo reflected by the particle.

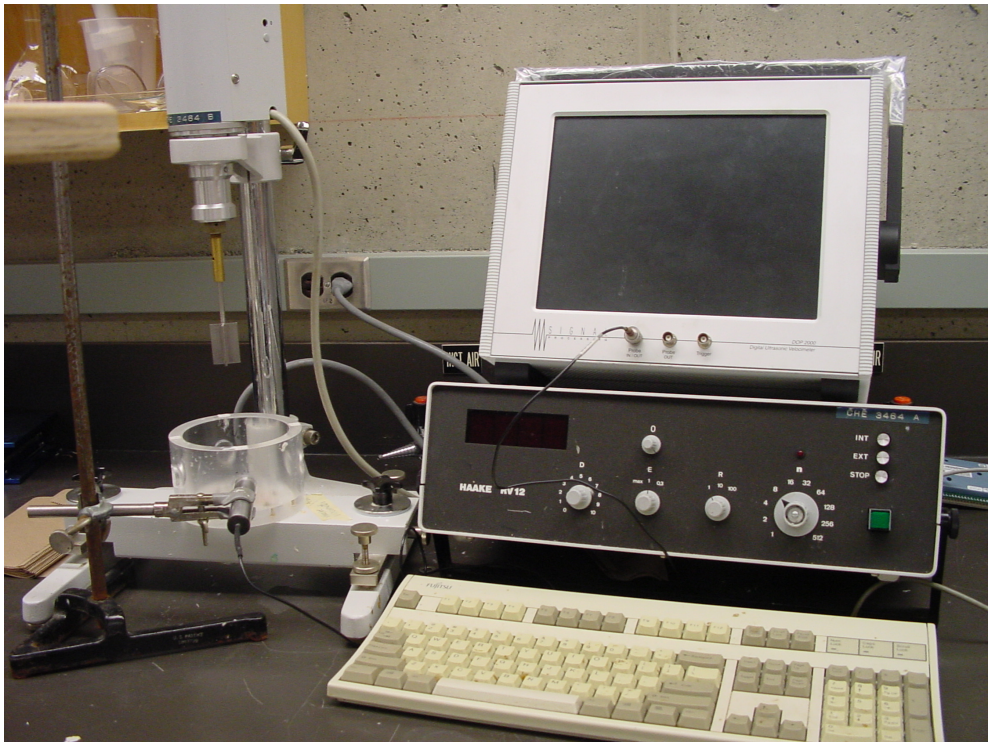

Figure A-1: Ultrasound Doppler velocimeter coupled with a rate controlled rheometer. The same transducer is used as an emitter and a receiver.

By having the time interval between two subsequent ultrasound bursts, T_{prf} , and the angle at which the particle is moving in relation to the axis of the ultrasound beam, θ, the change in depth of the particle can be measured by Eq. (A-2):

$$(y_2 - y_1) = v \times T_{prf} \times \cos\theta = \frac{c}{2} \times (T_2 - T_1) \qquad \text{(A-2)}$$

The time difference, T_2-T_1, is a function of the phase shift of the received echo, δ, and can be measured by Eq. (A-3):

$$T_2 - T_1 = \frac{\delta}{2\pi \times f_0} \qquad \text{(A-3)}$$

where f_0 is the ultrasound emitting frequency. The particle velocity can then be calculated by Eq. (A-4):

$$v = \frac{c \times \delta}{4\pi \times f_0 \times \cos\theta \times T_{prf}} = \frac{c \times f_d}{2 \times f_0 \times \cos\theta} \tag{A-4}$$

Therefore, the depth and the velocity of a moving particle can be measured in a fluid and in the direction of the ultrasound beam.

Advantages and Limitations

UDV is a non-intrusive technique which can be used to measure the velocity distribution within a moving fluid. Its main advantage is that it can be easily used with both transparent and opaque fluids, in contrast to the most of the other velocity measurement techniques. However, there are a number of limitations/assumptions in making use of such a technique. The main limitation is that there is a maximum velocity that can be measured for each pulse repetition frequency (PRF). This maximum velocity can be measured according to Eq. (A-5):

$$u_{\max} = \frac{c}{4 \times f_0 \times \cos\theta \times T_{prf}} \tag{A-5}$$

If a velocity higher than this maximum is measured, a phenomenon referred to as aliasing occurs which affects the accuracy of the measured data. This means that all frequencies above the half of the sampling frequency are folded back in the low frequency region.

Similarly, there is a limitation in the measurement of the maximum depth. The maximum measurable depth can be calculated by Eq. (A-6):

$$y_{\max} = \frac{T_{prf} \times c}{2} \tag{A-6}$$

From Eqs. (A-5) and (A-6) it is evident that reducing *PRF* or increasing T_{prf} will increase the measureable depth but decreases the maximum measurable velocity. This can be more clearly shown by Eq. (A-7):

$$y_{\max} u_{\max} = \frac{c^2}{8 f_e} \tag{A-7}$$

In other words, there is a maximum measurable depth corresponding to a maximum measureable velocity, this can often impose a limitation in the practical situations.

In addition to the above limitations, it is presumed that the ultrasound beam only travels in a straight line with a constant rate of attenuation. The speed of sound in the medium is assumed to be constant and the ultrasound beam is assumed to be infinitely thin with all echoes originating from its central axis. Obviously, these are not satisfied in all situations.

Resolution

Resolution is the ability of the instrument to distinguish two objects adjacent to each other in the fluid and is divided into spatial and temporal resolution. Spatial resolution in turn can be divided into axial and lateral resolution. Axial resolution is the ability of the instrument to identify objects in the direction of the ultrasound beam while lateral resolution is the ability to identify two objects perpendicular to the beam's direction. These resolutions have to be adjusted properly in order to be able to capture the true flow field of the fluid within the system.

The lateral resolution can be increased by decreasing the width of the ultrasound beam. The beam's width can be decreased by using a higher frequency transducer, focusing the beam or by decreasing the gain. The axial resolution on the other hand can be improved by using higher frequency transducers at the expense of decreasing the penetration. Therefore, higher frequencies are used to capture the structures close to the transducer. In this study the spatial resolution was set between 0.19–0.25 mm, with a temporal resolution of 45–55 ms/profile and velocity resolution of 0.025 mm/s.